



5-2014

Synthesizing Strong Donor Macrocyclic Tetracarbene Metal Complexes for Catalytic Aziridination

Steven Alan Cramer

University of Tennessee - Knoxville, scramer2@utk.edu

Follow this and additional works at: https://trace.tennessee.edu/utk_graddiss

 Part of the [Inorganic Chemistry Commons](#)

Recommended Citation

Cramer, Steven Alan, "Synthesizing Strong Donor Macrocyclic Tetracarbene Metal Complexes for Catalytic Aziridination. " PhD diss., University of Tennessee, 2014.
https://trace.tennessee.edu/utk_graddiss/2756

This Dissertation is brought to you for free and open access by the Graduate School at TRACE: Tennessee Research and Creative Exchange. It has been accepted for inclusion in Doctoral Dissertations by an authorized administrator of TRACE: Tennessee Research and Creative Exchange. For more information, please contact trace@utk.edu.

To the Graduate Council:

I am submitting herewith a dissertation written by Steven Alan Cramer entitled "Synthesizing Strong Donor Macrocyclic Tetracarbene Metal Complexes for Catalytic Aziridination." I have examined the final electronic copy of this dissertation for form and content and recommend that it be accepted in partial fulfillment of the requirements for the degree of Doctor of Philosophy, with a major in Chemistry.

David M. Jenkins, Major Professor

We have read this dissertation and recommend its acceptance:

David C. Baker, Zi-ling Xue, Engin Serpersu

Accepted for the Council:

Carolyn R. Hodges

Vice Provost and Dean of the Graduate School

(Original signatures are on file with official student records.)

**Synthesizing Strong Donor Macrocyclic Tetracarbene Metal
Complexes for Catalytic Aziridination**

A Dissertation Presented for the

Doctor of Philosophy

Degree

The University of Tennessee, Knoxville

Steven Alan Cramer

May 2014

Copyright © 2014 by Steven Alan Cramer

All rights reserved.

DEDICATION

I would like to dedicate my dissertation to my parents and my wife. My father William Cramer has always inspired me by example to never quit any task and always work as hard as possible. My mother Sherri Cramer has made endless efforts to make sure I excel academically and technologically, whether it be through rewards for good grades or a nightly competition while watching Jeopardy on television. Finally, my wife Natalie Cramer has supported me with love, kindness, and words of encouragement everyday throughout my life journey. Without each of these three individuals I can honestly say that I would not be writing this dissertation and likely would not have achieved my current level of success in life.

ACKNOWLEDGEMENTS

I would like to acknowledge Dr. David Jenkins and Dr. Zheng Lu. Dr. Jenkins has been instrumental in molding my thought process to think abstractly through chemical problems. Due to his efforts, my breadth of chemistry knowledge has grown exponentially. Additionally, Dr. Jenkins has taught me to prepare a plan for every synthetic challenge and try to pinpoint all the possible outcomes. Dr. Lu has shaped how I perform chemistry in a tangible way. In addition to the vast knowledge he has shown me how to use certain instrumentation and setup reactions, he also taught me not to “overthink” chemistry and instead try a reaction if there is a possibility that it may work. With the mentoring from Dr. Jenkins and Dr. Lu, I have realized that it is critical to conceptually understand everything possible in the beginning of a reaction or problem but be open-minded when the outcome was not foreseen in the original plan, because, after all, we are scientists and we apply rules and when those rules fail it is up to us to make new rules.

ABSTRACT

A small ringed macrocyclic tetracarbene ligand was developed due to the inherent ability of *N*-heterocyclic carbenes (NHCs) to stabilize high oxidation states of transition metals. This new strong donor ligand was prepared by first synthesizing an 18-atom ringed macrocyclic tetraimidazolium ligand precursor. The tetraimidazolium can be prepared by a two-step procedure. This ligand precursor was deprotonated to prepare a monomeric platinum tetracarbene complex.

A new iron macrocyclic tetra-carbene complex was synthesized by an in situ strong base deprotonation strategy of the ligand precursor. The iron tetracarbene complex was found to catalyze the aziridination of a wide array of functionalized aryl azides and a variety of substituted aliphatic alkenes, including tetra-substituted.

The aziridination intermediate was probed by mass spectrometry and found to likely be an iron(IV) imido. Further investigation of this intermediate discovered that an iron(IV) tetrazene forms when excess aryl azide was added, probably by a 1,3-cycloaddition of an additional equivalent of azide to an imido. Utilizing single-crystal X-ray diffraction, NMR spectroscopy, and Mossbauer spectroscopy the metal center was formally assigned as a low spin ($S = 0$) iron(IV). Additional reactivity studies indicate this tetrazene is capable of performing aziridination and therefore is an additional reaction pathway in the catalytic cycle.

A large disadvantage of the aforementioned iron tetracarbene catalyst is poor yield. To overcome low yields and to prepare several transition metal tetracarbene complexes, a dimeric macrocyclic tetracarbene silver complex was synthesized. This complex was shown to successfully extend transmetallation of polydentate NHCs beyond bidentate NHCs. The silver complex was utilized in the preparation of a variety of mononuclear tetracarbene complexes ranging from early first row to late third row transition metals in moderate to high.

In an attempt to move toward improving solubility of the tetracarbene catalysts, a second generation variant with two borate moieties in the ligand backbone was utilized. With this dianionic 18-atom macrocyclic tetracarbene ligand, the first tetracarbene complexes of Group 13 and 14 metals were synthesized. The tin, indium, and aluminium tetracarbene complexes are structurally analogous to their catalytically active porphyrin or salen analogues.

TABLE OF CONTENTS

Chapter 1 Introduction	1
Chapter 2 Preparation of an 18-Atom Macrocyclic Tetra-Imidazolium as a Tetra- <i>N</i> -Heterocyclic Carbene Ligand Precursor.....	8
Abstract	9
Introduction	10
Synthesis and Characterization of Tetra-imidazolium Ligand Precursor	12
Synthesis and Characterization of a Platinum(II) Tetracarbene Complex	14
Conclusion	17
Experimental	18
Chapter 3 Synthesis of Aziridines from Alkenes and Aryl Azides with a Reusable Macrocyclic Tetracarbene Iron Catalyst.....	25
Abstract	26
Introduction	26
Synthesis and Characterization of an Iron(II) Tetracarbene Complex	28
Catalytic Aziridination with Aryl Azides and Aliphatic Alkenes.....	31
Conclusion	38
Experimental	39
Chapter 4 Development of a Silver Transmetallating Reagent to Synthesize Macrocyclic Tetracarbene Complexes	55
Abstract	56
Introduction	57

Synthesis and Characterization of Silver Complex.....	58
Synthesis of Tetracarbene Complexes.....	60
Structural Characterization of Tetracarbene Complexes.....	65
Conclusion	69
Experimental	70
Chapter 5 Characterization and Reactivity of an Fe(IV) Tetrazene Complex.....	77
Abstract	78
Introduction	78
Characterization and Reactivity of Fe(IV) Tetrazene.....	81
Conclusion	86
Experimental	87
Chapter 6 Overcoming NHCs Neutrality: Installing Tetracarbenes on Group 13 and 14 Metals	94
Abstract.....	95
Introduction	95
Synthesis and Characterization of Tetracarbene Main Group Complexes	97
Conclusion	104
Experimental	104
Chapter 7 Conclusion	112
References	116
VITA.....	141

LIST OF TABLES

Table 3.1. Aziridination reactions with $[(^{\text{Me,Et}}\text{TC}^{\text{Ph}})\text{Fe}(\text{NCCH}_3)_2](\text{PF}_6)_2$	32
Table 3.2. Aziridination of functionalized aryl azides and 1-decene with $[(^{\text{Me,Et}}\text{TC}^{\text{Ph}})\text{Fe}(\text{NCCH}_3)_2](\text{PF}_6)_2$	36
Table 3.3. Aziridination reaction re-using $[(^{\text{Me,Et}}\text{TC}^{\text{Ph}})\text{Fe}(\text{NCCH}_3)_2](\text{PF}_6)_2$ with <i>cis</i> - cyclooctene.....	37
Table 4.1. Transmetallation results for metal complexes.	63

LIST OF FIGURES

Figure 1.1. Isolated late transition metal imide complexes.....	4
Figure 1.2. Group theory of a 5-coordinate d^4 bent square pyramidal metal complex.	5
Figure 1.3. Mononuclear tetra- <i>N</i> -heterocyclic carbene complexes	6
Figure 2.1. Crystal structure of $(^{Me,Et}TC^{Ph})(I)_4$	15
Figure 2.2. Crystal structure of $[(^{Me,Et}TC^{Ph})Pt](PF_6)_2$	17
Figure 2.3. Labelled 1H NMR spectra of $[(^{Me,Et}TC^{Ph})Pt](PF_6)_2$ and ^{13}C NMR highlight of Pt-NHC chemical shift.	24
Figure 3.1. X-ray crystal structure of $[(^{Me,Et}TC^{Ph})Fe(NCCH_3)_2](PF_6)_2$	30
Figure 3.2. ESI/MS of $[(^{Me,Et}TC^{Ph})Fe=N(p-CF_3-Ph)](PF_6)_2$	38
Figure 3.3. Diagram of organic azides that were prepared.	42
Figure 3.4. 1H NMR of 2,2,3,3-tetramethyl-1-(<i>p</i> -tolyl)aziridine in $CDCl_3$	53
Figure 3.5. ^{13}C NMR of 2,2,3,3-tetramethyl-1-(<i>p</i> -tolyl)aziridine in $CDCl_3$	54
Figure 4.1. X-ray crystal structure of $[(^{Me,Et}TC^{Ph})Ag]_2Ag_2](PF_6)_4$	61
Figure 4.2. Graphical representation of $[(^{Me,Et}TC^{Ph})Rh(I)_2]PF_6$	67
Figure 4.3. X-ray crystal structure of $[(^{Me,Et}TC^{Ph})Cr(Cl)_2](PF_6)$	68
Figure 5.1. Gade's classes of N_4 binding modes found in tetrazene ligands.	80
Figure 5.2. X-ray crystal structure of $[(^{Me,Et}TC^{Ph})Fe(ArN_4Ar)](PF_6)_2$	84
Figure 5.3. Mössbauer spectra of complexes $[(^{Me,Et}TC^{Ph})Fe(CH_3CN)_2](PF_6)_2$ and $[(^{Me,Et}TC^{Ph})Fe(ArN_4Ar)](PF_6)_2$	85

Figure 5.4. Modified proposed aziridination mechanism with catalyst

$[(^{Me,Et}TC^{Ph})Fe(CH_3CN)_2](PF_6)_2$86

Figure 5.5. Decomposition of $[(^{Me,Et}TC^{Ph})Fe(ArN_4Ar)](PF_6)_2$ as followed by 1H

NMR91

Figure 5.6. 1H NMR of the extracted organic products from the decomposition of

$[(^{Me,Et}TC^{Ph})Fe(ArN_4Ar)](PF_6)_2$ in the presence of excess cyclooctene.92

Figure 6.1. Contrasting Group 13 and 14 metal complexes.....96

Figure 6.2. X-ray crystal structure of $(^{BMe_2,Et}TC^H)SnBr_2$101

Figure 6.3. X-ray crystal structure of $(^{BMe_2,Et}TC^H)InBr$ and $(^{BMe_2,Et}TC^H)AlCl$103

Figure 6.4. Graphical representation of $(^{B(Me)_2,Et}TC^H)AlBr$ 110

Figure 6.5. NMR data for $(^{B(Me)_2,Et}TC^H)SnBr_2$111

LIST OF SCHEMES

Scheme 1.1. Cenini's catalytic aziridination.	2
Scheme 2.1. Synthesis of Macrocyclic Ligand Precursor.	13
Scheme 2.2. Synthesis of $[(^{\text{Me,Et}}\text{TC}^{\text{Ph}})\text{Pt}](\text{PF}_6)_2$	16
Scheme 3.1. Synthesis of $[(^{\text{Me,Et}}\text{TC}^{\text{Ph}})\text{Fe}(\text{NCCH}_3)_2](\text{PF}_6)_2$	28
Scheme 3.2. Sample catalytic aziridination reaction with $[(^{\text{Me,Et}}\text{TC}^{\text{Ph}})\text{Fe}(\text{NCCH}_3)_2](\text{PF}_6)_2$	31
Scheme 3.3. Proposed reaction mechanism for aziridination	37
Scheme 4.1. Synthesis of silver complexes from $(^{\text{Me,Et}}\text{TC}^{\text{Ph}})(\text{X})_4$	59
Scheme 4.2. Synthesis of metal complexes from $[(^{\text{Me,Et}}\text{TC}^{\text{Ph}})\text{Ag}]_2\text{Ag}_2(\text{X})_4$	62
Scheme 5.1. Synthesis of $[(^{\text{Me,Et}}\text{TC}^{\text{Ph}})\text{Fe}(\text{ArN}_4\text{Ar})](\text{PF}_6)_2$	81
Scheme 6.1. Synthesis of tetracarbene main group metal complexes.	98

Chapter 1

Introduction

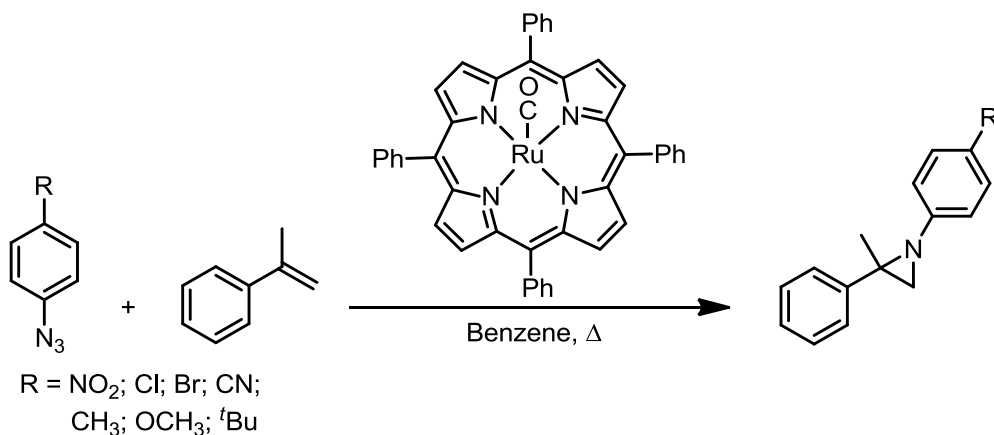
Aziridines are a significant functional group since they are the nitrogen analog of epoxides.¹ Epoxides have found themselves as important functional groups in many reactions such as polymerization.² However, aziridines have been an afterthought due to their limited and difficult means of synthesis.¹ The aziridine ring can be found in natural products, such as mitomycin C, that exhibit antitumor properties.³ More importantly these strained rings are capable of undergoing organic manipulations such as ring opening⁴ and ring expansion⁵ reactions. Aziridines could find an equally important place in chemistry as epoxides if there were an analogous catalytic manner to prepare this critical functional group in a manner similar to Jacobsen epoxidation.

A similar synthetic strategy to Jacobsen epoxidation for aziridines can be classified as a “C₂+N₁” aziridination strategy.¹ This strategy combines an alkene fragment and a nitrene source to form the aziridine ring. Several tosyl nitrene sources have been utilized in conjunction with a catalyst and alkenes to form aziridines in relatively high yield.⁶ Generally these tosyl nitrene sources have evolved from hypervalent PhI=NTs and chloroamine-T to tosyl azide.⁷ Although the byproducts of these reactions have improved from iodobenzene or NaCl to N₂, all the examples still leave a tosyl group on the nitrogen atom of the final aziridine product. The problem with this method is an additional step to deprotect the nitrogen is required and can often include reagents which can degrade the

aziridine ring.^{6b, 8} A more atom economical approach to this strategy is to perform the catalysis with a nitrene source which can place the final desired organic moiety on the aziridine nitrogen during the catalysis.

In an effort to propel catalytic aziridination forward, Cenini utilized a Ru-porphyrin catalyst in conjunction with *p*-nitrophenylazide and saturated alkenes to form aziridines.⁹ Later, Cenini found that utilizing the same catalyst with styrene derivatives as the alkene source allowed for electron donating aryl azides, such as *p*-methoxyphenylazide, were capable of forming aziridine products as well (Scheme 1.1).¹⁰ While this catalytic system is effective and leads to only N₂ as the side product, the starting reagents are either limited to a variety of aryl azides and styrene derivatives or to *p*-nitrophenylazide and the desired alkene.

Scheme 1.1. Cenini's catalytic aziridination.



In order to design a new catalyst capable of performing catalytic aziridination, the metal-nitrene intermediate should be taken into consideration.

Although in the case of Cenini's Ru-porphyrin catalyst the aziridination intermediate may follow several different reaction pathways, a Ru-imido is not thought to be the reaction intermediate. Yet the transfer of a nitrene from an imido complex is a possible target for a potential reaction intermediate. Upon examining isolated late transition metal imido complexes, it becomes apparent that strong σ -donor mono-, bi-, and tridentate ligands can be used to stabilize the metal ligand multiple bond (Figure 1.1A-C, respectively).¹¹ In one example by Peters, it is found that the iron trisphosphinoborate complex (Figure 1.1C) can even activate an organic azide, however, the resulting imido complex is too stable and therefore cannot transfer the imide to form an aziridine.^{11a} In another case by Hillhouse it was found that although the starting Ni-complex would not activate an organic azide, a Ni-imido could be prepared synthetically (Figure 1.1B) and the nitrene does transfer to an alkene to form an aziridine.^{11c} Still the lack of a system which can combine both the activation step and the transfer step is critical in order to make a complete catalytic cycle.

Transition metal imide complexes have been prepared with mono-, bi-, and tridentate strong σ -donor ligands,¹¹ yet no examples of strong σ -donor tetradentate ligands have been used to prepare metal imide complexes. This is particularly surprising given the tetradentate Ru-porphyrin complex has been the most successful aziridination catalyst to date. Group theory suggests a d^4 metal-imido complex with a bent square pyramidal geometry would be low spin and much more stable than the high spin alternative that would result from a weak

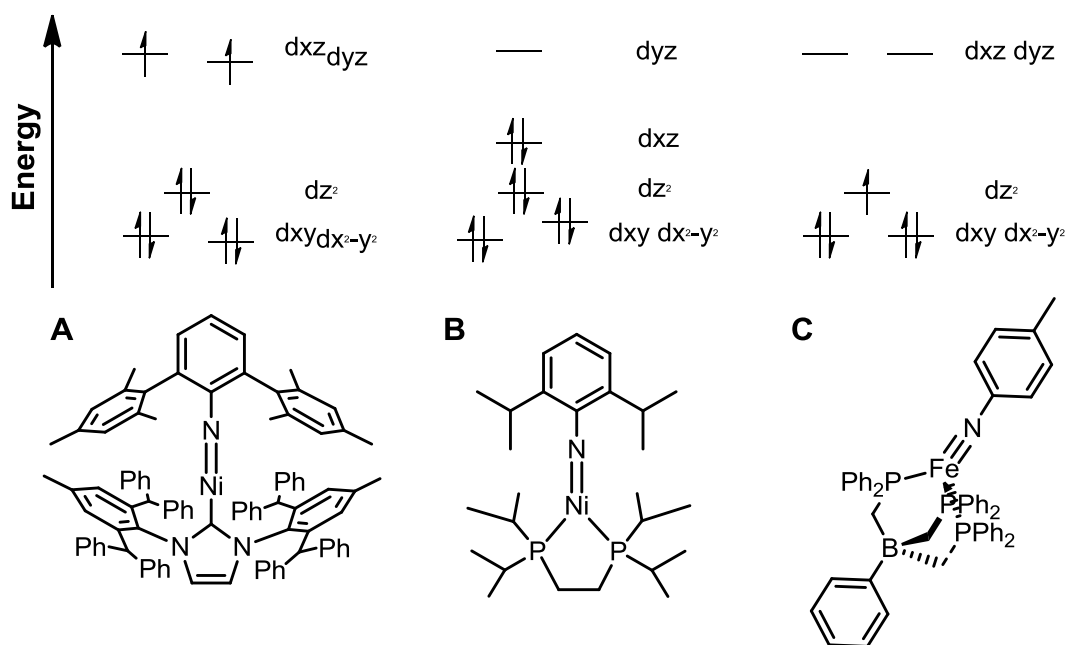


Figure 1.1. Isolated late transition metal imide complexes. Metal-imido bonds are stabilized by monodentate (A, Hillhouse), bidentate (B, Hillhouse), and tridentate (C, Peters) strong σ -donor ligands and respective orbital splitting diagram for each complex.

donor ligand (Figure 1.2). In order to achieve this desired geometry a strong donor macrocyclic ligand, similar to a porphyrin, would be highly desirable. Traditionally, phosphines have been the strong σ -donor ligand of choice, however, recently *N*-heterocyclic carbenes (NHCs) have been used as an alternative due to their decreased sensitivity toward oxygen.¹²

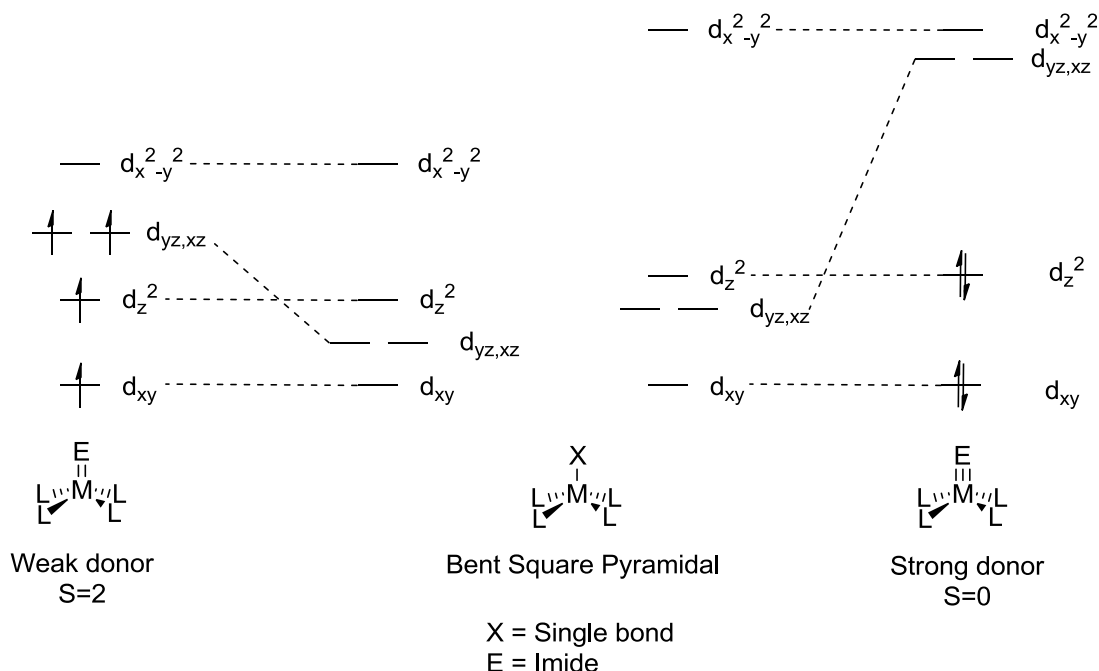


Figure 1.2. Group theory of a 5-coordinate d^4 bent square pyramidal metal complex. d-orbital splitting diagram shown with weak field donor ligands (left) and strong field donor ligands (right) with and without π -bonds.

Several NHC complexes have been prepared that have four NHCs in one plane around a central metal atom, yet these examples mostly consist of four monodentate-NHCs or two bis-bidentate NHC ligands.¹³ While these offer interesting insight, they are not macrocyclic ligands that would stay in one plane on all metal centers. Hahn, however, did prepare a 16-atom ringed macrocyclic tetra-NHC platinum complex (Figure 1.3A).¹⁴ Unfortunately the templating methodology employed to prepare the macrocyclic ligand cannot be transferred

to other no*N*-group 10 metals nor could the tetra-chelated ligand be removed for later use.

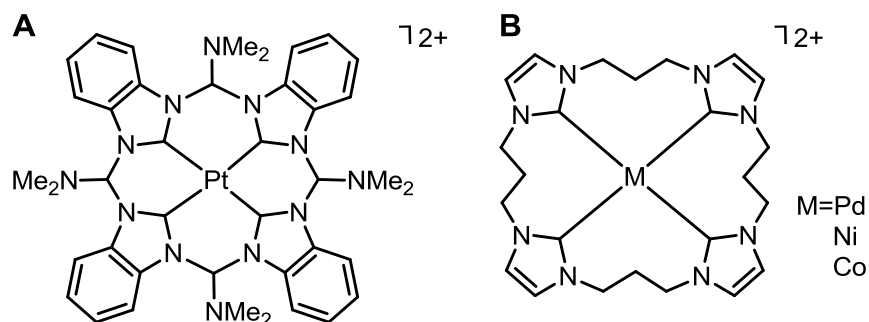


Figure 1.3. Mononuclear tetra-*N*-heterocyclic carbene complexes. Selected examples by Hahn (A) and Murphy (B).

In order to prepare a macrocyclic tetra-NHC which can be utilized to prepare a variety of metal complexes, a ligand precursor must be developed. Murphy achieved this goal with the preparation of a free tetra-imidazolium salt which could be later deprotonated to synthesize three mononuclear transition metal complexes on Pd, Ni, and Co (Figure 1.3B).¹⁵ The problem with this ligand was later found to be that the linkers were too bulky once ligated to a metal center. Large linkers, particularly for aziridination, would mean no metal site is open for catalytic transformations to occur. The other problem with the ligand is that due to the linker length the ligand is not forced to stay in the equatorial plane around the metal center which causes the geometry and therefore the control over the metal electronics to be lost.

The goal of my research is to develop a new 18-atom ringed tetraimidazolium ligand precursor. Utilizing this tetraimidazolium several mononuclear transition metal complexes should be synthesizable and have open metal sites for catalytic transformations to occur at. The metal complexes should then be screened for catalytic activity as well as attempt to isolate reactive reaction intermediates.

Chapter 2

Preparation of an 18-Atom Macrocyclic Tetra-Imidazolium as a Tetra *N*-Heterocyclic Carbene Ligand Precursor

A version of this chapter was originally published by Heather M. Bass, S. Alan Cramer, Julia L. Price, and David M. Jenkins:

Bass, H. M.; Cramer, S. A.; Price, J. L.; Jenkins, D. M. "18-Atom-Ringed Macrocyclic Tetraimidazoliums for Preparation of Monomeric Tetracarbene Complexes." *Organometallics* **2010**. 29, 3235-3238.

and by Chi-Linh Do-Thanh, Neelam Khanal, Zheng Lu, S. Alan Cramer, David M. Jenkins, and Michael D. Best:

Do-Thanh, C.; Khanal, N.; Lu, Z.; Cramer, S. A.; Jenkins, D. M.; Best, M. D. "Chloride Binding by a Polyimidazolium Macrocycle Detected via Fluorescence, NMR, and X-ray Crystallography." *Tetrahedron* **2011**. 133, 19342-19345.

All work presented in this chapter was altered from the original publication to only include work completed by S. Alan Cramer.

Abstract

An 18-atom ringed macrocyclic tetra-imidazolium ligand have been synthesized by a two-step procedure and is the smallest free tetra-imidazolium to date. The structure of the tetra-imidazolium was characterized by multi-nuclear NMR, high resolution ESI/MS, and single-crystal X-ray diffraction to distinguish it

from the potential di-imidazolium species. The tetra-imidazolium ligand forms a monomeric tetra-carbene complex with platinum through in situ deprotonation.

Introduction

The stabilization of complexes that contain metal-ligand multiple bonds, such as oxo and nitride ligands, is dependent on the symmetry and donor strength of the auxiliary ligands bound to the transition metal.¹⁶ Recent advancements in the preparation of iron oxos and nitrides for bioinorganic models of O₂ and N₂ activation have employed neutral tetra-dentate weak σ -donors, such as cyclam, as the auxiliary macrocyclic ligand.¹⁷ Current research on three-fold symmetry complexes of iron^{11a, 18} and cobalt¹⁹ has demonstrated that increasing the σ -donor strength of the auxiliary ligands stabilizes novel imidos and nitrides complexes. To our knowledge, few neutral tetra-dentate strong σ -donor ligands have been synthesized. In fact, few macrocyclic tetra-dentate phosphines have been prepared and isolated, due to their difficult syntheses, instability, and sensitivity to O₂.^{12a-c} Lately, *N*-heterocyclic carbenes (NHCs) have become a more attractive alternative to phosphines for many catalytic applications.²⁰ In addition to strong σ -donation, NHCs exhibit other beneficial properties, in particular their resistance to degradation in the presence of O₂.^{12d} This chapter presents an easy to synthesize strong σ -donor macrocyclic tetra-NHC that exclusively produces a mononuclear transition metal complex.

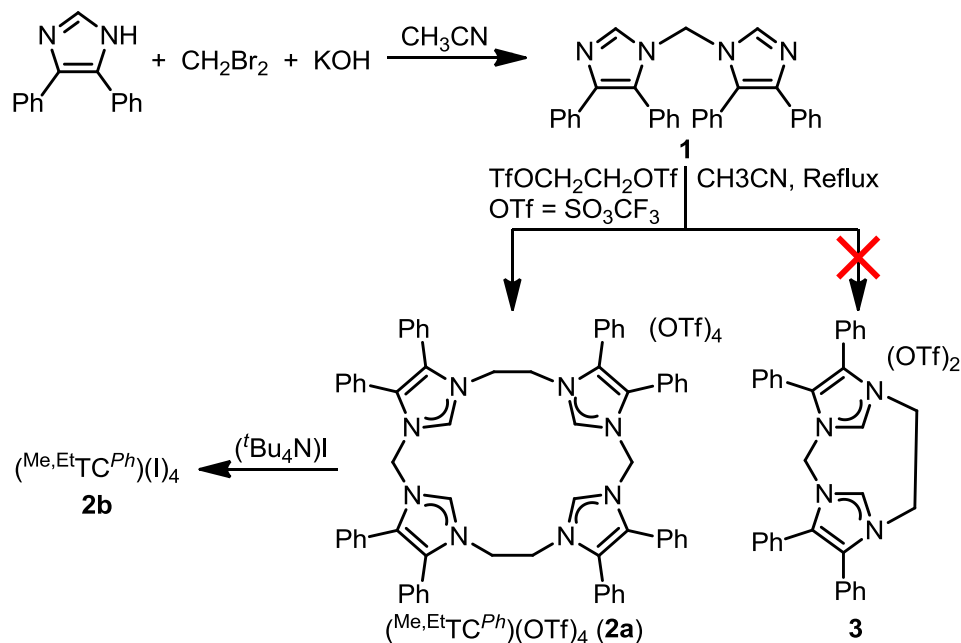
Recently synthesized tetra-*N*-heterocyclic carbene complexes include the classes of tetra-monodentate-carbenes, bis-bidentate-carbenes and macrocyclic tetradentate-carbenes.¹³ These tetra-carbene complexes have found potential applications as near UV-phosphorescent emitters,²¹ radiopharmaceuticals,²² and catalyst precursors.²³ Yet, of these tetra-NHCs, only three examples of monomeric macrocyclic tetra-carbene complexes have been prepared, and both synthetic approaches are somewhat limited in scope. Hahn's synthesis of the first macrocyclic tetra-carbene complex requires a templating reaction on platinum.¹⁴ In addition to requiring a tetra-isocyanide complex as a precursor to the monodentate carbene ligands, the synthesis also requires harsh reagents like phosgene. The other two examples have been prepared from a macrocyclic tetra-imidazolium ligand and, although a few macrocyclic tetra-imidazoliums have been synthesized,²⁴ only one of these species has been employed as a ligand for synthesizing tetra-carbene complexes. Murphy's group was able to prepare a 24-atom ringed tetra-imidazolium using 1,3-diiodopropane as the key dielectrophile for ring formation.^{15b} This tetra-carbene ligand is so large and flexible that some metal complexes are monomeric, such as palladium^{15b} and cobalt,^{15c} but others are dimeric, such as silver^{15b} and copper.^{15b} Since most NHC-carbene complexes are prepared from imidazoliums, this approach provides a wider-ranging scope than templating.

Synthesis and Characterization of Tetra-imidazolium Ligand

Precursor

We have synthesized an 18-atom ringed tetra-imidazolium macrocycle that should exclusively favor mononuclear and monomeric complexation. This imidazolium was synthesized in multi-gram quantities using a simple two-step process starting from commercially available imidazole and without the use of dilute solvent conditions (Scheme 2.1). We synthesized 1,1'-methylene-bis(4,5-diphenylimidazole) (**1**) in high yield by adding dibromomethane to a basic solution of 4,5-diphenylimidazole in acetonitrile (Scheme 1). Although previous syntheses of macrocyclic tetra-imidazolium species have employed dihaloalkanes or dihaloxylenes as the key dielectrophile for ring formation,^{24,15b} we were unsuccessful in our attempts at similar reactions to produce smaller-sized macrocycles with reagents such as diiodomethane and 1,2-diiodoethane. However, utilizing the stronger dielectrophile 1,2-bis-(trifoxy)ethane²⁵ allowed us to prepare the 18-atom ringed macrocyclic tetra-imidazolium, $(^{\text{Me,Et}}\text{TC}^{\text{Ph}})(\text{OTf})_4$ (**2a**) shown in Scheme 1, in greater than 15% yield and within three days. We were then able to exchange the counteranions from triflates to iodides by mixing **2a** with excess $(^n\text{Bu}_4\text{N})\text{I}$ in an acetonitrile solution to yield $(^{\text{Me,Et}}\text{TC}^{\text{Ph}})(\text{I})_4$ (**2b**).

Scheme 2.1. Synthesis of Macrocyclic Ligand Precursor.



One challenge in these syntheses is distinguishing between the diimidazolium species (**3**) shown in Scheme 1 and the desired macrocyclic species (**2a**) since they are often synthesized concurrently.^{24b,15b} ^1H and ^{13}C NMR for the white solids formed were consistent with imidazolium formation, and although this evidence was not sufficient to distinguish between **2a** and **3**,²⁶ high resolution ESI/MS conclusively confirmed the formation of **2a**, as opposed to **3**. The ESI/MS spectrum exhibited peaks at 369.8 and 1407.2 m/z that are associated with $\{(\text{Me,EtTC}^{\text{Ph}})(\text{OTf})\}^{3+}$ and $\{(\text{Me,EtTC}^{\text{Ph}})(\text{OTf})_3\}^+$, respectively, and are unique to **2a**. In addition, the peak at 629.2 m/z exhibited isotopomers that were $\frac{1}{2}$ of a mass unit apart, which is consistent with $\{(\text{Me,EtTC}^{\text{Ph}})(\text{OTf})_2\}^{2+}$ from **2a** and not with the 1+ ion of **3-OTf**. The ratio of the isotopomers at 629.1 m/z is

consistent with only **2a** and not a mixture of **2a** and **3**. Furthermore, no peak was found at 240.2 m/z which would match the 2+ ion of **3-2OTf**. Combined, these data demonstrate that only the macrocyclic 18-atom ring, **2a**, was isolated from the reaction.

Finally, to further characterize this new ligand we turned to X-ray crystallography. Single-crystals suitable for single-crystal X-ray diffraction of **2b** were obtained from slow evaporation of an acetonitrile solution. The X-ray crystal structure confirmed the formation of the desired macrocyclic tetraimidazolium (Figure 2.1). The structure of **2b** (Figure 2.1) shows two adjacent imidazolium rings are hydrogen bonding to an iodide above the plane of the macrocycle and the other 2 imidazoliums are hydrogen bonding to another iodide below the plane.

Synthesis and Characterization of a Platinum(II) Tetracarbene Complex

To test the ability of **2** to form monomeric metal complexes, we synthesized a platinum complex (Scheme 2.2). Bis-bidentate platinum^{21,22} and palladium²⁷ carbene complexes that are similar in size to **4** have been prepared previously via in situ deprotonation with a weak base from the free imidazolium ligands. Thallium(I) hexafluorophosphate was employed in the reaction to remove any iodide ions and prevent anion confusion during purification. Spectroscopic characterization of **4** was consistent with a tetra-carbene complex. The ESI/MS of **4** shows peaks at 576.2 and 1297.3 m/z that are associated with

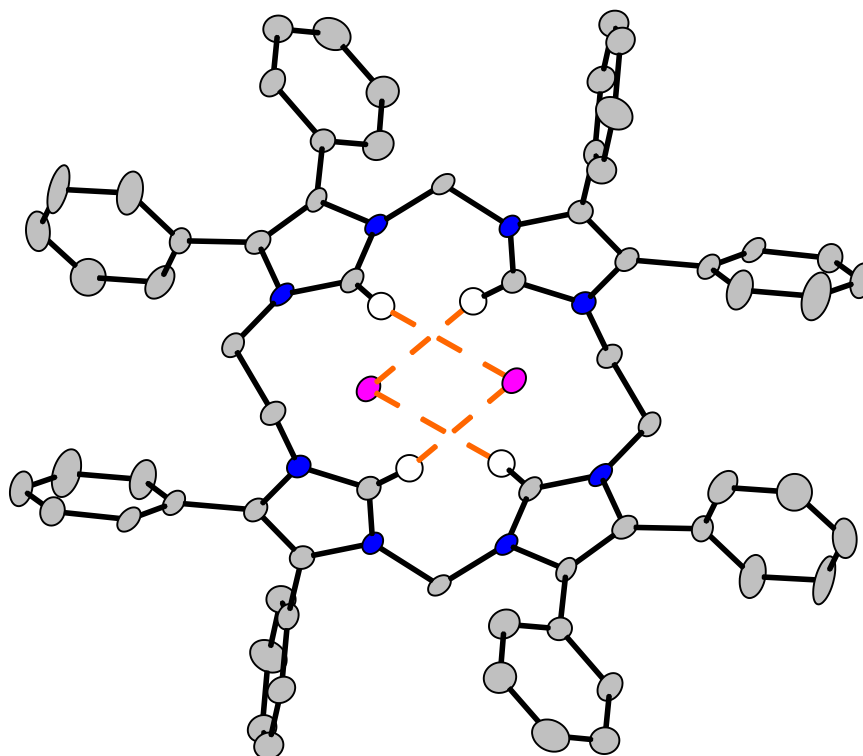
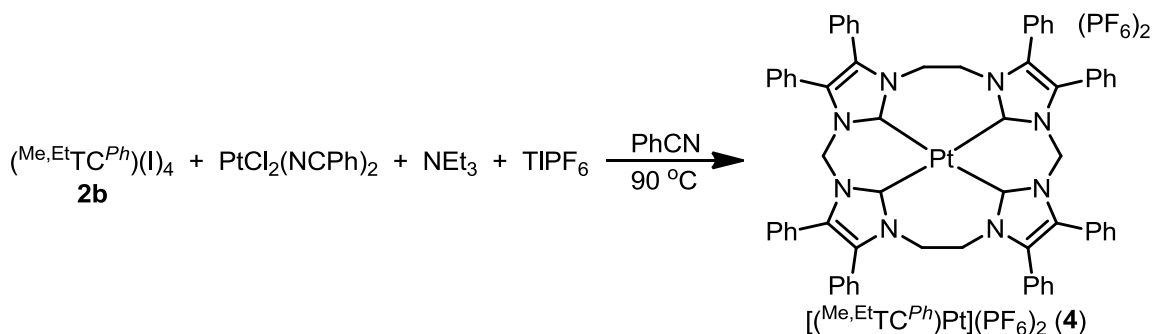


Figure 2.1. Crystal structure of $(^{\text{Me,Et}}\text{TC}^{\text{Ph}})(\text{I})_4$ (2b). Purple, blue, and grey ellipsoids (50% probability) represent I, N and C, respectively. White spheres represent H. Non-hydrogen bonding counteranions and hydrogens, and solvent molecules have been omitted for clarity.

$[(^{Me,Et}TC^{Ph})Pt]^{2+}$ and $\{[(^{Me,Et}TC^{Ph})Pt](PF_6)\}^+$, respectively. The geminal AB splitting pattern in the 1H NMR of the protons on the methylene position on **4** demonstrates the rigidity of the ligand in solution,^{21,27b} which is in direct contrast to Murphy's complex.^{15b} The ^{13}C NMR of **4a** is consistent with NHC formation with the carbene peak at 158 ppm, although the platinum satellites on the carbene carbon in the ^{13}C NMR could not be resolved.¹⁴ To confirm the conformation of **4**, a single-crystal was examined and a structure demonstrating connectivity of the macrocyclic ligand was obtained (Figure 2.2).

Scheme 2.2. Synthesis of $[(^{Me,Et}TC^{Ph})Pt](PF_6)_2$.



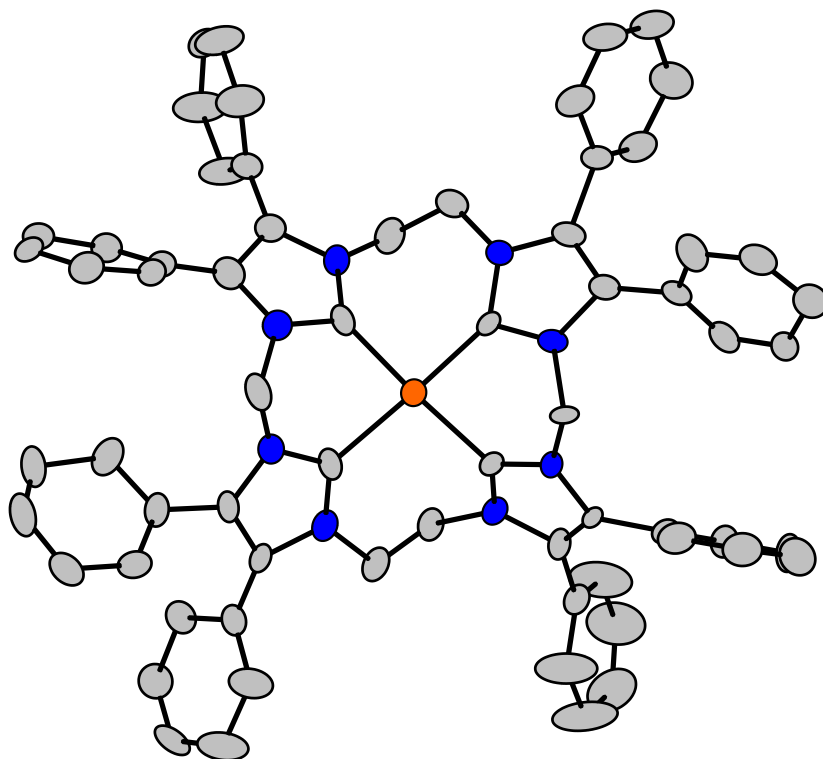


Figure 2.2. Crystal structure of $[(^{\text{Me,Et}}\text{TC}^{\text{Ph}})\text{Pt}](\text{PF}_6)_2$ (**4**). Orange, blue, and grey ellipsoids (50% probability) represent Pt, N and C, respectively. Counteranions, solvent molecules and hydrogens have been omitted for clarity.

Conclusion

In conclusion, we have demonstrated a facile, two step synthesis of an 18-atom ringed tetra-imidazolium ligand that employed 1,2-bis-(trifoxyl)ethane as the key dielectrophile. The ligand was prepared on a multi-gram scale quickly and cleanly without the use of dilute solvent conditions. This 18-atom ringed tetra-imidazolium (**2**) ligates to form a mononuclear transition metal complex (**4**).

Experimental

Syntheses of organic compounds were performed under normal atmospheric conditions. Syntheses of platinum complexes were performed under a dry nitrogen atmosphere with the use of either a dry box or standard Schlenk techniques. Solvents were dried on an Innovative Technologies (Newburgport, MA) Pure Solv MD-7 Solvent Purification System and degassed by three freeze-pump-thaw cycles on a Schlenk line to remove O₂ prior to use. DMSO-*d*₆, acetonitrile-*d*₃, and chloroform-*d* were degassed by three freeze-pump-thaw cycles prior to drying over activated molecular sieves. These NMR solvents were then stored under N₂ in a glovebox. The compound 1,2-diyl-bis(trifluoromethanesulfonate)ethane (also called 1,2-bis-(trifoxy)ethane)²⁵ was prepared as described previously. All other reagents were purchased from commercial vendors and used without purification. ¹H, ¹³C{¹H}, and ¹⁹F NMR spectra were recorded at ambient temperature on a Varian Mercury 300 MHz or a Varian INOVA 600 MHz narrow-bore broadband system. ¹H and ¹³C NMR chemical shifts were referenced to the residual solvent. ¹⁹F NMR chemical shifts are reported relative to an external standard of neat CFC_l₃. All mass spectrometry analyses were conducted at the Mass Spectrometry Center located in the Department of Chemistry at the University of Tennessee. The DART analyses were performed using a JEOL AccuTOF-D time-of-flight (TOF) mass spectrometer with a DART (direct analysis in real time) ionization source from JEOL USA, Inc. (Peabody, MA). The ESI/MS analyses were performed using a

QSTAR Elite quadrupole time-of-flight (QTOF) mass spectrometer with an electrospray ionization source from AB Sciex (Concord, Ontario, Canada). All mass spectrometry sample solutions were prepared in acetonitrile. Infrared spectra were collected on a Thermo Scientific Nicolet iS10 with a Smart iTR accessory for attenuated total reflectance. Carbon, hydrogen, and nitrogen analyses were obtained from Atlantic Microlab, Norcross, GA.

Synthesis of 1,1'-methylene-bis(4,5-diphenyl-imidazole), (1). 4,5-Diphenylimidazole (13.2 g, 0.0610 mol) and potassium hydroxide powder (5.0 g, 0.089 mol) were added to a 240-mL glass jar with a Teflon lid and dissolved with 100 mL of acetonitrile and stirred for 15 min. Dibromomethane (5.2 g, 0.030 mol) was then diluted with 3 mL of acetonitrile and this solution was slowly added to the glass jar. The reaction was then stirred for 72 h. After the reaction was complete, 16 mL of ice cold water were added to the mixture and stirred for an additional 15 min, which precipitated a white solid. The white solid was collected over a 150-mL medium sintered-glass frit and dried under reduced pressure to give the product (12 g, 89% yield). ^1H NMR (CDCl_3 , 300.1 MHz): δ 7.51 (m, 6H), 7.40 (dd, $J_1 = 7.8$ Hz, $J_2 = 1.8$ Hz, 4H), 7.19 (m, 10H), 6.77 (s, 2H), 5.73 (s, 2H). ^{13}C NMR (CDCl_3 , 75.46 MHz): δ 139.1, 136.7, 133.8, 131.1, 129.8, 129.7, 129.6, 128.3, 127.4, 126.9, 126.6, 53.1. IR (neat): 3059, 1600, 1500, 1442, 1357, 1304, 1231, 1193, 1072, 1017, 950, 922, 790, 774 cm^{-1} . DART MS (m/z): $[\text{M}-\text{H}]^+$

453.3. Anal. Calcd for $C_{31}H_{24}N_4$: C, 82.27; H, 5.35; N, 12.38. Found: C, 82.11; H, 5.21; N, 12.19.

Synthesis of 4,5,10,11,15,16,21,22-octaphenyl-3,9,14,20-tetraaza-1,6,12,17-tetraazoniapentacyclo-hexacosane-1(23),4,6(26),10,12(25),15,17(24),21-

octaene tetra-trifluoromethanesulfonate ((^{Me,Et}TC^{Ph})(OTf)₄), (2a). 1,1'-

Methylene-bis(4,5-diphenyl-imidazole) (**1**) (10.0 g, 0.0222 mol) was added to a 500-mL round-bottom flask, dissolved with acetonitrile (175 mL) and stirred for 20 min. 1,2-diyl-bis(trifluoromethanesulfonate)ethane (7.23 g, 0.0222 mol) was diluted with acetonitrile (5 mL) and pipetted into the round-bottom flask. The reaction mixture was heated to reflux for 72 h. After cooling to room temperature, a white solid was collected by slowly pouring the solution over a 150-mL medium sintered-glass frit a few mL at a time. Each aliquot was filtered through before adding the next one. This slow filtration yielded the product which was dried under reduced pressure (3.25 g, 18.9% yield). ¹H NMR (DMSO-*d*₆, 300.1 MHz): δ 10.02 (s, 4H), 7.46 (m, 16H), 7.29 (t, *J* = 7.2 Hz, 8H), 7.18 (d, *J* = 6.0 Hz, 8H), 7.00 (d, *J* = 6.9 Hz, 8H), 6.61 (s, 4H), 4.68 (s, 8H). ¹³C NMR (DMSO-*d*₆, 75.46 MHz): δ 136.8, 132.7, 132.3, 131.0, 130.7, 130.2, 129.4, 129.3, 123.2, 122.4, 120.6 (q, *J*_{F-C} = 322 Hz), 56.0, 46.8. ¹⁹F NMR (DMSO-*d*₆, 282.3 MHz): δ -77.8. IR (neat): 3145, 3067, 1560, 1445, 1372, 1336, 1278, 1254, 1241, 1226, 1177, 1027, 765 cm⁻¹. ESI MS (*m/z*): [M-OTf]⁺ 1407.2, [M-2OTf]²⁺

629.2, [M-3OTf]³⁺ 369.8. Anal. Calcd for C₇₀H₅₆F₁₂N₈O₁₂S₄: C, 53.98; H, 3.62; N, 7.19. Found: C, 53.84; H, 3.47; N, 7.37.

Synthesis of 4,5,10,11,15,16,21,22-octaphenyl-3,9,14,20-tetraaza-1,6,12,17-tetraazoniapentacyclo-hexacosane-1(23),4,6(26),10,12(25),15,17(24),21-octaene tetraiodide ((^{Me,Et}TC^{Ph})(I)₄), (2b). (^{Me,Et}TC^{Ph})(OTf)₄ (2a) (9.36 g, 0.00602 mol) was added as a solid to an acetonitrile (300 mL) solution of tetrabutylammonium iodide (8.89 g, 0.0241 mol) in a 500-mL Erlenmeyer flask. This mixture was stirred overnight and the white solid was collected on a 150-mL medium sintered-glass frit and dried under reduced pressure to yield the pure product (8.84 g, 93.7% yield). ¹H NMR (DMSO-*d*₆, 300.1 MHz): δ 10.65 (s, 4H), 7.59 (d, *J* = 6.6 Hz, 8H), 7.47 (m, 24 H), 7.21 (d, *J* = 7.5 Hz, 8H), 6.97 (s, 4H), 4.75 (s, 8H). ¹³C NMR (DMSO-*d*₆, 75.46 MHz): δ 136.0, 133.2, 132.2, 131.7, 131.5, 131.2, 131.1, 129.6, 129.5, 123.8, 123.4, 57.7, 46.5. IR (neat): 2964, 1561, 1488, 1446, 1373, 1252, 1215, 1030, 759 cm⁻¹. Anal. Calcd for C₆₆H₅₆I₄N₈: C, 53.97; H, 3.84; N, 7.63. Found: C, 52.33; H, 3.89; N, 7.26.

Synthesis of [(^{Me, Et}TC^{Ph})Pt](PF₆)₂, (4). (^{Me,Et}TC^{Ph})(I)₄ (2b) (0.153 g, 0.104 mmol) was dissolved in benzonitrile (10 mL) in a 20-mL vial. Dichlorobis(benzonitrile)platinum(II) (0.0492 g, 0.104 mmol) was dissolved in 2 mL of benzonitrile and was added to the (^{Me,Et}TC^{Ph})(I)₄ solution. Triethylamine (0.0528 g, 0.521 mmol) was then added to the reaction mixture. This solution

was heated to 90 °C and stirred for 24 h. After the reaction mixture was removed from the heat and allowed to cool to room temperature, thallium(I) hexafluorophosphate (0.219 g, 0.626 mmol) was dissolved in benzonitrile (2 mL), added to the reaction mixture, and stirred for 24 h. The reaction mixture was then filtered over Celite to remove thallium(I) iodide. Benzonitrile was then removed under reduced pressure to leave the crude solid. The crude solid was dissolved in acetone (5 mL) and filtered over Celite. The product was crystallized via vapor diffusion of ether into the acetone solution. The collected crystals were washed with methylene chloride (2 mL) and diethyl ether (3 x 10 mL) (0.010 g, 6.6% yield). ^1H NMR (DMSO- d_6 , 300.1 MHz): δ 7.45 (m, 16H), 7.39 (t, J = 7.9 Hz, 8H), 7.25 (t, J = 7.7 Hz, 8H), 7.13 (d, J = 7.1 Hz, 8H), 6.14 (d, J = 14.1 Hz, 2H), 5.72 (d, J = 14.2 Hz, 2H), 4.79 (m, 4H), 4.5 (m, 4H). ^{13}C NMR (DMSO- d_6 , 150.9 MHz): δ 158.8, 132.2, 131.1, 130.9, 130.2, 129.8, 129.7, 128.9, 128.8, 126.0, 125.3, 58.1, 46.8. ^{19}F NMR (DMSO- d_6 , 282.3 MHz): δ -70.1 (d, J = 711 Hz). IR (neat): 1489, 1467, 1404, 1369, 1235, 828, 786, 766, 735 cm^{-1} . ESI MS (m/z): $[\text{M-PF}_6]^+$ 1297.34, $[\text{M-2PF}_6]^{2+}$ 576.19. Anal. Calcd for $\text{C}_{66}\text{H}_{52}\text{F}_{12}\text{N}_8\text{P}_2\text{Pt}$: C, 54.97; H, 3.63; N, 7.77. Found: C, 54.69; H, 3.54; N, 7.79.

X-ray Structure Determinations. X-ray diffraction measurements were performed on single-crystals coated with Paratone oil and mounted on Kapton loops. Each crystal was frozen under a stream of N_2 while data were collected on a Bruker APEX diffractometer. A matrix scan using at least 20 centered

reflections was used to determine initial lattice parameters. Reflections were merged and corrected for Lorentz and polarization effects, scan speed, and background using SAINT 4.05. Absorption corrections, including odd and even ordered spherical harmonics were performed using SADABS. Space group assignments were based upon systematic absences, *E* statistics, and successful refinement of the structure. The structure was solved by Patterson maps with the aid of successive difference Fourier maps, and was refined against all data using the SHELXTL 5.0 software package. The structure of **4** was solved in the space group Cc. The crystal suffered from twinning, which led to a lower quality structure. Despite repeated attempts with different solvent combinations, we were unable to grow crystals that did not exhibit twinning. The carbon, nitrogen, platinum and phosphorous atoms were refined anisotropically, while the disordered fluorine atoms were refined isotropically. Three of the fluorine atoms (F4, F7, and F11) were split equally over two positions to improve the electron density model of the PF₆'s. The solvent molecules in the unit cell were modeled as ethers. They are disordered and were refined isotropically.

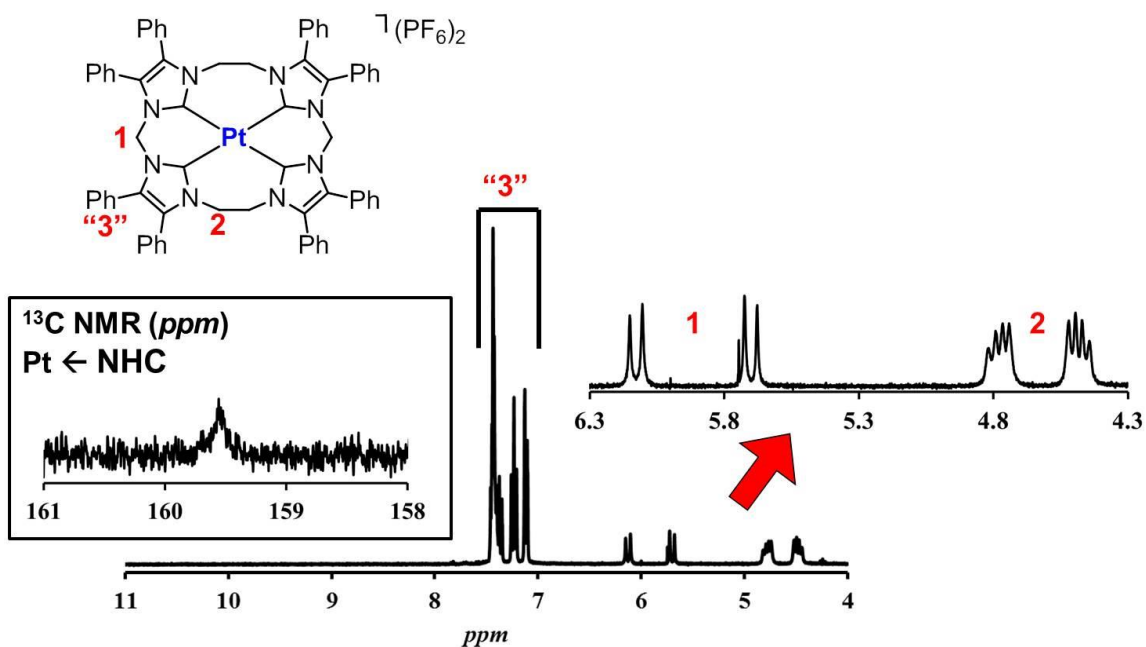


Figure 2.3. Labelled 1H NMR spectra of $[(^{Me, Et}TC^{Ph})Pt](PF_6)_2$ and ^{13}C NMR highlight of Pt-NHC chemical shift.

Chapter 3

Synthesis of Aziridines from Alkenes and Aryl Azides with a Reusable Macrocyclic Tetracarbene Iron Catalyst

A version of this chapter was originally published by S. Alan Cramer and David M. Jenkins:

Cramer, S. A.; Jenkins, D. M. "Synthesis of Aziridines from Alkenes and Aryl Azides with a Reusable Macrocyclic Tetracarbene Iron Catalyst." *J. Am. Chem. Soc.* **2011**. 133, 19342-19345.

Abstract

A new iron aziridination catalyst supported by a macrocyclic tetra-carbene ligand has been synthesized. The catalyst, $[(^{\text{Me,Et}}\text{TC}^{\text{Ph}})\text{Fe}(\text{NCCH}_3)_2](\text{PF}_6)_2$, was synthesized from the tetra-imidazolium precursor $(^{\text{Me,Et}}\text{TC}^{\text{Ph}})(\text{I})_4$ and was characterized by NMR spectroscopy, ESI mass spectrometry, and single-crystal X-ray diffraction. This iron complex catalyzes the aziridination of a wide array of functionalized aryl azides and a variety of substituted aliphatic alkenes, including tetra-substituted, in a "C₂ + N₁" addition reaction. Finally, the catalyst can be recovered and re-used up to three additional times without significant reduction in yield.

Introduction

Despite the successful development of catalytic epoxidation from alkenes over the last thirty years, the nitrogen analog, catalytic aziridination, has languished behind.¹ Part of the reason is the lack of nitrogenous variants of peroxides or dioxygen which are used to form epoxides in conjunction with

alkenes.²⁸ Since the aziridine functional group is found in natural products²⁹ and also is used in pharmaceuticals, broadening the scope of the aziridination reaction is significant.³⁰ Today, “C₂ + N₁” aziridination reactions that combine an alkene and a nitrene fragment typically use iodoimine reagents, such as PhI=NTs (Ts = tosylate),^{1, 28, 31} chloramine-T,³² or tosylazide,³³ as the nitrene reagent. The disadvantage of these reactions is that the tosyl group must be removed before the desired final substituent can be placed on the ring which reduces atom economy and can lead to ring degradation.¹

An alternative to these current nitrene reagents is organic azides. Aryl azides can be easily synthesized in one step from amines³⁴ and are tolerant of a wide variety of functional groups.³⁵ Finally, since the correct functionality on the organic azide can be installed prior to catalysis, using organic azides instead of PhI=NTs will improve the atom economy of these reactions, thereby eliminating the step of removing the tosylate group before installing the desired moiety on the nitrogen atom.³⁶ A catalytic “C₂ + N₁” aziridination that is successful with a wide variety of substrates, both for alkenes and organic azides, would be a significant advance in chemical synthesis.

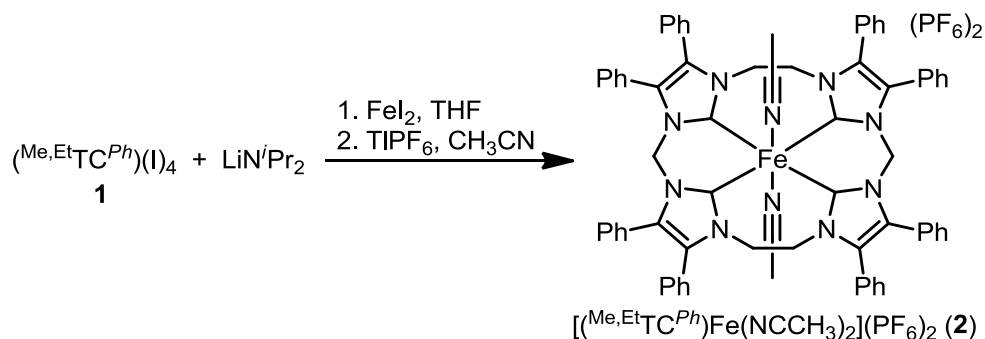
A very limited number of catalytic ruthenium and iron porphyrin systems have been developed that perform a “C₂ + N₁” aziridination with organic azides, but they are limited to strongly electron withdrawing aryl azides (such as *p*-nitro-phenylazide)^{10b, 37} and/or styrene derivatives for the alkene.^{10a} This chapter presents a new tetra-carbene iron(II) complex that acts as a catalyst for

aziridination with electron donating and withdrawing aryl azides and a variety of substituted aliphatic alkenes. In addition, the catalyst is robust and can be recovered and re-used for multiple aziridination runs.

Synthesis and Characterization of an Iron(II) Tetracarbene

Complex

Scheme 3.1. Synthesis of $[(^{\text{Me,Et}}\text{TC}^{\text{Ph}})\text{Fe}(\text{NCCH}_3)_2](\text{PF}_6)_2$.



We have previously reported the synthesis of the macrocyclic tetraimidazolium $(^{\text{Me,Et}}\text{TC}^{\text{Ph}})(\text{I})_4$, **1**, which can be deprotonated in the presence of divalent transition metals such as Pt to prepare tetra-carbene complexes.³⁸ Unlike our previously reported platinum complex, $[(^{\text{Me,Et}}\text{TC}^{\text{Ph}})\text{Pt}](\text{PF}_6)_2$,³⁸ an iron complex could not be prepared via deprotonation with a weak base. However, an *in situ* carbene strategy proved successful in ligating the macrocyclic carbene to the iron center (Scheme 3.1).^{13, 39} Lithium di-isopropylamide deprotonates $(^{\text{Me,Et}}\text{TC}^{\text{Ph}})(\text{I})_4$, **1**, at room temperature in THF in five minutes. Addition of a THF

solution of iron(II) iodide to this mixture followed by the addition of thallium hexafluorophosphate in acetonitrile gives the octahedral complex $[(^{\text{Me,Et}}\text{TC}^{\text{Ph}})\text{Fe}(\text{NCCH}_3)_2](\text{PF}_6)_2$, **2**. Complex **2** constitutes a tetra-carbene iron complex with easily accessible coordination sites for catalytic reactions.⁴⁰

Spectroscopic characterization of **2** is consistent with a tetra-carbene complex. The ESI/MS of **2** shows peaks at 506.2 *m/z*, associated with $[(^{\text{Me,Et}}\text{TC}^{\text{Ph}})\text{Fe}]^{2+}$, and at 1157.3 *m/z*, associated with $\{[(^{\text{Me,Et}}\text{TC}^{\text{Ph}})\text{Fe}](\text{PF}_6)\}^+$ with the correct isotopic ratios. ¹H NMR demonstrates that the acetonitrile ligands on **2** exchange in CD₃CN solution since **2** which has been crystallized from CH₃CN solution (see below) shows peaks only for unbound acetonitrile. ¹³C NMR shows a resonance for the carbene carbon at 196.65 ppm which is consistent with other Fe^{II} NHC-carbene complexes.⁴¹ In addition, complex **2** is air stable in the solid state.

The X-ray crystal structure of **2** shows that the acetonitrile ligands are bound in the solid state (Figure 3.1) giving an octahedral complex. The average Fe-C bond distance is 2.01 Å which is slightly longer than the only other Fe^{II} tetra-carbene which has been previously reported (1.96 Å).⁴⁰ The *trans* C-Fe-C angles are 169.7 and 172.2 degrees which demonstrates that there is only a minimal distortion about the equatorial plane formed by the macrocycle. Unlike four-coordinate Co and Ni complexes which have a 24-atom ringed macrocyclic tetra-carbene ligand,¹⁵ **2** has space for apical ligands to bind to the metal center.

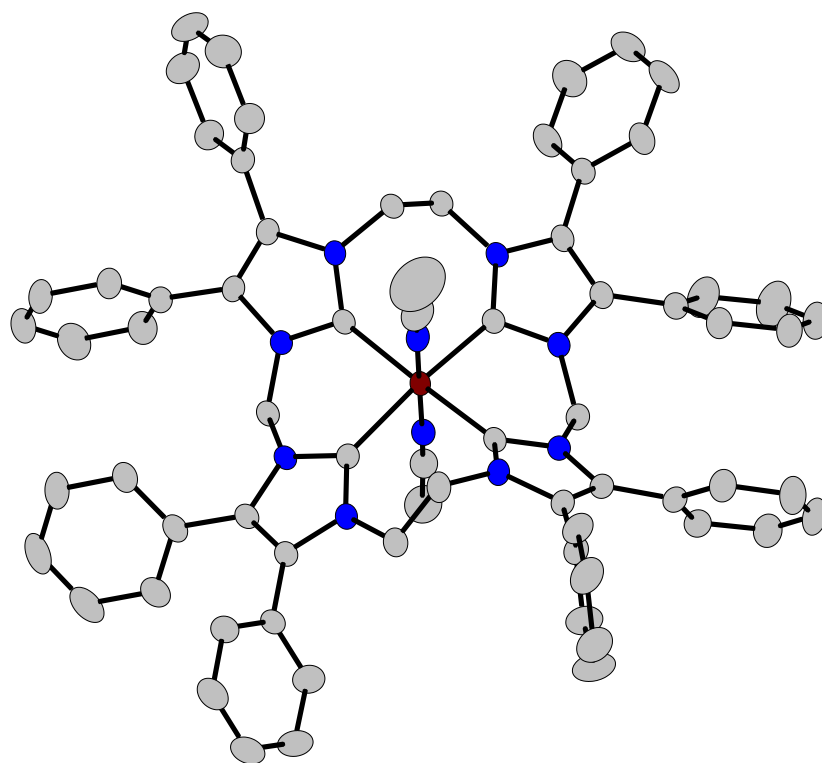


Figure 3.1. X-ray crystal structure of $[(^{\text{Me,Et}}\text{TC}^{\text{Ph}})\text{Fe}(\text{NCCH}_3)_2](\text{PF}_6)_2$, (2). Red, blue and grey ellipsoids (50% probability) represent Fe, N, and C, respectively. Counteranions, solvent molecules and hydrogens have been omitted for clarity.

Catalytic Aziridination with Aryl Azides and Aliphatic Alkenes

To determine the best catalytic reaction conditions for aziridination with an electron donating aryl azide, a series of test reactions were run with *p*-tolyl-azide, 1-decene and **2**. The best results were obtained by using 0.1 mol% catalyst loading of **2** with 29-fold excess of alkene and no additional solvent (Scheme 3.2). After 18 hours at 90 °C the reaction was complete (all organic azide had reacted) and the reaction mixture was cooled to room temperature and the catalyst was removed by filtration over Celite. Removal of the remaining organics under reduced pressure followed by column chromatography yielded pure 2-octyl-(*p*-tolyl)-aziridine in 70% isolated yield (Table 3.1, Entry 1). The identity of the product was determined by ¹H and ¹³C NMR spectroscopy, GC/MS, and HR MS. Increasing the catalyst loading to 1% (Table 3.1, Entry 2) improved the isolated yield to 82%. One advantage of this methodology is the ease of catalyst separation from the product since **2** is insoluble in the reaction mixture at room temperature.

To test the effectiveness of the catalytic system, additional azides and alkenes were evaluated (Table 3.1). The catalyst successfully performed aziridination with electron withdrawing azides, such as 1-azido-4-(trifluoromethyl)benzene (Table 3.1, Entry 3), and 1-decene with a slightly higher yield compared to previously reported Ru-porphyrin systems.^{37a} Di-substituted alkenes, including *cis* and *trans* substituted examples were both successful

Scheme 3.2. Sample catalytic aziridination reaction with $[(^{\text{Me,Et}}\text{TC}^{\text{Ph}})\text{Fe}(\text{NCCH}_3)_2](\text{PF}_6)_2$.

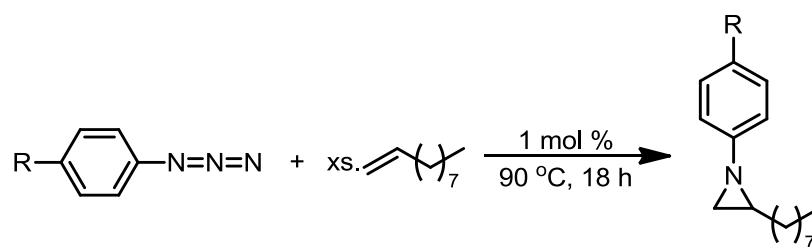


Table 3.1. Aziridination reactions with $[(^{\text{Me,Et}}\text{TC}^{\text{Ph}})\text{Fe}(\text{NCCH}_3)_2](\text{PF}_6)_2$.

Entry	Alkene	Azide R-group	Catalyst Loading	Temp (°C)	Time (h)	Aziridine	Yield ^a
1	1-decene	-CH ₃	0.1%	90	18		70% ^b
2	1-decene	-CH ₃	1%	90	18		82% ^b
3	1-octene	-CF ₃	0.1%	90	18		37% ^b
4	<i>cis</i> -cyclo-octene	-CH ₃	0.1%	90	12		97%
5	<i>trans</i> -4-octene	-CH ₃	1%	90	144		30% ^b
6	1-methyl-cyclo-hexene	-CH ₃	1%	90	144		39% ^b
7	2,3-dimethyl-2-butene	-CH ₃	0.1%	70	160		20% ^b

^a all reported yields are isolated yields. ^b required chromatography.

(Table 3.1, Entries 4 and 5 respectively). The yield for 9-(*p*-tolyl)-9-azabicyclo-[6.1.0]nonane (Table 3.1, Entry 4) was almost quantitative (97% yield) with just 0.1% catalyst loading. The reaction with *trans*-4-octene (Table 3.1, Entry 5) was much slower and lower yielding, probably due to the steric bulk of the propyl groups. Furthermore, tri- and tetra-substituted alkenes, such as 2,3-dimethyl-2-butene, were successful (Table 3.1, Entries 6 and 7). The reaction with 2,3-dimethyl-2-butene was run at 70° due to its lower boiling point which may have contributed to the lower yield. In contrast, Gallo's group reported the tri-substituted alkenes did not react with aryl azides and a Ru porphyrin catalyst.^{10a} Likewise, previous examples of similar tetra-substituted aziridines have only been prepared by photolysis of electron-withdrawing organic azides to make the free nitrene prior to reaction with alkene.⁴² In these two cases (Table 3.1, Entries 5 and 6), we have catalyzed the first example of a "C₂ + N₁" aziridination between those classes of alkene and an aryl azide.

In order to expand upon this catalytic system the functional group tolerance of **2** needed to be determined. A "C₂+N₁" aziridination catalyst has yet to effectively yield aziridines with a wide range of functional groups and non-conjugated alkene. Following the same approach as seen in Scheme 3.2, 1-decene and 13 additional functional groups (in the para-position with respect to the azide) were screened with **2** at 0.1% catalyst loading (Table 3.2). In direct contrast to work published by Cenini^{37a} with a Ru-porphyrin catalyst electron donating aryl azides were determined to be higher yielding than electron

withdrawing examples. The chloro, dimethylamine, methoxy, and bromo examples (Table 3.2, Entry 1-4, respectively) were all comparable to the previously discussed electron donating *p*-tolyl-azide. An alkynyl variant gave a moderate 57.9% yield (Table 3.2, Entry 5). The next 6 examples were all electron withdrawing groups which gave relatively similar moderately low yields (Table 3.2, Entry 6-11) but includes synthetically valuable examples such as the boronic ester which can potentially be manipulated in Pd-catalyzed cross coupling reactions (Table 3.2, Entry 8). Unfortunately, protic examples do not exhibit the formation of aziridine product (Table 3.2, Entry 12 and 13).

Since the catalyst, **2**, is insoluble in the reaction mixture at room temperature, we believed that it could be recovered and re-used once the catalysis was complete. Since the reactions with *cis*-cyclooctene (Table 3.1, Entry 4) gave the best yields with low catalyst loading, we repeated the reaction three times with the same batch of catalyst. The results demonstrate the catalyst is reusable for this reaction with only a negligible decrease in yield by the fourth run (Table 3.2). In addition to improving the atom economy of the reaction by using aryl azides, the ability to re-use the catalyst without significant loss of yield is quite beneficial.

Based on previously studied aziridination reactions with aryl azides a potential intermediate in this reaction mechanism is an iron(IV) imide, **3** (Scheme 3.3).³¹ Three-fold symmetric strong σ -donor ligands have been demonstrated to stabilize iron imides in the 2+,⁴³ 3+,^{11a, 44} and 4+⁴⁵ oxidation states, but these

complexes do not react with alkenes to give aziridines. While we have not been able to isolate $[(^{\text{Me,Et}}\text{TC}^{\text{Ph}})\text{Fe}=\text{NAr}](\text{PF}_6)_2$, **3**, ESI/MS data is consistent with its formation. Addition of 1-azido-4-(trifluoromethyl)benzene to a solution of **2** at room temperature in acetonitrile gives an ESI/MS with a peak at 585.7 m/z , associated with $[(^{\text{Me,Et}}\text{TC}^{\text{Ph}})\text{Fe}=\text{N}(p\text{-CF}_3\text{-Ph})]^{2+}$ (Figure 3.2).

Table 3.2. Aziridination of functionalized aryl azides and 1-decene with $[(^{\text{Me,Et}}\text{TC}^{\text{Ph}})\text{Fe}(\text{NCCH}_3)_2](\text{PF}_6)_2$.

Entry	Azide R-group	Cat. Loading	Temp. (°C)	Time (h)	Yield ^a
1	-Cl	0.1%	90	18	70.8
2	-N(CH ₃) ₂	0.1%	90	18	68.1
3	-OCH ₃	0.1%	90	18	65.3
4	-Br	0.1%	90	18	62.0
5	-CCH	0.1%	90	18	57.9
6	-CHO	0.1%	90	18	42.1
7	-OAc	0.1%	90	18	41.3
8	-B(pin)	0.1%	90	18	40.3
9	-COOCH ₃	0.1%	90	18	40.1
10	-CN	0.1%	90	18	37.6
11	-NO ₂	0.1%	90	18	33.3
12	-OH	0.1%	90	18	---
13	-COOH	0.1%	90	18	---

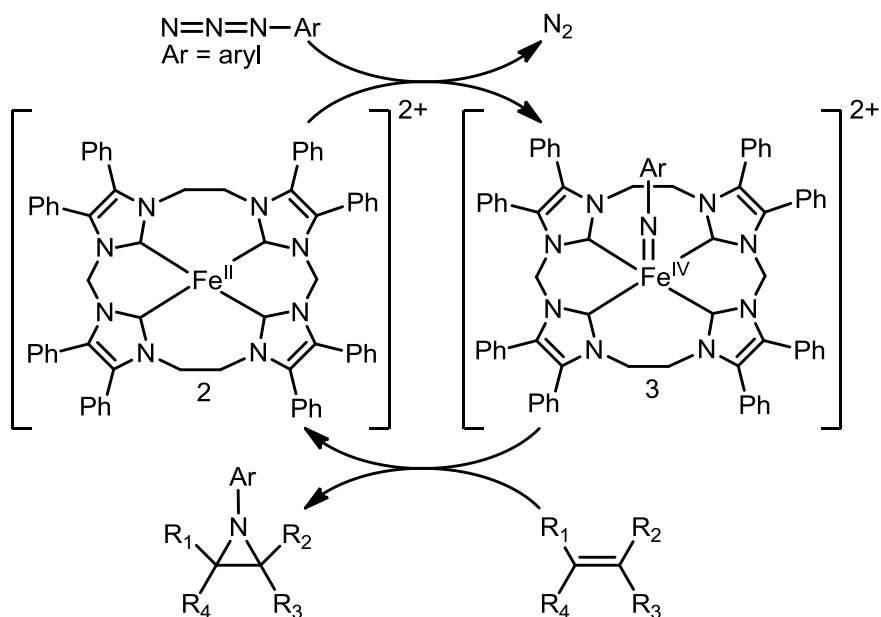
^a all reported yields are isolated yields.

Table 3.3. Aziridination reaction re-using $[(^{Me,Et}TC^{Ph})Fe(NCCH_3)_2](PF_6)_2$ with *cis*-cyclooctene.

Run	Azide	Catalyst Loading	Temp (°C)	Time (h)	Aziridine	Yield ^a
1	<i>p</i> -tolyl azide	0.1%	90	12	See Table 1, Entry 4	97%
2	<i>p</i> -tolyl azide	0.1%	90	12	See Table 1, Entry 4	95%
3	<i>p</i> -tolyl azide	0.1%	90	12	See Table 1, Entry 4	97%
4	<i>p</i> -tolyl azide	0.1%	90	12	See Table 1, Entry 4	89%

^aall reported yields are isolated yields.

Scheme 3.3. Proposed reaction mechanism for aziridination



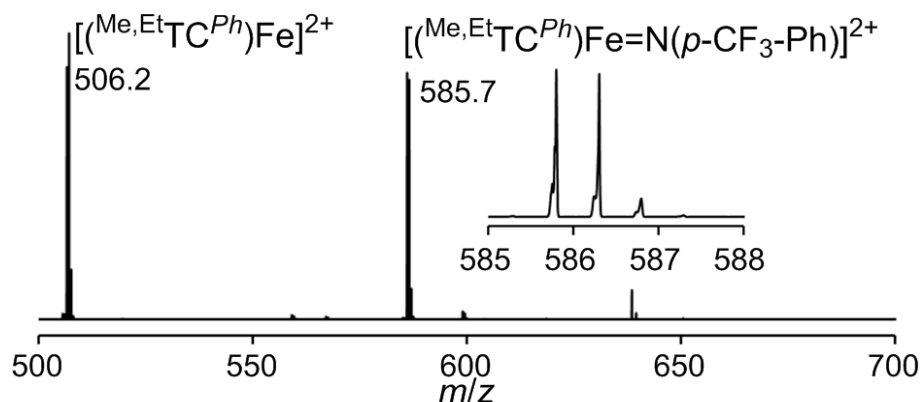


Figure 3.2. ESI/MS of $[(^{\text{Me,Et}}\text{TC}^{\text{Ph}})\text{Fe}=\text{N}(p\text{-CF}_3\text{-Ph})](\text{PF}_6)_2$. The inset shows the highlight for the $[(^{\text{Me,Et}}\text{TC}^{\text{Ph}})\text{Fe}=\text{N}(p\text{-CF}_3\text{-Ph})]^{2+}$ ion.

Conclusion

In conclusion, we have synthesized a new iron aziridination catalyst supported by a macrocyclic tetra-carbene ligand. This tetra-carbene iron complex, $[(^{\text{Me,Et}}\text{TC}^{\text{Ph}})\text{Fe}(\text{NCCH}_3)_2](\text{PF}_6)_2$, was synthesized from the tetra-imidazolium precursor $(^{\text{Me,Et}}\text{TC}^{\text{Ph}})(\text{I})_4$ and characterized by spectroscopy and single-crystal X-ray diffraction. This catalyst reacts with aryl azides and a wide variety of substituted aliphatic alkenes to give aziridines in a “ $\text{C}_2 + \text{N}_1$ ” addition reaction. We were able to form 9-(*p*-tolyl)-9-azabicyclo-[6.1.0]nonane in nearly quantitative yield from *cis*-cyclooctene and tolyl-azide. In addition, we were able to synthesize aziridines with 2,3-dimethyl-butene, a tetra-substituted alkene. These aliphatic alkenes are generally considered more challenging reagents than styrene variants which have been previously studied. Furthermore, the catalyst

can be recovered and re-used up to three additional times with only a nominal reduction in yield. To investigate the potential intermediate in the reaction, mass spectrometry data was collected and is consistent with an Fe(IV) imide. These results showcase a more direct approach to the formation of aziridines from readily available substrates while improving atom economy.

Experimental

All reactions were performed under a dry nitrogen atmosphere with the use of either a drybox or standard Schlenk techniques. Solvents were dried on an Innovative Technologies (Newburgport, MA) Pure Solv MD-7 Solvent Purification System and degassed by three freeze pump-thaw cycles on a Schlenk line to remove O₂ prior to use. DMSO-*d*₆, acetonitrile-*d*₃, benzene-*d*₆, and chloroform-*d* were degassed by three freeze-pump-thaw cycles prior to drying over activated molecular sieves. These NMR solvents were then stored under N₂ in a glovebox. The compound (^{Me,Et}TC^{Ph})(I)₄³⁸ was prepared as described previously. All other reagents except variants of **3** were purchased from commercial vendors and used without purification. ¹H, ¹³C{¹H}, and ¹⁹F NMR spectra were recorded at ambient temperature on a Varian Mercury 300 MHz or a Varian VNMRs 500 MHz narrow-bore broadband system. ¹H and ¹³C NMR chemical shifts were referenced to the residual solvent. ¹⁹F NMR chemical shifts are reported relative to an external standard of neat CFCI₃. All mass spectrometry analyses were conducted at the Mass Spectrometry Center located in the Department of Chemistry at the University of Tennessee. The DART analyses were performed

using a JEOL AccuTOF-D time-of-flight (TOF) mass spectrometer with a DART (direct analysis in real time) ionization source from JEOL USA, Inc. (Peabody, MA). The ESI/MS analyses were performed using a QSTAR Elite quadrupole time-of-flight (QTOF) mass spectrometer with an electrospray ionization source from AB Sciex (Concord, Ontario, Canada). The GC/MS analyses were performed using a Hewlett-Packard 6890 gas chromatography system with Hewlett-Packard 5973 mass spectrometer. Mass spectrometry sample solutions of metal complexes were prepared in acetonitrile. Mass spectrometry sample solutions of organic compounds from catalysis reactions were prepared in hexanes. Infrared spectra were collected on a Thermo Scientific Nicolet iS10 with a Smart iTR accessory for attenuated total reflectance. UV-vis measurements were taken inside a dry glovebox on an Ocean Optics USB4000 UV-vis system with 1 cm path length quartz crystal cell. Cyclic voltammetry measurements were made inside a dry glovebox using a BAS Epsilon electrochemical analyzer with a platinum working electrode, platinum wire counter electrode, and Ag/AgNO₃ reference electrode. All potentials were measured versus an external standard of ferrocene. Carbon, hydrogen, and nitrogen analyses were obtained from Atlantic Microlab, Norcross, GA.

Synthesis of [(^{Me,Et}TC^{Ph})Fe(NCCH₃)₂](PF₆)₂, 2. (^{Me,Et}TC^{Ph})(I)₄ (**1**) (2.570 g, 1.750 mmol) was added to tetrahydrofuran (20 mL) in a 100-mL round-bottom flask and stirred for 10 min. Lithium di-isopropyl amide (0.562 g, 5.25 mmol) was dissolved

in 5 mL of tetrahydrofuran and was added to the stirring ($^{\text{Me,Et}}\text{TC}^{\text{Ph}}\text{)(I)}_4$ mixture. After 3 min, iron(II) iodide (0.542 g, 1.75 mmol) which had been previously dissolved in tetrahydrofuran (20 mL) was added to the reaction mixture. After 10 min, additional solid lithium di-isopropyl amide (0.188g, 1.75 mmol) was added to the reaction mixture and the mixture was allowed to stir for 24 h. All volatiles were removed under reduced pressure and diethyl ether (50 mL) was added to the crude solid and the ether mixture was stirred for 4 h. The slurry was then filtered over Celite and the filtered ether solution was discarded. The remaining solid in the flask was dissolved in methylene chloride (20 mL) and added to the top of the Celite filter flask and the solution was collected and the methylene chloride removed under reduced pressure. The resulting solid was dissolved in acetonitrile (50 mL) and thallium(I) hexafluorophosphate (1.223 g, 3.500 mmol) was added to the solution and allowed to stir for 4 h. The subsequent mixture was then filtered over Celite to remove thallium iodide and the collected acetonitrile solution was reduced in volume to 1 mL. The pure product was crystallized via vapor diffusion of diethyl ether into the acetonitrile solution and the bright red crystals were collected after 5 d (0.279 g, 11.5% yield). ^1H NMR (CD_3CN , 499.74 MHz): δ 7.41 (m, 8H), 7.33 (m, 16H), 7.21 (t, J = 8.0 Hz, 8H), 7.12 (d, J = 7.0 Hz, 8H), 5.96 (s, 4H), 4.44 (s, 8H). ^{13}C NMR (CD_3CN , 125.66 MHz): δ 196.65, 135.44, 133.89, 132.39, 131.52, 130.39, 130.23, 129.83, 129.80, 129.10, 128.21, 57.44, 48.04. ^{19}F NMR (CD_3CN , 282.3 MHz): δ -72.9 (d, J = 706 Hz). IR (neat): 2975, 2255, 1979, 1602, 1488, 1445, 1365, 1181, 1075,

829, 769, 698 cm^{-1} . UV-vis (CH_3CN) λ_{max} , nm (ϵ): 357 (33000), 435 (11000). ESI/MS (m/z): $[\text{M-PF}_6]^+$ 1157.18, $[\text{M-2PF}_6]^{2+}$ 506.16. Electrochemistry (vs ferrocene in CH_3CN with $[\text{TBA}][\text{PF}_6]$ as supporting electrolyte): $\text{Fe}^{\text{III}}/\text{Fe}^{\text{II}}$, +40 mV. Anal. Calcd for $\text{C}_{70}\text{H}_{58}\text{F}_{12}\text{Fe}_1\text{N}_{10}\text{P}_2$: C, 60.70; H, 4.22; N, 10.11. Found: C, 60.21; H, 4.14; N, 9.88.

General Procedure for the Preparation of Azides 1a-l. Previously synthesized azides 3a-m were prepared by diazotization from the commercially available aniline, followed by treatment with sodium azide based on a standard procedure.³⁴ All azides were characterized based on physical and/or spectral data as shown in Figure 3.3(3a,⁴⁶ 3b,⁴⁷ 3c,⁴⁸ 3d,⁴⁹ 3e,⁴⁶ 3f,⁵⁰ 3g,⁵¹ 3h,⁵² 3i,⁵³ 3j⁵⁴, 3k,⁵⁵ 3l,⁵⁶ and 3m⁵⁷).

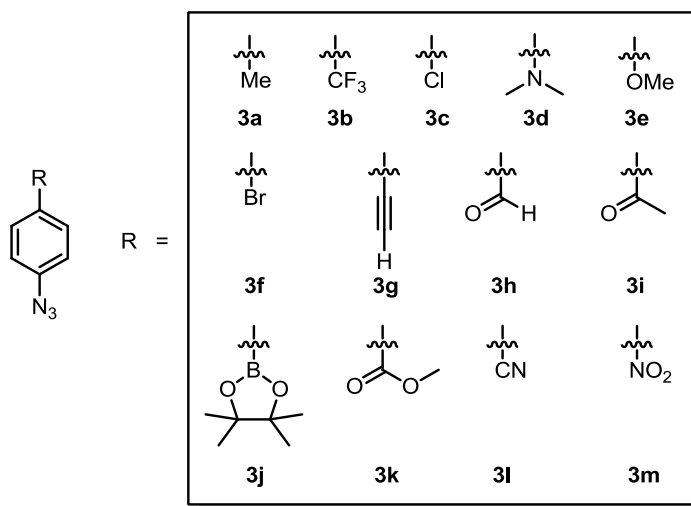


Figure 3.3. Diagram of organic azides that were prepared.

General Catalytic Reaction. $[(^{\text{Me,Et}}\text{TC}^{\text{Ph}})\text{Fe}(\text{NCCH}_3)_2](\text{PF}_6)_2$ (**2**) was added to a 20-mL vial (100 mL pressure vial for Table 1 entry 5 and 6) followed by the addition of the alkene. The reaction mixture was heated and stirred for 10 min. The aryl azide was then added to the reaction and allowed to stir at the designated temperature. Once aryl azide was no longer present (as determined by GC/MS) the mixture was removed from heat and $[(^{\text{Me,Et}}\text{TC}^{\text{Ph}})\text{Fe}(\text{NCCH}_3)_2](\text{PF}_6)_2$ was filtered away over Celite. $[(^{\text{Me,Et}}\text{TC}^{\text{Ph}})\text{Fe}(\text{NCCH}_3)_2](\text{PF}_6)_2$ can be recollected for re-use by adding acetonitrile to the filter and collecting the solution. Removal of the acetonitrile under reduced pressure gives (**2**). The volatiles were removed under reduced pressure and, if needed, the product was purified by column chromatography on silica gel using a 9:1 ratio of hexanes to ethyl acetate as eluent.

Synthesis of 2-octyl-1-(*p*-tolyl)aziridine (Table 3.1, Entry 1). *0.1% catalyst loading:* *p*-Tolyl azide (0.240 g, 1.81 mmol), 1-decene (7.410 g, 52.83 mmol), and **2** (0.0025 g, 0.0018 mmol) were used in the General Catalytic Reaction described above yielding 0.312 g, 70.4%. **(Table 3.1, Entry 2)** *1% catalyst loading:* *p*-Tolyl azide (0.103 g, 0.773 mmol), 1-decene (2.223 g, 15.85 mmol), and **2** (0.0107 g, 0.00773 mmol) were used in the General Catalytic Reaction described above yielding 0.156 g, 82.1%. ^1H NMR (CDCl_3 , 499.74 MHz): δ 7.03 (d, $J = 7.5$ Hz, 2H), 6.89 (d, $J = 7.0$ Hz, 2H), 2.28 (s, 3H), 2.03 (m, 3H), 1.59 (m, 4H), 1.40 (m, 2H), 1.31 (m, 8H), 0.91 (t, $J = 6.0$ Hz, 3H). ^{13}C NMR (CDCl_3 ,

125.66 MHz): δ 152.77, 131.45, 129.51, 120.65, 40.33, 34.17, 33.41, 32.02, 29.74, 29.69, 29.42, 27.85, 22.80, 20.78, 14.24. GC/MS (m/z): 245.2. DART HR MS (m/z): $[M+H]^+$ 246.2211 (found); $C_{17}H_{28}N$ 246.2222 (calcd).

Synthesis of 2-hexyl-1-(4-(trifluoromethyl)phenyl)aziridine (Table 3.1, Entry 3). 1-azido-4-(trifluoromethyl)- benzene (0.392 g, 2.09 mmol), 1-octene (3.575 g, 31.90 mmol), and **2** (0.0029 g, 0.0021 mmol) were used in the General Catalytic Reaction described above yielding 0.212 g, 37.3%. 1H NMR ($CDCl_3$, 499.74 MHz): δ 7.47 (d, J = 8.0 Hz, 2H), 7.03 (d, J = 8.0 Hz, 2H), 2.13 (m, 2H), 2.09 (d, J = 6.0 Hz, 1H), 1.58 (m, 4H), 1.41 (m, 2H), 1.34 (m, 4H), 0.92 (t, J = 6.5 Hz, 3H). ^{13}C NMR ($CDCl_3$, 125.66 MHz): δ 158.40, 126.27 (q, J = 3.8 Hz), 124.60 (q, J = 270.0 Hz), 124.19 (q, J = 32.7 Hz), 120.83, 40.55, 34.23, 33.16, 31.97, 29.32, 27.71, 22.75, 14.18. ^{19}F NMR ($CDCl_3$, 470.2 MHz): δ -61.7. GC/MS (m/z): 271.1. DART HR MS (m/z): $[M+H]^+$ 272.1609 (found); $C_{15}H_{21}F_3N$ 272.1626 (calcd).

Synthesis of 9-(*p*-tolyl)-9-azabicyclo[6.1.0]nonane (Table 3.1, Entry 4). *p*-Tolyl azide (0.192 g, 1.44 mmol) and *cis*-cyclooctene (4.230 g, 38.40 mmol), and **2** (0.0020 g, 0.0014 mmol) were used in the General Catalytic Reaction described above yielding 0.302 g, 97.1%. 1H NMR ($CDCl_3$, 499.74 MHz): δ 7.02 (d, J = 8.5 Hz, 2H), 6.88 (d, J = 8.0 Hz, 2H), 2.32 (dd, J_1 = 13.5 Hz, J_2 = 2.5 Hz, 2H), 2.28 (s, 3H), 2.05 (d, J = 9.5 Hz, 2H), 1.65 (m, 4H), 1.50 (m, 6H). ^{13}C NMR ($CDCl_3$, 125.66 MHz): δ 153.08, 131.14, 129.41, 120.15, 43.73, 27.36, 27.20,

26.59, 20.77. GC/MS (m/z): 215.1. DART HR MS (m/z): $[M+H]^+$ 216.1748 (found); $C_{15}H_{22}N$ 216.1752 (calcd).

Synthesis of 2,3-dipropyl-1-(*p*-tolyl)aziridine (Table 3.1, Entry 5). *p*-Tolyl azide (0.113 g, 0.852 mmol), *trans*-4-octene (3.705 g, 33.02 mmol), and **2** (0.0118 g, 0.0085 mmol) were used in the General Catalytic Reaction described above yielding 0.055 g, 30%. 1H NMR ($CDCl_3$, 499.74 MHz): δ 7.02 (d, J = 7.5 Hz, 2H), 6.80 (d, J = 8.5 Hz, 2H), 2.28 (s, 3H), 2.03 (t, J = 5.5 Hz, 2H), 1.62 (m, 2H), 1.53 (m, 4H), 1.10 (m, 2H), 0.96 (t, J = 7.0 Hz, 6H) ^{13}C NMR ($CDCl_3$, 125.66 MHz): δ 148.10, 130.91, 129.36, 120.95, 44.99, 33.29, 21.11, 20.80, 14.18. GC/MS (m/z): 217.2. DART HR MS (m/z): $[M+H]^+$ 218.1901 (found); $C_{15}H_{24}N$ 218.1909 (calcd).

Synthesis of 1-methyl-7-(*p*-tolyl)-7-azabicyclo[4.1.0]heptane (Table 3.1, Entry 6). *p*-Tolyl azide (0.100 g, 0.751 mmol), 1-methyl-cyclohexene (4.055 g, 42.20 mol), and **2** (0.0104 g, 0.00751 mmol) were used in the General Catalytic Reaction described above yielding 0.059 g, 39%. 1H NMR ($CDCl_3$, 499.74 MHz): δ 7.02 (d, J = 7.5 Hz, 2H), 6.75 (d, J = 6.5 Hz, 2H), 2.28 (s, 3H), 2.15 (m, 1H), 2.02 (m, 1H), 1.99 (m, 2H), 1.64 (m, 1H), 1.55 (m, 2H), 1.35 (m, 1H), 1.25 (m, 1H), 0.99 (s, 3H) ^{13}C NMR ($CDCl_3$, 125.66 MHz): δ 148.74, 130.52, 129.27, 120.49, 44.17, 41.60, 32.41, 24.62, 21.16, 20.85, 20.81, 20.65. GC/MS (m/z): 201.1. DART HR MS (m/z): $[M+H]^+$ 202.1594 (found); $C_{15}H_{22}N$ 202.1596 (calcd).

Synthesis of 2,2,3,3-tetramethyl-1-(*p*-tolyl)aziridine (Table 3.1, Entry 7). *p*-Tolyl azide (0.231 g, 1.73 mmol), 2,3-dimethyl-2-butene (3.540 g, 42.06 mmol), and **2** (0.0024 g, 0.0017 mmol) were used in the General Catalytic Reaction described above yielding 0.067 g, 20%. ¹H NMR (CDCl₃, 499.74 MHz): δ 7.00 (d, *J* = 8.0 Hz, 2H), 6.62 (d, *J* = 8.0 Hz, 2H), 2.27 (s, 3H), 1.25 (s, 12H). ¹³C NMR (CDCl₃, 125.66 MHz): δ 145.46, 129.54, 129.24, 120.50, 44.14, 20.80, 20.55. GC/MS (*m/z*): 189.1. DART HR MS (*m/z*): [M+H]⁺ 190.1601 (found); C₁₃H₂₀N 190.1596 (calcd).

Control Reactions. Selected control reactions following the method of the General Catalytic Reaction were attempted but without **2**. These reactions either gave lower yields for aziridines or almost no isolable aziridine. Two example cases are shown. *2-octyl-1-(p-tolyl)aziridine*. *p*-Tolyl azide (0.096 g, 0.72 mmol) and 1-decene (1.853 g, 13.2 mmol) were used in the General Catalytic Reaction described above yielding 0.078 g, 43% yield. *1-methyl-7-(p-tolyl)-7-azabicyclo[4.1.0]heptane*. *p*-Tolyl azide (0.203 g, 1.53 mmol) and 1-methylcyclohexene (4.055 g, 42.2 mol) were used in the General Catalytic Reaction described above yielding 0.007 g, 2% yield.

General Functional Group Tolerance Catalytic Reaction. The catalyst was added to a 20-mL vial followed by the addition of 5 mL of 1-decene. The reaction mixture was heated and stirred for 10 min. The aryl azide was then added to the

reaction mixture and allowed to stir at 90 °C. Once the aryl azide was no longer present (as determined by GC/MS) the mixture was cooled to room temperature and the catalyst was removed by filtering over Celite. The volatiles were removed under reduced pressure. The product was purified by flash chromatography on silica gel using 9:1 ratio of hexanes to ethyl acetate as eluent in all reactions at 0.1% catalyst loading with **2** for characterization.

Synthesis of 1-(4-chlorophenyl)-2-octylaziridine (Table 3.2, Entry 1). *0.1% catalyst loading:* 1-azido-4-chlorobenzene (0.2993 g, 1.949 mmol) and **2** (0.0027 g, 0.0020 mmol) were used in the General Catalytic Reaction described above yielding 0.366 g, 70.7%. ¹H NMR (CDCl₃, 499.74 MHz): δ 7.15 (d, *J* = 8.8 Hz, 2H), 6.88 (d, *J* = 8.7 Hz, 2H), 2.06 (d, *J* = 3.5, 1H), 2.03 (m, 1H), 1.99 (d, *J* = 6.2, 1H), 1.55 (m, 4H), 1.40 (m, 2H), 1.30 (m, 8H), 0.90 (t, *J* = 7.0 Hz, 3H). ¹³C NMR (CDCl₃, 125.66 MHz): δ 153.80, 128.82, 126.97, 121.93, 40.47, 34.17, 33.15, 31.94, 29.65, 29.60, 29.34, 27.70, 22.73, 14.16. GC/MS (*m/z*): 265.1. DART HR MS (*m/z*): [M+H]⁺ 266.16658 (found); C₁₆H₂₅ClN₁ 266.16755 (calcd).

Synthesis of *N,N*-dimethyl-4-(2-octylaziridin-1-yl)aniline (Table 3.2, Entry 2). *0.1% catalyst loading:* 4-azido-*N,N*-dimethylaniline (0.2576 g, 1.588 mmol) and **2** (0.0022 g, 0.0016 mmol) were used in the General Catalytic Reaction described above yielding 0.297 g, 68.1%. ¹H NMR (CDCl₃, 499.74 MHz): δ 6.93 (d, *J* = 8.9 Hz, 2H), 6.69 (d, *J* = 8.9 Hz, 2H), 2.89 (s, 6H), 2.01 (m, 3H), 1.59 (m, 4H), 1.44

(m, 2H), 1.34 (m, 8H), 0.94 (t, $J = 7.0$ Hz, 3H). ^{13}C NMR (CDCl_3 , 125.66 MHz): δ 146.58, 121.20, 113.90, 41.35, 40.25, 34.10, 33.37, 31.92, 29.66, 29.60, 29.32, 27.80, 22.70, 14.14. GC/MS (m/z): 274.2. DART HR MS (m/z): $[\text{M}+\text{H}]^+$ 275.24756 (found); $\text{C}_{18}\text{H}_{31}\text{N}_2$ 275.24872 (calcd). *HMBC shows both quaternary aryl carbons are overlapping at 146.58 ppm

Synthesis of 1-(4-methoxyphenyl)-2-octylaziridine (Table 3.2, Entry 3). 0.1% catalyst loading: 1-azido-4-methoxybenzene (0.4200 g, 2.816 mmol) and **2** (0.0039 g, 0.0028 mmol) were used in the General Catalytic Reaction described above yielding 0.481 g, 65.3%. ^1H NMR (CDCl_3 , 499.74 MHz): δ 6.89 (d, $J = 9.0$ Hz, 2H), 6.75 (d, $J = 9.0$ Hz, 2H), 3.71 (s, 3H), 1.98 (m, 3H), 1.56 (m, 4H), 1.40 (m, 2H), 1.32 (m, 8H), 0.91 (t, $J = 7.0$ Hz, 3H). ^{13}C NMR (CDCl_3 , 125.66 MHz): δ 154.83, 148.43, 121.25, 114.08, 55.27, 40.27, 34.04, 33.23, 31.85, 29.58, 29.53, 29.26, 27.69, 22.63, 14.05. GC/MS (m/z): 261.2. DART HR MS (m/z): $[\text{M}+\text{H}]^+$ 262.21623 (found); $\text{C}_{17}\text{H}_{28}\text{N}_1\text{O}_1$ 262.21709 (calcd).

Synthesis of 1-(4-bromophenyl)-2-octylaziridine (Table 3.2, Entry 4). 0.1% catalyst loading: 1-azido-4-bromobenzene (0.4146 g, 2.094 mmol) and **2** (0.0029 g, 0.0021 mmol) were used in the General Catalytic Reaction described above yielding 0.403 g, 62.0%. ^1H NMR (CDCl_3 , 499.74 MHz): δ 7.29 (d, $J = 8.7$ Hz, 2H), 6.83 (d, $J = 8.7$ Hz, 2H), 2.06 (d, $J = 3.5$, 1H), 2.02 (m, 1H), 1.98 (d, $J = 6.2$, 1H), 1.55 (m, 4H), 1.39 (m, 2H), 1.31 (m, 8H), 0.90 (t, $J = 6.9$ Hz, 3H). ^{13}C NMR

(CDCl₃, 125.66 MHz): δ 154.26, 131.72, 122.39, 114.43, 40.40, 34.10, 33.11, 31.91, 29.63, 29.57, 29.32, 27.67, 22.71, 14.16. GC/MS (m/z): 309.1. DART HR MS (m/z): [M+H]⁺ 310.11613 (found); C₁₆H₂₅BrN₁ 310.11704 (calcd).

Synthesis of 1-(4-ethynylphenyl)-2-octylaziridine (Table 3.2, Entry 5). 0.1% catalyst loading: 1-azido-4-ethynylbenzene (0.2791 g, 1.949 mmol) and **2** (0.0027 g, 0.0020 mmol) were used in the General Catalytic Reaction described above yielding 0.289 g, 57.9%. ¹H NMR (CDCl₃, 499.74 MHz): δ 7.34 (d, J = 8.6 Hz, 2H), 6.89 (d, J = 8.6 Hz, 2H), 2.99 (s, 1H), 2.07 (m, 2H), 2.03 (m, 1H), 1.57 (m, 4H), 1.41 (m, 2H), 1.3 (m, 8H), 0.90 (t, J = 7.0 Hz, 3H). ¹³C NMR (CDCl₃, 125.66 MHz): δ 155.72, 132.90, 120.62, 115.45, 83.89, 76.03, 40.37, 34.06, 33.12, 31.92, 29.62, 29.57, 29.32, 27.66, 22.71, 14.14. GC/MS (m/z): 255.2. DART HR MS (m/z): [M+H]⁺ 256.20561 (found); C₁₈H₂₆N₁ 256.20652 (calcd).

Synthesis of 4-(2-octylaziridin-1-yl)benzaldehyde (Table 3.2, Entry 6). 0.1% catalyst loading: 4-azidobenzaldehyde (0.2125 g, 1.444 mmol) and **2** (0.0020 g, 0.0014 mmol) were used in the General Catalytic Reaction described above yielding 0.158 g, 42.1%. ¹H NMR (CDCl₃, 499.74 MHz): δ 9.82 (s, 1H), 7.71 (d, J = 8.5 Hz, 2H), 7.02 (d, J = 8.5 Hz, 2H), 2.15 (m, 2H), 2.10 (m, 1H), 1.56 (m, 4H), 1.37 (m, 2H), 1.27 (m, 8H), 0.86 (t, J = 7.0 Hz, 3H). ¹³C NMR (CDCl₃, 125.66 MHz): δ 190.83, 161.09, 131.20, 131.04, 120.93, 40.54, 34.19, 32.99, 31.89,

29.59, 29.54, 29.29, 27.59, 22.69, 14.14. GC/MS (m/z): 259.2. DART HR MS (m/z): $[M+H]^+$ 260.20059 (found); $C_{17}H_{26}N_1O_1$ 260.20144 (calcd).

Synthesis of 1-(4-(2-octylaziridin-1-yl)phenyl)ethanone (Table 3.2, Entry 7).

0.1% catalyst loading: 1-(4-azidophenyl)ethanone (0.2909 g, 1.804 mmol) and **2** (0.0025 g, 0.0018 mmol) were used in the General Catalytic Reaction described above yielding 0.204 g, 41.3%. 1H NMR ($CDCl_3$, 499.74 MHz): δ 7.82 (d, J = 8.6 Hz, 2H), 6.96 (d, J = 8.6 Hz, 2H), 2.49 (s, 3H), 2.12 (m, 2H), 2.08 (m, 1H), 1.56 (m, 4H), 1.38 (m, 2H), 1.29 (m, 8H), 0.87 (t, J = 7.0 Hz, 3H). ^{13}C NMR ($CDCl_3$, 125.66 MHz): δ 196.68, 159.75, 131.42, 129.75, 120.39, 77.41, 76.91, 40.39, 34.08, 33.01, 31.87, 29.58, 29.52, 29.27, 27.59, 26.29, 22.67, 14.11. GC/MS (m/z): 273.2. DART HR MS (m/z): $[M+H]^+$ 274.21615 (found); $C_{18}H_{28}N_1O_1$ 274.21709 (calcd).

Synthesis of 2-octyl-1-(4-(4,4,5,5-tetramethyl-1,3,2-dioxaborolan-2-yl)phenyl)aziridine (Table 3.2, Entry 8). *0.1% catalyst loading:* 2-(4-azidophenyl)-4,4,5,5-tetramethyl-1,3,2-dioxaborolane (0.637 g, 2.60 mmol) and **2** (0.0036 g, 0.0026 mmol) were used in the General Catalytic Reaction described above yielding 0.374 g, 40.3%. 1H NMR ($CDCl_3$, 499.74 MHz): δ 7.70 (d, J = 8.4 Hz, 2H), 6.98 (d, J = 8.4 Hz, 2H), 2.11 (m, 2H), 2.04 (m, 1H), 1.59 (m, 4H), 1.41 (m, 2H), 1.32 (m, 20H), 0.91 (t, J = 7.0 Hz, 3H). ^{13}C NMR ($CDCl_3$, 125.66 MHz): 158.04, 135.83, 120.11, 83.49, 40.16, 33.96, 33.21, 31.93, 29.65, 29.59, 29.34,

27.65, 24.90, 22.72, 14.17. GC/MS (m/z): 358.2. DART HR MS (m/z): $[M+H]^+$ 358.29033 (found); $C_{22}H_{37}B_1N_1O_2$ 358.29173 (calcd).

Synthesis of methyl 4-(2-octylaziridin-1-yl)benzoate (Table 3.2, Entry 9).

0.1% catalyst loading: methyl 4-azidobenzoate (0.3710 g, 2.094 mmol) and **2** (0.0029 g, 0.0021 mmol) were used in the General Catalytic Reaction described above yielding 0.243 g, 40.1%. 1H NMR ($CDCl_3$, 499.74 MHz): δ 7.89 (d, J = 8.6 Hz, 2H), 6.95 (d, J = 8.6 Hz, 2H), 3.84 (s, 3H), 2.12 (m, 2H), 2.07 (m, 1H), 1.56 (m, 4H), 1.38 (m, 2H), 1.27 (m, 8H), 0.87 (t, J = 7.0 Hz, 3H). ^{13}C NMR ($CDCl_3$, 125.66 MHz): δ 166.89, 159.59, 130.83, 123.81, 120.37, 51.80, 40.41, 34.11, 33.09, 31.92, 29.63, 29.57, 29.32, 27.63, 22.72, 14.15. GC/MS (m/z): 289.2. DART HR MS (m/z): $[M+H]^+$ 290.21091 (found); $C_{18}H_{28}N_1O_2$ 290.21200 (calcd).

Synthesis of 4-(2-octylaziridin-1-yl)benzonitrile (Table 3.2, Entry 10).

0.1% catalyst loading: 4-azidobenzonitrile (0.2394 g, 1.166 mmol) and **2** (0.0023 g, 0.0016 mmol) were used in the General Catalytic Reaction described above yielding 0.160 g, 37.6%. 1H NMR ($CDCl_3$, 499.74 MHz): δ 7.47 (d, J = 8.6 Hz, 2H), 6.98 (d, J = 8.7 Hz, 2H), 2.17 (m, 1H), 2.13 (m, 1H), 2.09 (m, 1H), 1.58 (m, 4H), 1.38 (m, 2H), 1.27 (m, 8H), 0.87 (t, J = 7.0 Hz, 3H). ^{13}C NMR ($CDCl_3$, 125.66 MHz): δ 159.30, 133.20, 121.28, 119.41, 104.98, 40.65, 34.25, 32.94, 31.91, 29.60, 29.54, 29.30, 27.61, 22.71, 14.16. GC/MS (m/z): 256.2. DART HR MS (m/z): $[M+H]^+$ 257.21081 (found); $C_{17}H_{25}N_2$ 257.20177 (calcd).

Synthesis of 1-(4-nitrophenyl)-2-octylaziridine (Table 3.2, Entry 11). 0.1% catalyst loading: 1-azido-4-nitrobenzene (0.4266 g, 2.599 mmol) and **2** (0.0036 g, 0.0026 mmol) were used in the General Catalytic Reaction described above yielding 0.239 g, 33.3%. ¹H NMR (CDCl₃, 499.74 MHz): δ 8.05 (d, *J* = 9.1 Hz, 2H), 6.97 (d, *J* = 9.1 Hz, 2H), 2.19 (m, 2H), 2.13 (m, 1H), 1.55 (m, 4H), 1.35 (m, 2H), 1.26 (m, 8H), 0.85 (t, *J* = 7.0 Hz, 3H). ¹³C NMR (CDCl₃, 125.66 MHz): δ 161.33, 142.36, 125.05, 120.57, 40.81, 34.37, 32.83, 31.86, 29.55, 29.49, 29.26, 27.52, 22.67, 14.10. GC/MS (*m/z*): 276.2. DART HR MS (*m/z*): [M+H]⁺ 277.19241 (found); C₁₆H₂₅N₂O 277.19160 (calcd).

X-ray Structure Determinations. X-ray diffraction measurements were performed on single-crystals coated with Paratone oil and mounted on glass fibers. Each crystal was frozen under a stream of N₂ while data were collected on a Bruker APEX diffractometer. A matrix scan using at least 12 centered reflections was used to determine initial lattice parameters. Reflections were merged and corrected for Lorenz and polarization effects, scan speed, and background using SAINT 4.05. Absorption corrections, including odd and even ordered spherical harmonics, were performed using SADABS, if necessary. Space group assignments were based upon systematic absences, *E* statistics, and successful refinement of the structure. The structures were solved by direct methods with the aid of successive difference Fourier maps, and were refined

against all data using the SHELXTL 5.0 software package. The structure of **2** has two types of disorder. First, one of the PF₆ counteranions has fluorine atoms that are split over multiple positions to improve the electron density map. Second, one of the solvent positions is disordered between one ether molecule and two acetonitrile molecules. This was modeled including each of these moieties (1 CH₃CH₂OCH₂CH₃ or 2 CH₃CN) at 50% weighting. All of the solvent molecules were refined isotropically.

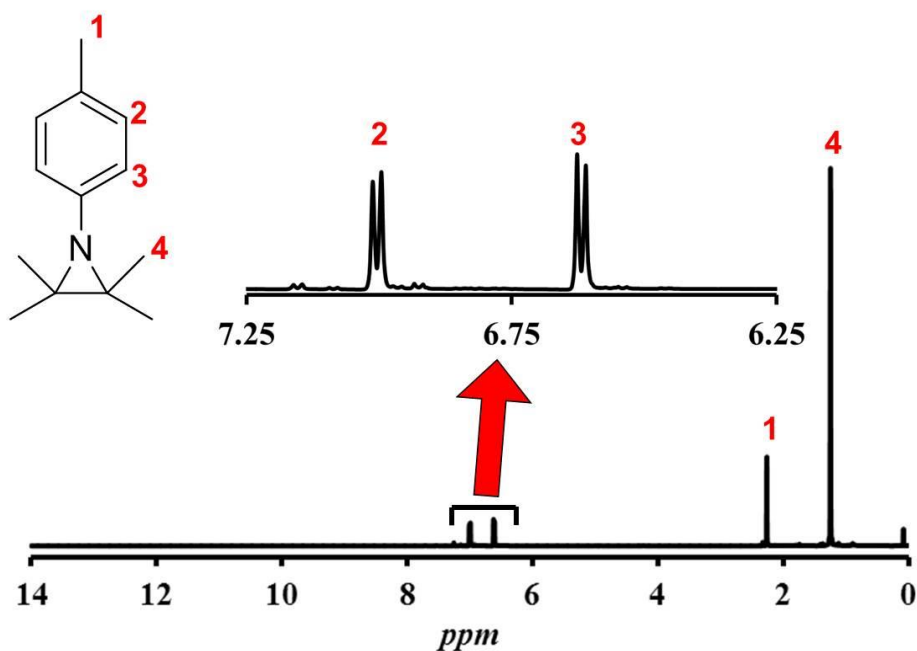


Figure 3.4. ¹H NMR of 2,2,3,3-tetramethyl-1-(*p*-tolyl)aziridine in CDCl₃.

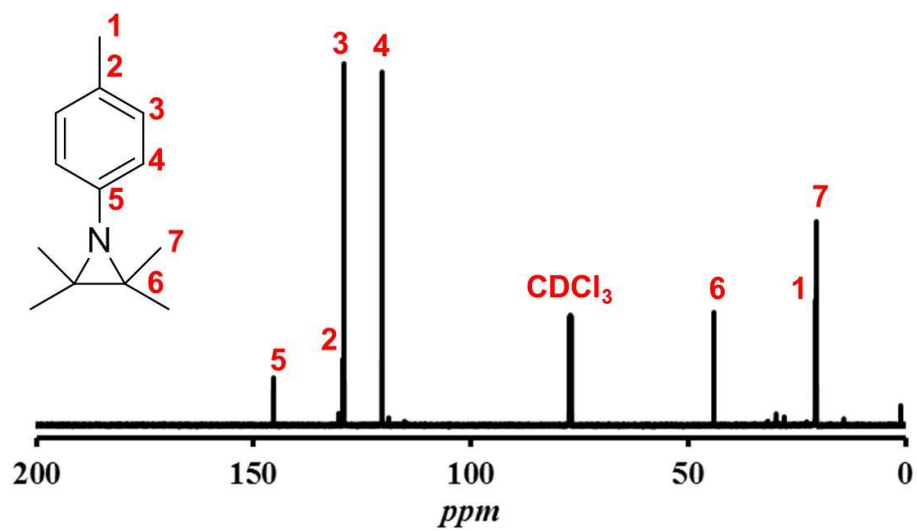


Figure 3.5. ^{13}C NMR of 2,2,3,3-tetramethyl-1-(*p*-tolyl)aziridine in CDCl_3 .

Chapter 4

Development of a Silver Transmetallating Reagent to Synthesize Macrocyclic Tetracarbene Complexes

A version of this chapter was originally published by Zheng Lu, S. Alan Cramer, and David M. Jenkins:

Lu, Z.; Cramer, S. A.; Jenkins, D. M. "Exploiting a Dimeric Silver Transmetallating Reagent to Synthesize Macrocyclic Tetracarbene Complexes." *Chem. Sci.* **2012**, 3, 3081-3087.

All work presented in this chapter was altered from the original publication to only include work completed by S. Alan Cramer unless otherwise noted within the text.

Abstract

A dimeric macrocyclic tetra-*N*-heterocyclic carbene (NHC) silver complex was synthesized and shown to successfully extend transmetallation of polydentate NHCs beyond bidentate NHCs. The silver complex was utilized in the preparation of a variety of monomeric tetra-NHC complexes ranging from early first row to late third row transition metals in moderate to high yield for a total of nine examples of transmetallation. Among these complexes are rare examples of silver transmetallation with first row transition metals: chromium, iron, and cobalt. Additionally, the first examples of tetracarbenes on chromium and gold are reported. All compounds were characterized by single-crystal X-ray diffraction, ESI-MS, and spectroscopic techniques.

Introduction

The facile synthesis of bidentate⁵⁸ and tridentate⁵⁸⁻⁵⁹ *N*-heterocyclic carbenes (NHCs) coupled with their resistance to oxidation^{12d} has made these chelating ligands a complementary choice to phosphines for many applications. Bidentate NHCs have been employed as auxiliary ligands for catalysts ranging from Pd catalysed coupling⁶⁰ to olefin hydrogenation.⁶¹ In addition to their use in catalysis,⁶² tridentate NHCs have been utilized in the stabilization of novel metal ligand multiple bonds, such as iron nitrides^{18b, 44d, 63} and cobalt imidos.^{19b} Despite numerous uses for these strong σ -donor ligands, one class of chelating NHCs that has not been as thoroughly investigated is tetradentate carbenes.⁶⁴ Macrocyclic tetradentate carbenes would be structurally similar to, but electronically distinct from, other important tetradentate macrocycles such as cyclam^{17a} or porphyrin.⁶⁵

The lack of research with these tetradentate ligands is primarily due to the limited number of metal complexes which have been synthesized. Since Hahn's elegant templated synthesis of the first macrocyclic tetracarbene on Pt in 2005,¹⁴ there have only been five other examples of monomeric macrocyclic tetracarbene complexes, all of which were prepared by in situ deprotonation of imidazoliums.^{15, 38, 66} Despite the very limited number of examples with this ligand motif, these complexes have been quite significant for systems such as electron transfer reactions^{15a, 15c} and catalytic aziridination.⁶⁶ While the ability to prepare sufficient quantities of the precursor macrocyclic tetraimidazoliums is

now well known,^{15b, 38} no general methodology for complexing these ligands to form tetracarbenes has been demonstrated prior to this work.

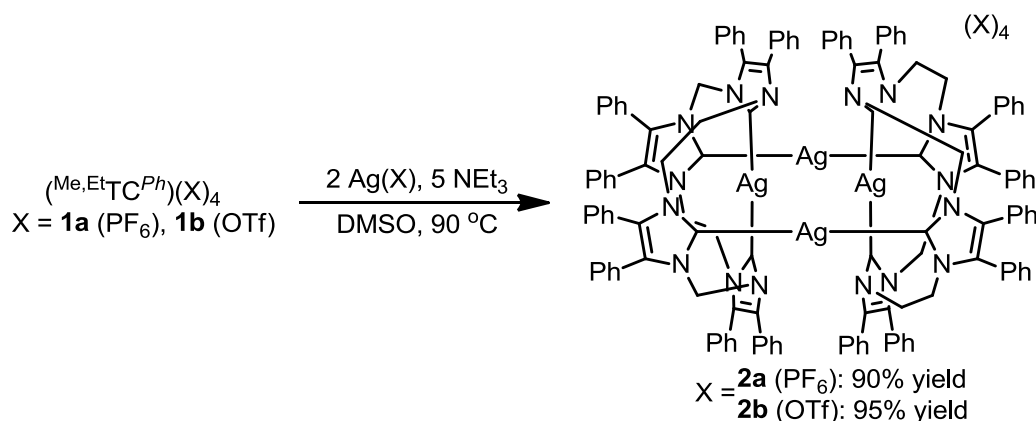
The development of a silver transmetallating reagent for tetracarbenes would have many advantages from a synthetic perspective.⁶⁷ Reactions with metal halide salts typically only give silver halide by-products. Furthermore, since the carbene is already formed, reaction conditions can often be much milder since no base is required during the reaction.³⁹ Transmetallation reactions have been successful in yielding monomeric metal complexes with mono⁶⁸ and bidentate⁶⁹ NHC ligands.⁷⁰ However, a disilver tetracarbene complex prepared by Murphy and Spicer, using a 24-atom ringed macrocycle has not been demonstrated to transmetallate the NHCs to other metals from the silver.^{15b} Another concern with polydentate carbenes is that, with rare exceptions, transmetallation of NHCs from silver is limited to the late transition metals Ru, Rh, Ir, Ni, Pd, Pt, Cu, and Au.⁶⁷ This communication presents a general synthetic methodology for preparing macrocyclic tetracarbenes with first, second, and third row transition metals from both sides of the periodic table by utilizing a dimeric silver transmetallating reagent

Synthesis and Characterization of Silver Complex

We have previously reported the synthesis of the macrocyclic tetraimidazolium $(^{\text{Me,Et}}\text{TC}^{\text{Ph}})(\text{OTf})_4$ and $(^{\text{Me,Et}}\text{TC}^{\text{Ph}})(\text{I})_4$.³⁸ As iodides are undesirable for the synthesis of a transmetallation reagent a counteranion exchange was performed by adding 4 equivalents of TIPF_6 to $(^{\text{Me,Et}}\text{TC}^{\text{Ph}})(\text{I})_4$, to

yield $(^{\text{Me,Et}}\text{TC}^{\text{Ph}})(\text{PF}_6)_4$. Addition of two equivalents of $\text{Ag}(\text{X})$, **1** and NEt_3 in DMSO at 90 °C gave the dimeric, tetranuclear silver complex, $[\{(^{\text{Me,Et}}\text{TC}^{\text{Ph}})\text{Ag}\}_2\text{Ag}_2](\text{X})_4$ (**2a**) in 90% yield (Scheme 4.1). This work was performed in collaboration with Dr. Zheng Lu, a postdoctoral researcher in the Jenkins lab, where he synthesized the triflate variant **2b**. Like many silver NHC complexes, the metal ion is two coordinate.⁶⁷ Although Ag_2O is often used to prepare transmetallating reagents,⁶⁷ we found the yield of **2** to be lower under similar conditions.

Scheme 4.1. Synthesis of silver complexes from $(^{\text{Me,Et}}\text{TC}^{\text{Ph}})(\text{X})_4$.



Spectroscopic characterization of **2a** was consistent with this novel dimeric structure. Electrospray ionization mass spectrometry (ESI-MS) analysis of **3a** showed peaks at m/z 586.37 associated with $[\{(^{\text{Me,Et}}\text{TC}^{\text{Ph}})\text{Ag}\}_2\text{Ag}_2]^{4+}$, 829.82 associated with $\{[\{(^{\text{Me,Et}}\text{TC}^{\text{Ph}})\text{Ag}\}_2\text{Ag}_2](\text{PF}_6)\}^{3+}$, and 1317.70 associated with $\{[\{(^{\text{Me,Et}}\text{TC}^{\text{Ph}})\text{Ag}\}_2\text{Ag}_2](\text{PF}_6)_2\}^{2+}$. ^{13}C NMR for **2a** shows two resonances for the carbene carbons at 182.83 and 176.85 ppm. These two peaks are both split into

pairs of doublets due to the coupling to both ^{107}Ag and ^{109}Ag . By comparing the ^{13}C NMR of a mononuclear silver complex prepared by Dr. Zheng Lu which only has a resonance at 178.38 ppm for the carbene carbon, we can conclude that the carbene bound to the inter-macrocycle bridging silver gives the peak at 183.18 ppm in **2a**. The ^{13}C NMR and the ESI-MS demonstrate that **2a** maintains its geometry in solution. Complexes **2a** and **2b** are both air and moisture stable.

The X-ray crystal structure of **2a** shows the dimeric structure of the tetrasilver complex (Figure 4.1). The intra-macrocycle C1-Ag1-C3 and C67-Ag2-C69 bond angles are 162.7° and 161.8° , respectively, while the bridging inter-macrocycle C2-Ag3-C68 and C4-Ag4-C70 bond angles are 170.0° and 173.3° , respectively. These relatively linear bond angles suggest that there is little distortion due to the size of the macrocycle. The Ag1-C and Ag2-C bond distances average 2.14 Å while the Ag3-C and Ag4-C bond distances average 2.09 Å. The bond distances and angles are typical for two coordinate Ag-NHC complexes.^{70a, 71}

Synthesis of Tetracarbene Complexes

Since there is a stoichiometric ratio of two Ag^{I} ions per macrocyclic ligand, we believed that the preferred metal salts for the formation of monomeric tetracarbene complexes would be di- or trivalent metals with two or more halides. To canvass the periodic table, we decided to use commercially available di- and trivalent metal salts with particular attention paid to metals which had few or no

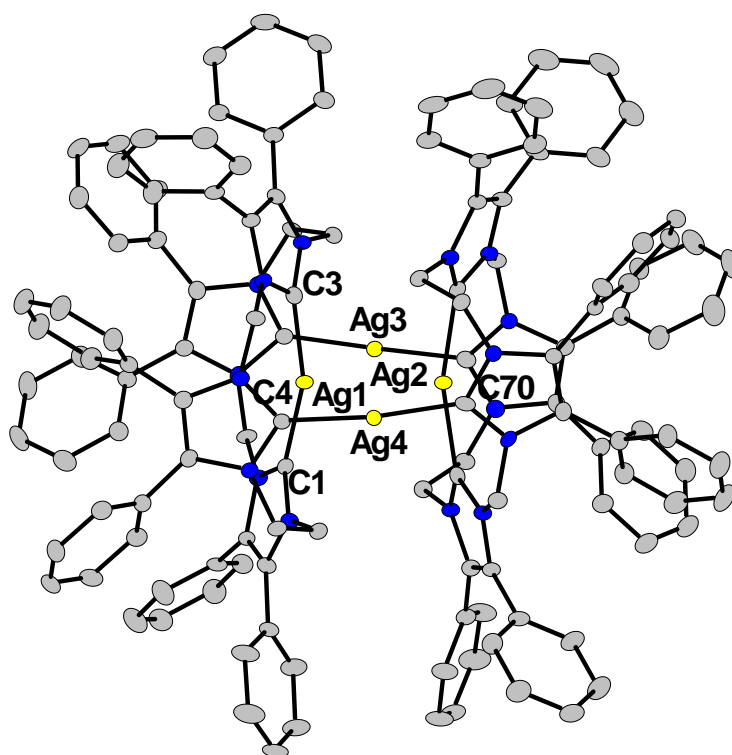
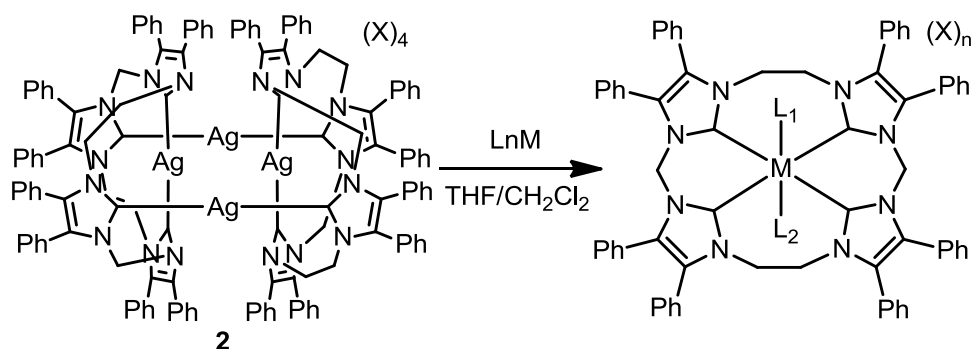


Figure 4.1. X-ray crystal structure of $[(^{\text{Me,Et}}\text{TC}^{\text{Ph}})\text{Ag}]_2\text{Ag}_2(\text{PF}_6)_4$ (**3a**). Light yellow, blue, grey, and white ellipsoids (50% probability) represent Ag, N, C, and H, respectively. Counteranions, solvent molecules, and H atoms have been omitted for clarity. Bond distances (Å) and angles (deg): Ag1-C1, 2.143(3); Ag1-C3, 2.144(3); Ag4-C4, 2.092(3); Ag4-C70, 2.077(3); C1-Ag1-C3, 162.7(1); C4-Ag4-C70, 173.3(1).

examples of NHCs prepared via silver transmetallation. Addition of **2** to these metal salts in a 50/50 mixture of THF and CH_2Cl_2 yielded nine examples of macrocyclic tetracarbene complexes in moderate to high yield (Scheme 4.2 and

Table 4.1). In each case, the tetracarbene ligand binds to the four sites in the equatorial plane around the metal. As this work was completed in a collaborative effort, metal complexes **5**, **6**, **8**, **9**, and **12** were all isolated and characterized by Dr. Zheng Lu. As the synthesis of these complexes demonstrate the importance of **2**, yields of new metal complexes are shown in Table 2 but these new complexes will not be discussed beyond comparing to similar complexes that I prepared myself.

Scheme 4.2. Synthesis of metal complexes from $[\{(\text{Me},\text{EtTC}^{\text{Ph}})\text{Ag}\}_2\text{Ag}_2](\text{X})_4$.



Since group 10 metals are excellent candidates for silver transmetallation of carbenes,⁶⁷ we synthesized the platinum, palladium, and nickel complexes. The platinum complex, $[(\text{Me},\text{EtTC}^{\text{Ph}})\text{Pt}](\text{PF}_6)_2$ (**3**), was previously synthesized via an alternate synthetic strategy.³⁸ While the imidazolium deprotonation approach with NEt_3 led to a 7% isolated yield, however, transmetallation led to an 82% yield of **3**. ESI-MS of **3** showed two peaks at m/z 576.19, associated with

Table 4.1. Transmetallation results for metal complexes.

Complex	L _n M	M	L ₁	L ₂	(X) _n	Yield
3	Pt(NCPh) ₂ Cl ₂	Pt	–	–	PF ₆	82%
4	PdI ₂	Pd	–	–	(OTf) ₂	70%
5	Ni(PPh ₃) ₂ Cl ₂	Ni	–	–	(OTf) ₂	87%
6	RhI ₃	Rh	I	I	PF ₆	72% ^{ab}
7	CoCl ₂	Co	OTf	–	OTf	68%
8	FeI ₂	Fe	CH ₃ CN	CH ₃ CN	(PF ₆) ₂	92% ^c
9	Ru(DMSO) ₄ Cl ₂	Ru	DMSO	DMSO	(OTf) ₂	40% ^b
10	CrCl ₂	Cr	Cl	Cl	PF ₆	58% ^d
11	HAuCl ₄	Au	–	–	(OTf) ₃	47% ^e

^a Reaction performed in THF and DMSO; ^b Reaction heated to 60 °C; ^c CH₃CN added during work-up; ^d Excess CrCl₂ used in reaction; ^e An additional equivalent of Ag(OTf) was used.

$[(^{Me,Et}TC^{Ph})Pt]^{2+}$, and 1297.34, associated with $\{[(^{Me,Et}TC^{Ph})Pt](PF_6)\}^+$. The isostructural palladium and nickel complexes, $[(^{Me,Et}TC^{Ph})Pd](OTf)_2$ (**5**) and $[(^{Me,Et}TC^{Ph})Ni](OTf)_2$ (**3**), can be synthesized similarly and also in high yields. All three group ten complexes show a geminal AB splitting pattern in the ¹H NMR of the protons on the methylene and ethylene bridges which demonstrates the rigidity of the ligand in solution.^{21, 27b, 38}

To demonstrate that the transmetallation strategy for these macrocyclic tetracarbenes is more general, we chose to expand the reaction to group 8 and 9 metals. Addition of **2a** to RhI₃ in THF and DMSO yielded $[(^{Me,Et}TC^{Ph})Rh(I)_2](PF_6)$

(**6**). Unexpectedly, the Ag ion failed to remove one of the bound iodides from the rhodium; however, this result is consistent with a previous example of a silver transmetallation yielding a tetracarbene rhodium complex with bound halides by Youngs.⁷² Complex **6** shows a doublet carbene peak in the ¹³C NMR at 167.4 ppm ($J_{Rh-C} = 33.2$ Hz). In direct contrast to **6** is another group 9 metal complex prepared by Dr. Lu which is instead a 5 coordinate cobalt tetracarbene (**7**) that only has one of its two anions bound to the metal center.

The iron complex, $[(^{Me,Et}TC^{Ph})Fe(NCCH_3)_2](PF_6)_2$ (**8**), was synthesized in 92% yield from **2a** and FeI₂. While **8** has been demonstrated to be an excellent aziridination catalyst,⁶⁶ one of the limitations of this catalyst's development was that it could only be synthesized in 11% yield using an in situ deprotonation of the imidazoliums with lithium diisopropyl amide. Complex **8** is the second example of a tetracarbene on iron⁴⁰ and the second case of successful transmetallation of an NHC to iron from silver.⁷³ An isostructural ruthenium tetracarbene, $[(^{Me,Et}TC^{Ph})Ru(DMSO)_2](OTf)_2$ (**9**), was prepared by Dr. Lu albeit in significantly lower yield. The yield is likely a result of decreased solubility. The lessened solubility of **9** is likely due to slow exchange of tightly bound solvent molecules as evidenced by ESI/MS and ¹H NMR data. Unlike complex **9** which exchanges the DMSOs over a period of days, the solvent ligands of **8** exchange rapidly in solution which accounts for the lack of geminal splitting in the ¹H NMR.

To further establish the transmetallation of these macrocyclic NHCs, we examined whether this reaction would be successful with metals on which no

examples of tetracarbene complexes have previously been reported. The two test metals that we evaluated were chromium and gold. Dr. Lu found the transmetallation reagent to be effective at preparing a tricationic gold tetracarbene. In the chromium case, the transmetallation reagent **2a** was non-innocent and the silver behaved as an oxidant which was confirmed by powder X-ray diffraction of the solid precipitate. Similar non-innocent silver NHC transmetallation was observed by Peris⁷⁴ for Rh and Ir and Arnold⁷⁵ for Ru. By adding five equivalents of the metal instead of two equivalents used in the general methodology, after work-up, the reaction yielded $[(^{\text{Me,Et}}\text{TC}^{\text{Ph}})\text{Cr}(\text{Cl})_2](\text{PF}_6)$ (**10**) (See below of X-ray structure). ESI-MS characterization confirmed the trivalent oxidation state of the complex as m/z peaks at 336.15 ($[(^{\text{Me,Et}}\text{TC}^{\text{Ph}})\text{Cr}]^{3+}$), 521.66 ($[(^{\text{Me,Et}}\text{TC}^{\text{Ph}})\text{Cr}(\text{Cl})]^{2+}$), and 1078.25 ($[(^{\text{Me,Et}}\text{TC}^{\text{Ph}})\text{Cr}(\text{Cl})_2]^{+}$) were observed. Complex **10** is the first example of a tetracarbene on chromium and, to our knowledge, just the second example of silver transmetallation of a NHC to a group 7 or earlier metal.⁷⁶

Structural Characterization of Tetracarbene Complexes

Due to the ease of synthesis of a wide variety of monomeric complexes of the tetracarbene ligand $^{\text{Me,Et}}\text{TC}^{\text{Ph}}$, we have been able to collect crystal structures from metals across the periodic table. In each case, the tetracarbene ligand binds to four equatorial positions around the metal center. The *trans*-NHC bond angles in each case are between 170° and 180°. This minimization of distortion suggests that the 18-atom ring size of the macrocycle comfortably fits a variety of

metals with different ionic radii while also allowing additional ligands to bind to the metal center. The transition metal complexes from group 10 and 11 form square planar structures while the complexes formed from group 8 and earlier have an octahedral geometry.

Structurally characterized tetracarbenes are much rare on group 9 metals. Despite multiple crystallization conditions, we were unable to obtain a high-quality X-ray crystal structure of complex **6**, but it is possible to determine the connectivity about the rhodium. The crystal structure of **6** clearly shows two bound iodide ligands (Figure 4.2), which is consistent with Youngs's similar rhodium tetracarbene.⁷²

Since the chromium complex (**10**) is the first examples of a tetracarbene on chromium, the X-ray structure is of particular importance (Figure 4.3). Complex **10** has an octahedral geometry about the metal center and the Cr-C bonds are all between 2.09 and 2.14 Å showing a modest distortion in the chromium carbene bonds (Table 2). These bond distances are comparable to Cr-C bond distances in the rare Cr^{III} dicarbene complexes that have been structurally characterized.⁷⁷ The C1-Cr-C3 and C2-Cr-C4 bond angles of **11** are 172.6 and 170.6, respectively, which again show a modest distortion from an idealized equatorial plane about the metal center.

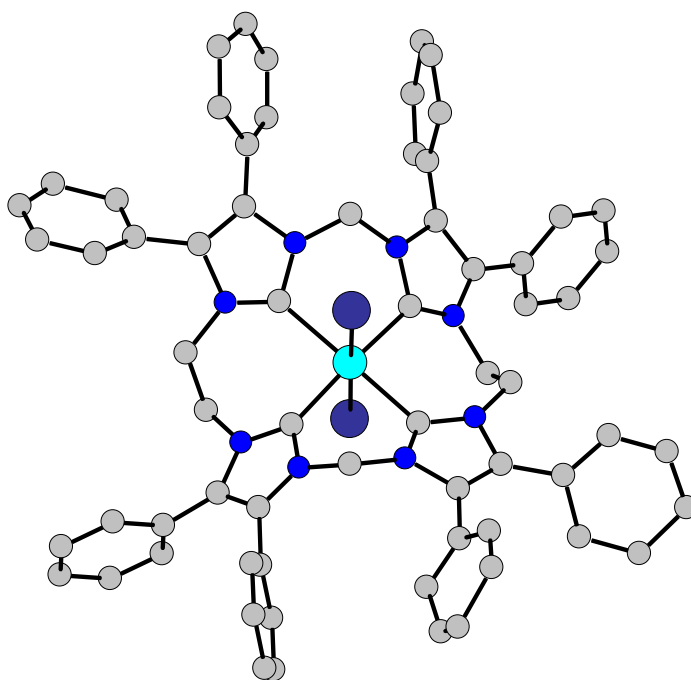


Figure 4.2. Graphical representation of $[\{(\text{Me},\text{Et}\text{-TC}^{\text{Ph}})\text{Rh}(\text{I})_2\}]\text{PF}_6$ (**6**) based on X-ray analysis. Light blue, purple, blue, and gray spheres represent Rh, I, N, and C, respectively. Counteranions, solvent molecules and H atoms have been omitted for clarity.

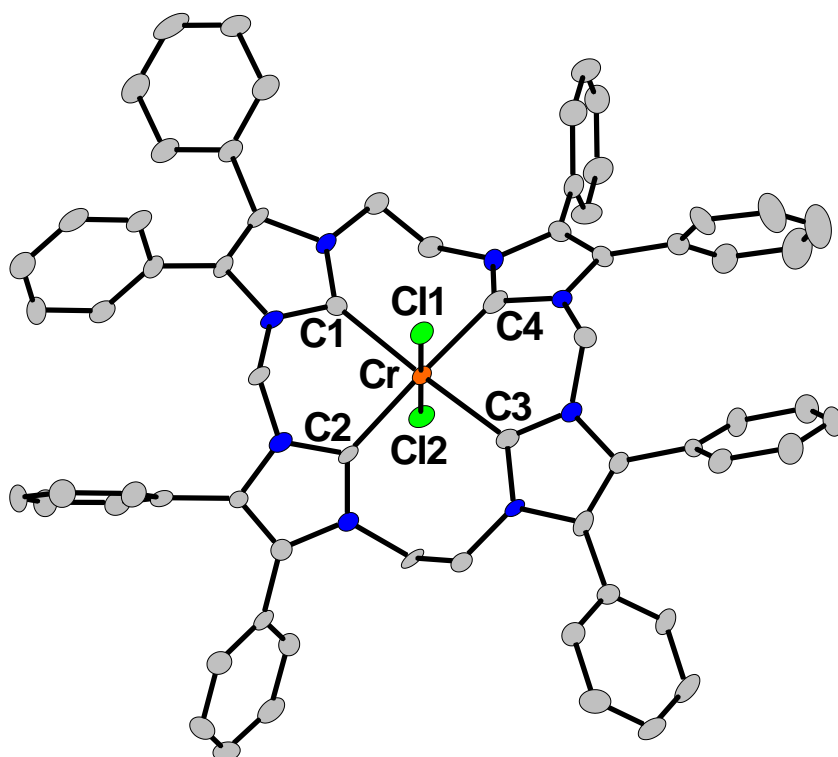


Figure 4.3. X-ray crystal structure of $[(^{\text{Me,Et}}\text{TC}^{\text{Ph}})\text{Cr}(\text{Cl})_2](\text{PF}_6)$ (10). Orange, blue, grey, and light green ellipsoids (50% probability) represent Cr, N, C, and Cl, respectively. Counteranions, solvent molecules, and H atoms have been omitted for clarity. Bond distances (Å) and angles (deg): Cr-C1, 2.135(5); Cr-C2, 2.101(5); Cr-C3, 2.142(5); Cr-C4, 2.094(6); Cr-Cl1, 2.340(2); Cr-Cl2, 2.356(2); C1-Cr-C3, 172.6(2); C2-Cr-C4, 170.6(2).

Conclusion

In conclusion, we have synthesized a dimeric silver NHC transmetallating reagent that reacts with a wide variety of di- and trivalent metal halides to give mononuclear tetracarbene complexes. These silver complexes were characterized by ^1H and ^{13}C NMR spectroscopy, ESI-MS and single-crystal X-ray diffraction, all of which demonstrate that they are dimeric in the solid-state and in solution. These silver reagents transmetallate NHCs to nine different metal salts from the first to third row on the periodic table in moderate to high yield. All of the metal tetracarbene complexes were structurally characterized by single-crystal X-ray diffraction, as well as ESI-MS and other spectroscopic techniques. The X-ray crystal structures demonstrate that the ligand only undergoes minimal distortions to bind each site on the equatorial plane of the metal. The complexes formed for the three first-row metals, chromium, iron and cobalt, are rare examples of silver NHC transmetallation to these metals. The redox active transmetallation to chromium is particularly significant since early metal NHC chemistry is underdeveloped, and this complex is the first tetracarbene on this metal. Likewise, the gold complex is the first example of a tetracarbene on gold. Given the importance of the few macrocyclic tetracarbenes that have been previously synthesized, this transmetallation strategy demonstrates that macrocyclic tetracarbenes can be prepared on metals across the periodic table.

Experimental

All reactions were performed under a dry nitrogen atmosphere with the use of either a drybox or standard Schlenk techniques. Solvents were dried on an Innovative Technologies (Newburgport, MA) Pure Solv MD-7 Solvent Purification System and degassed by three freeze-pump-thaw cycles on a Schlenk line to remove O₂ prior to use. DMSO-*d*₆, acetonitrile-*d*₃, and chloroform-*d* were degassed by three freeze-pump-thaw cycles prior to drying over activated molecular sieves. These NMR solvents were then stored under N₂ in a glovebox. (^{Me,Et}TC^{Ph})(OTf)₄ and (^{Me,Et}TC^{Ph})(I)₄,³⁸ were prepared as described previously. Characterization of [(^{Me,Et}TC^{Ph})Pt](PF₆)₄ and [(^{Me,Et}TC^{Ph})Fe(NCCH₃)₂](PF₆)₄ have been previously reported.^{38, 66} All other reagents were purchased from commercial vendors and used without purification. ¹H, ¹³C{¹H}, and ¹⁹F NMR spectra were recorded at ambient temperature, unless otherwise noted, on a Varian Mercury 300 MHz or a Varian VNMRs 500 MHz narrow-bore broadband system. ¹H and ¹³C NMR chemical shifts were referenced to the residual solvent. ¹⁹F NMR chemical shifts are reported relative to an external standard of neat CFCl₃. All mass spectrometry analyses were conducted at the Mass Spectrometry Center located in the Department of Chemistry at the University of Tennessee. The ESI/MS analyses were performed using a QSTAR Elite quadrupole time-of-flight (QTOF) mass spectrometer with an electrospray ionization source from AB Sciex (Concord, Ontario, Canada). Mass spectrometry sample solutions of metal complexes were prepared in acetonitrile. Infrared

spectra were collected on a Thermo Scientific Nicolet iS10 with a Smart iTR accessory for attenuated total reflectance. UV-vis measurements were taken inside a dry glovebox on an Ocean Optics USB4000 UV-vis system with 1 cm path length quartz crystal cell. Cyclic voltammetry measurements were made inside a dry glovebox using a BAS Epsilon electrochemical analyzer with a platinum working electrode, platinum wire counter electrode, and Ag/AgNO₃ reference electrode. All potentials were measured versus an external standard of ferrocene. Carbon, hydrogen, and nitrogen analyses were obtained from Atlantic Microlab, Norcross, GA.

Synthesis of $(^{\text{Me,Et}}\text{TC}^{\text{Ph}})(\text{PF}_6)_4$ (1a). $(^{\text{Me,Et}}\text{TC}^{\text{Ph}})(\text{I})_4$ (2.933g, 1.997 mmol) and thallium hexafluorophosphate (2.790g, 7.987 mmol) were added to a 100-mL round-bottom flask followed by the addition of 10 mL of DMSO and 60 mL of acetonitrile. The slurry was allowed to stir for 24 hours. The mixture was then filtered over Celite into a 500-mL Erlenmeyer flask. Water (200 mL) was added to the solution to yield a white precipitate which was collected on a fine sintered frit as the pure white powder product (2.612 g, 84.9% yield). ^1H NMR (DMSO- d_6 , 499.74 MHz): δ 10.04 (s, 4H), 7.44 (m, 16H), 7.26 (t, J = 7.5 Hz, 8H), 7.17 (d, J = 7.5 Hz, 8H), 6.98 (d, J = 7.5 Hz, 8H), 6.63 (s, 4H), 4.67 (s, 8H). $^{13}\text{C}\{^1\text{H}\}$ NMR (DMSO- d_6 , 125.66 MHz): δ 136.7, 132.7, 132.5, 131.0, 130.6, 130.2, 129.4, 123.1, 122.2, 55.9, 46.8. ^{19}F NMR (DMSO- d_6 , 470.39 MHz): δ -70.55 (d, J = 705.6 Hz). IR (neat): 3145, 3067, 1560, 1445, 1372, 1336, 1278, 1254, 1241,

1226, 1177, 1027, 765 cm^{-1} . ESI/MS (m/z): $[\text{M-PF}_6]^+$ 1395.36, $[\text{M-2PF}_6]^{2+}$ 625.19, $[\text{M-3PF}_6]^{3+}$ 368.48. Anal. Calcd for $\text{C}_{66}\text{H}_{56}\text{F}_{24}\text{N}_8\text{P}_4$: C, 51.44; H, 3.66; N, 7.27. Found: C, 50.64; H, 3.78; N, 7.17.

Synthesis of $[\{(\text{Me},\text{EtTC}^{Ph})\text{Ag}\}_2\text{Ag}_2](\text{PF}_6)_4$ (2a**).** $(\text{Me},\text{EtTC}^{Ph})(\text{PF}_6)_4$ (1.455 g, 0.9442 mmol) (**1a**) and silver(I) hexafluorophosphate (0.477 g, 1.89 mmol) were added to a 20-mL vial wrapped in aluminum foil and dissolved in 15 mL of DMSO while stirring and heating to 90 °C. After 10 min, triethylamine (0.477 g, 4.72 mmol) was added and allowed to stir for 48 h. The reaction mixture was cooled to rt and brought out of the glovebox. The solution was added to a 200-mL beaker and quenched with 150 mL of water to yield a white precipitate. The white powder was collected on a 60-mL fine sintered glass frit. The powder was then purified by dissolving in 40 mL of acetone in the sintered frit, filtering, and triturating with excess water (200 mL). The resulting fine powder was collected on a 60-mL fine sintered glass frit, which yielded the pure white powder product (1.24 g, 89.6% yield). Single-crystals suitable for X-ray diffraction were grown by layering an acetone solution of **2a** with water to give colorless needles. ^1H NMR (CD_3CN , 499.74 MHz): δ 7.65 (t, $J = 7.5$ Hz, 4H), 7.58 (t, $J = 6.5$ Hz, 4H), 7.48 (t, $J = 8.0$ Hz, 8H), 7.41 (t, $J = 7.5$ Hz, 4H), 7.36 (t, $J = 8.0$ Hz, 4H), 7.26 (t, $J = 8.0$ Hz, 8H), 7.19 (m, 16H), 7.09 (s, 8H), 6.96 (d, $J = 7.0$ Hz, 8H), 6.79 (s, 8H), 6.62 (d, $J = 14.5$ Hz, 4H), 6.10 (d, $J = 7.5$ Hz, 8H), 6.02 (d, $J = 13.5$ Hz, 4H), 5.05 (td, $J_1 = 13.5$ Hz, $J_2 = 3.5$ Hz, 4H), 4.82 (dd, $J_1 = 15.5$ Hz, $J_2 = 2.0$ Hz, 4H), 4.44 (m,

4H), 4.03 (d, $J = 14.0$ Hz, 4H). ^{13}C NMR (CD_3CN , 125.66 MHz): δ 182.83 ($J^{109}_{\text{Ag-C}} = 214.9$ Hz, $J^{107}_{\text{Ag-C}} = 181.0$ Hz), 176.85 ($J^{109}_{\text{Ag-C}} = 218.7$ Hz, $J^{107}_{\text{Ag-C}} = 188.5$ Hz), 137.00 (d, $J_{\text{Ag-C}} = 5.8$ Hz), 135.91 (d, $J_{\text{Ag-C}} = 5.3$ Hz), 135.21 (d, $J_{\text{Ag-C}} = 5.3$ Hz), 133.95 (d, $J_{\text{Ag-C}} = 5.0$ Hz), 132.25, 131.99, 131.81, 131.71, 131.62, 131.47, 131.28, 131.11, 130.55, 130.20, 130.09, 126.91, 126.30, 125.53, 125.48, 61.85, 51.06, 49.16. ^{19}F NMR (CD_3CN , 470.39 MHz): δ -72.81 (d, $J = 705.6$ Hz). IR (neat): 2950, 2917, 2868, 2837, 1709, 1488, 1447, 1376, 1359, 1321, 1261, 1221, 1168, 1074, 1019, 827, 761, 739, 696 cm^{-1} . ESI/MS (m/z): $[\text{M}-2\text{PF}_6]^{2+}$ 1317.70, $[\text{M}-3\text{PF}_6]^{3+}$ 829.82, $[\text{M}-4\text{PF}_6]^{4+}$ 586.37. Electrochemistry (vs. ferrocene in CH_3CN with $(\text{TBA})(\text{PF}_6)$ as supporting electrolyte): -1848 mV (rev.), -2005 mV (rev.). Anal. Calcd for $\text{C}_{132}\text{H}_{104}\text{Ag}_4\text{F}_{24}\text{N}_{16}\text{P}_4$: C, 54.19; H, 3.58; N, 7.66. Found: C, 53.20; H, 3.83; N, 7.59..

General Transmetallation Reaction. $[\{(\text{Me}, \text{EtTC}^{Ph})\text{Ag}\}_2\text{Ag}_2](\text{X})_4$ (**2**) and the corresponding metal salt was added to a 20-mL vial followed by 4 mL of methylene chloride and 4 mL of tetrahydrofuran. The reaction mixture was stirred and heated at the designated temperature overnight. After allowing the reaction to cool to room temperature, the silver halide was filtered away over Celite. The remainder of the work-up for each complex is described separately below.

Synthesis of $[(^{\text{Me,Et}}\text{TC}^{\text{Ph}})\text{Pt}](\text{PF}_6)_2$ (3**).** The general transmetallation reaction was followed using platinum(II)bisbenzonitrile chloride (0.0318 g, 0.067 mmol) and **2a** (0.0986 g, 0.0337 mmol) in acetonitrile (10 mL) at room temperature. Removal of volatiles under reduced pressure yielded the pure product as a white powder (0.080 g, 0.055 mmol, 82% yield).

Synthesis of $[(^{\text{Me,Et}}\text{TC}^{\text{Ph}})\text{Rh}(\text{I})_2](\text{PF}_6)$ (6**).** The general transmetallation reaction was followed using rhodium(III) iodide (0.0146 g, 0.0301 mmol) and **2a** (0.0441 g, 0.0151 mmol) in THF (5 mL) and DMSO (1 mL) and was heated to 60 °C. The volatiles were removed from the resulting solution under reduced pressure to yield the pure red powder (0.032 g, 72% yield). Crystals suitable for single-crystal X-ray diffraction were obtained by layering water into a solution of **6** in acetonitrile to yield red plates. ^1H NMR (CD_3CN , 599.77 MHz): δ 7.43 (m, 10H), 7.37 (m, 10H), 7.29 (t, $J = 7.8$ Hz, 4H), 7.22 (d, $J = 7.2$ Hz, 6H), 7.17 (t, $J = 7.8$ Hz, 6H), 7.09 (d, $J = 7.8$ Hz, 4H), 6.40 (s, 4H), 4.58 (s, 8H). ^{13}C NMR (150.83 MHz, CD_3CN): δ 167.37 ($J_{\text{Rh-C}} = 33.2$ Hz), 135.09, 132.31, 132.12, 131.75, 130.44, 129.79, 129.74, 128.38, 127.33, 50.57, 41.37. ^{19}F NMR (470.39 MHz, CD_3CN): δ -72.74 (d, $J = 705.6$ Hz). IR (neat) 3053, 2923, 2853, 1979, 1557, 1489, 1445, 1402, 1367, 1228, 1182, 1076, 1017, 833, 766, 740, 697 cm^{-1} . ESI/MS (m/z): $[\text{M-PF}_6]^+$ 1313.10, $[\text{M-2I-PF}_6]^{3+}$ 353.12; UV-vis (CH_2Cl_2) λ_{max} , nm (ϵ): 463 (740). Anal. Calcd for $\text{C}_{66}\text{H}_{52}\text{F}_6\text{I}_2\text{N}_8\text{P}_1\text{Rh}_1$: C, 54.34; H, 3.59; N, 7.68. Found: C, 53.23; H, 4.07; N, 7.31.

Synthesis of $[(^{\text{Me,Et}}\text{TC}^{\text{Ph}})\text{Fe}(\text{NCCH}_3)_2](\text{PF}_6)_2$ (8**).** The general transmetallation reaction was followed using iron(II) iodide (0.0302 g, 0.0975 mmol) and **2a** (0.1425 g, 0.04871 mmol). Addition of acetonitrile followed by removal of volatiles under reduced pressure yielded the pure product as a red powder (0.124 g, 0.0897 mmol, 92.0% yield). The product was crystallized by slow evaporation of diethyl ether into an acetonitrile solution of **8** to afford red crystals.

Synthesis of $[(^{\text{Me,Et}}\text{TC}^{\text{Ph}})\text{Cr}(\text{Cl})_2]\text{PF}_6$ (10**).** The general transmetallation reaction was followed using chromium(II) chloride (0.0232 g, 0.0189 mmol) and **2a** (0.111 g, 0.0378 mmol) at room temperature. The product was purified by crystallization via vapor diffusion of diethyl ether into the filtered reaction mixture to afford blue crystals (0.0532 g, 57.4% Yield). Crystals suitable for X-ray diffraction were grown by slow evaporation of an acetonitrile solution of **10** to yield blue plates. IR (neat) 2952, 1488, 1446, 1358, 1340, 1314, 1265, 1161, 1059, 1020, 836, 764, 735, 698 cm^{-1} . UV-vis (CH_3CN) λ_{max} , nm (ϵ): 570 (17). ESI/MS (m/z): $[\text{M-PF}_6]^+$ 1078.31, $[\text{M-PF}_6\text{-Cl}]^{2+}$ 521.67, $[\text{M-PF}_6\text{-2Cl}]^{3+}$ 336.12. Electrochemistry (vs. ferrocene in CH_3CN with $(\text{TBA})(\text{PF}_6)$ as supporting electrolyte): +1314 mV (irr.), -1995 mV (irr.). Anal. Calcd for $\text{C}_{67}\text{H}_{54}\text{Cl}_4\text{Cr}_1\text{F}_6\text{N}_8\text{P}_1$ (**11**· CH_2Cl_2): C, 61.43; H, 4.15; N, 8.55. Found: C, 61.41; H, 4.20; N, 8.66.

X-ray Structure Determinations. X-ray diffraction measurements were performed on single-crystals coated with Paratone oil and mounted on glass

fibers or mounted on nylon CryoLoops (Hampton Research). Each crystal was frozen under a stream of N₂ while data were collected on a Bruker APEX diffractometer. Initial scans of each specimen were taken to obtain preliminary unit cell parameters and to assess the mosaicity (i.e., breadth of spots between frames) of the crystal to select the required frame width for data collection. For all cases frame widths of 0.5° were judged to be appropriate, and full hemispheres of data were collected using the *Bruker APEX2* software suite to carry out overlapping ϕ and ω scans at detector setting of $2\theta = 28^\circ$. Following data collection, reflections were sampled from all regions of the Ewald sphere to redetermine unit cell parameters for data integration. Following exhaustive review of collected frames, the resolution of the dataset was judged, and, if necessary, regions of the frames where no coherent scattering was observed were removed from consideration for data integration using *Bruker SAINTplus* software. Data was integrated using a narrow frame algorithm and were subsequently corrected for absorption. Absorption corrections were performed for both samples using the *SADABS* program. Space group determination and tests for merohedral twinning were carried out using *XPREP*. In all cases, the highest possible space group was chosen.

Chapter 5

Characterization and Reactivity of an Fe(IV) Tetrazene Complex

All work in this chapter was completed by S. Alan Cramer except the Mössbauer spectroscopy which was collected by our collaborators Raul Sanchez and Dr. Theodore Betley at Harvard University.

Abstract

A new iron(IV) complex supported by both a tetra-NHC and a tetrazene ligand has been explored as an additional reactionary intermediate from starting aziridination catalyst $[(^{\text{Me,Et}}\text{TC}^{\text{Ph}})\text{Fe}(\text{NCCH}_3)_2](\text{PF}_6)_2$. The tetrazene complex, $[(^{\text{Me,Et}}\text{TC}^{\text{Ph}})\text{Fe}(\text{ArN}_4\text{Ar})](\text{PF}_6)_2$ (Ar = tolyl), has been characterized by NMR spectroscopy, mass spectrometry, Mössbauer spectroscopy, single-crystal X-ray diffraction, and other spectroscopic techniques. $[(^{\text{Me,Et}}\text{TC}^{\text{Ph}})\text{Fe}(\text{ArN}_4\text{Ar})](\text{PF}_6)_2$ has been shown to be able to decompose back to starting catalyst $[(^{\text{Me,Et}}\text{TC}^{\text{Ph}})\text{Fe}(\text{NCCH}_3)_2](\text{PF}_6)_2$ at 85 °C and even be able to perform nitrene transfer to an alkene source for aziridination.

Introduction

The synthesis of late transition metal imido complexes has been of considerable interest recently due to the expected reactivity from the metal ligand multiple bond.⁷⁸ Unlike early transition metals that favor high oxidation states, late transition metals usually do not favor metal ligand multiple bonds or higher oxidation states and therefore these reactive species are likely to be reactive transfer intermediates in processes such as amination or aziridination.⁷⁹ However, many efforts to prepare late transition metal imidos result in systems

which are not capable of performing the nitrene transfer in a catalytic manner. The incapability to perform nitrene transfer catalysis from an imido is generally problematic for one of 3 reasons: either the prepared imido complex has been stabilized by sterics and therefore cannot transfer to an external molecule,^{11b} the imido complex is too stable as compared to the starting material,^{19a} or the imido complex can perform a single transfer reaction but cannot regenerate the reactive imido intermediate.^{11c}

Organic azides are particularly desirable nitrene sources for the preparation of transition metal imido complexes due to the 'green' byproduct of N₂ that would result from following 'N-R' transfer catalytic reactions.^{7, 66} Although several imido complexes have been prepared with organic azides, most examples of metallo-tetrazene complexes were prepared from the attempted synthesis of imido complexes with organic azides.⁸⁰ The resulting tetrazene has been suggested to be a product of cycloaddition of an additional equivalent of organic azide to a reactive metal imido. Tetrazene ligands present different bonding modes depending on the electrophilicity of the metal that it is bound to. Gade defined these binding modes in three categories (Figure 5.1): a neutral donor ligand (Figure 5.1A), a delocalized π system including the metal atom (Figure 5.1B) and a dianionic ligand with a single localized N=N double bond (Figure 5.1C).⁸¹ Types A and B are common for late transition metals (M = Fe, Co, etc.) and type C is regarded as binding mode for early transition metals (M = Zr, Cr, etc.). Outside of thermal decomposition to produce the respective

diazene fragment and N_2 ,⁸² the group transfer reactivity of these ligands remains largely unexplored. We wanted to ask the question if a tetrazene is synthesized during a catalytic cycle, is it an end point or an additional side step in the cycle?

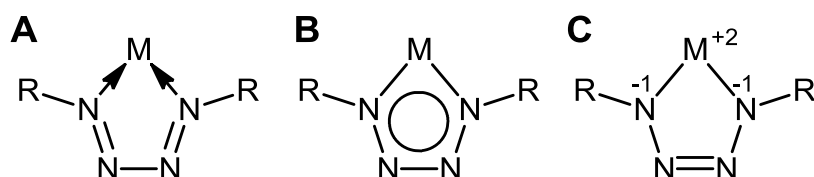


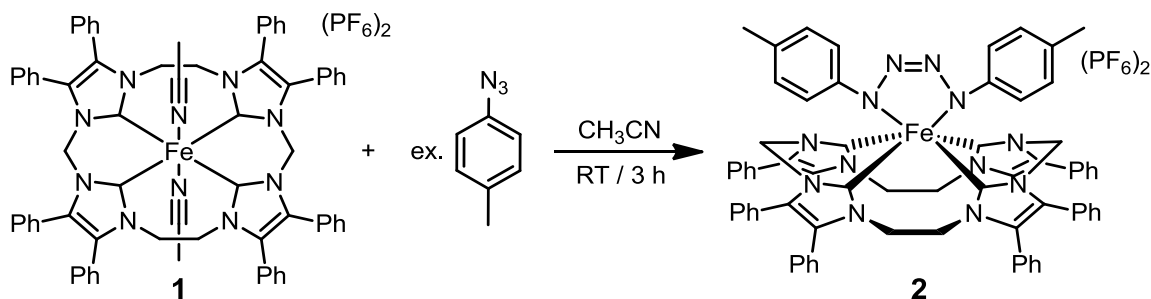
Figure 5.1. Gade's classes of N_4 binding modes found in tetrazene ligands.

Recently, our group has reported an Fe^{II} -tetracarbene that performs catalytic " C_2+N_1 " aziridination with aryl azides and mono-, di-, tri-, and tetrasubstituted aliphatic alkenes.⁶⁶ Although we were unable to isolate the reactionary intermediate, we proposed the intermediate was an $Fe(IV)$ imido as it was evidenced by ESI/MS. Although $Fe(IV)$ is very relevant biologically,⁸³ the synthesis of $Fe(IV)$ complexes is still in its infancy.^{17d, 18c, 84} One of these rare examples is a terminal $Fe(IV)$ -oxo supported by a macrocyclic tetracarbene ligand similar to the ligand used for catalytic aziridination.^{84b} Herein we report the isolation of the first 6-coordinate low spin ($S = 0$) $Fe(IV)$ complex, which is supported by both a tetracarbene and tetrazene ligand, and report its group transfer capabilities.

Characterization and Reactivity of Fe(IV) Tetrazene

We previously reported the synthesis of $[(^{\text{Me},\text{Et}}\text{TC}^{\text{Ph}})\text{Fe}(\text{NCCH}_3)_2](\text{PF}_6)_2$ (**1**) which performs aziridination with organic azides and aliphatic alkenes.⁶⁶ As previously reported **1** forms $[(^{\text{Me},\text{Et}}\text{TC}^{\text{Ph}})\text{Fe}=\text{NAr}](\text{PF}_6)_2$ with the addition aryl azide which was evidenced by ESI/MS; however, addition of excess tolyl azide in acetonitrile yields $[(^{\text{Me},\text{Et}}\text{TC}^{\text{Ph}})\text{Fe}(\text{ArN}_4\text{Ar})](\text{PF}_6)_2$ (**2**) (Ar = tolyl) in 2 hours at room temperature (Scheme 5.1). As previously reported with other tetrazene complexes,⁸⁰ it is likely this complex is formed by a 1,3-cycloaddition of an additional equivalent of tolyl azide to $[(^{\text{Me},\text{Et}}\text{TC}^{\text{Ph}})\text{Fe}=\text{NAr}](\text{PF}_6)_2$.

Scheme 5.1. Synthesis of $[(^{\text{Me},\text{Et}}\text{TC}^{\text{Ph}})\text{Fe}(\text{ArN}_4\text{Ar})](\text{PF}_6)_2$.



Spectroscopic characterization of **2** was consistent with the formation of a tetrazene. ESI/MS of **2** showed a peak at m/z 625.68 associated with $[(^{\text{Me},\text{Et}}\text{TC}^{\text{Ph}})\text{Fe}(\text{ArN}_4\text{Ar})]^{2+}$ and a peak at m/z 1395.43 associated with $\{[(^{\text{Me},\text{Et}}\text{TC}^{\text{Ph}})\text{Fe}(\text{ArN}_4\text{Ar})](\text{PF}_6)\}^+$, both of which had the expected isotopic distribution ratios. Diastereotopic splitting on the macrocyclic ligand of **2** is observable in ^1H NMR, which is indicative of the rigidity of **2** in solution. ^{13}C NMR

is also consistent with the addition of a tetrazene ligand. The Fe^{IV}-NHC chemical shift (169.79 ppm) is shifted significantly upfield from the starting Fe^{II}-NHC, **1** (196.65 ppm). Since **2** is the first diamagnetic Fe^{IV}-NHC complex, a valid comparison of ¹³C NMR chemical shifts to literature values is not possible. Additional characterization of **2** included electrochemical analysis, which showed a reversible one electron oxidation wave at -1055 mV in an acetonitrile solution, which can be assigned as Fe^{IV}/Fe^{III}. Complex **2** is also air stable in solution and solid state.

The X-ray crystal structure of **2** confirms the addition of the tetrazene ligand to **1** (Figure 5.2). Interestingly, the six-coordinate complex adopts a distorted trigonal prismatic geometry ($\phi_{\text{Ave}} = 10.4^\circ$) over an octahedral geometry as seen in the starting material, **1** (trigonal prismatic, $\phi = 0^\circ$; octahedral, $\phi = 60^\circ$).⁸⁵ This unusual coordination geometry is most likely due to the tetracarbene ligand not being flexible enough to adopt an octahedral geometry. Notably, the crystal structure provides a hint as to the process of the aziridination reaction. The alkene must be present near the metal imide prior to group transfer and the tetracarbene ligand is flexible enough to accommodate an additional ligand in a cis position. The average Fe-NHC bond length is 1.98 Å, which is slightly shorter than the average bond length for **1**, but is in line with Meyer's octahedral Fe^{IV}-oxo tetracarbene.^{84b} The shorter bond length of N₁₀-N₁₁ versus N₉-N₁₀ or N₁₁-N₁₂ is indicative of a dianionic tetrazene (Figure 5.1, Type C). If in fact the tetrazene ligand is dianionic, then the metal center must formally be Fe(IV). Typically iron

tetrazenes have adopted the Type B binding mode but a dianionic binding mode (Type C) has been prepared by reduction of the tetrazene ligand.^{80c}

In order to confirm the presence of a low spin ($S = 0$) Fe^{IV} complex, Mössbauer spectroscopy of **2** was necessary. For comparative purposes, the Mössbauer of the starting Fe^{II} tetracarbene complex, **1**, was collected (Figure 5.3A). The Mössbauer spectra collected for **1** contained a small impurity which has been modeled and is indicated by the modeled green line. The Mössbauer isomer shift and quadruple splitting of **1** ($\delta = 0.21$ mm/s and $|\Delta E_Q| = 1.98$ mm/s, respectively) are in agreement with Meyer's octahedral Fe^{II} tetracarbene ($\delta = 0.23$ mm/s and $|\Delta E_Q| = 2.10$ mm/s, respectively).^{84b} Mössbauer spectroscopy of **2** (Figure 5.3B) identifies the iron metal center as a low spin ($S = 0$) Fe^{IV} based on its reported isomer shift, quadruple splitting ($\delta = -0.01$ mm/s and $|\Delta E_Q| = 0.62$ mm/s, respectively) and due to apparent diamagnetism observed from NMR.

While a number of examples of tetrazene complexes have now been prepared,⁸⁰ with the exception of decomposition products,⁸² reactivity of these ligands have largely been unexplored. Complex **2** was initially tested to determine if the tetrazene fragment does in fact decompose to form the corresponding azobenzene derivative as reported by other previously reported tetrazene complexes. As determined by NMR and TGA analysis, at 85 °C, N_2 is evolved and the azobenzene derivative was detected by ^1H NMR and DART/MS. We wanted to take the process a step further and determine if the tetrazene

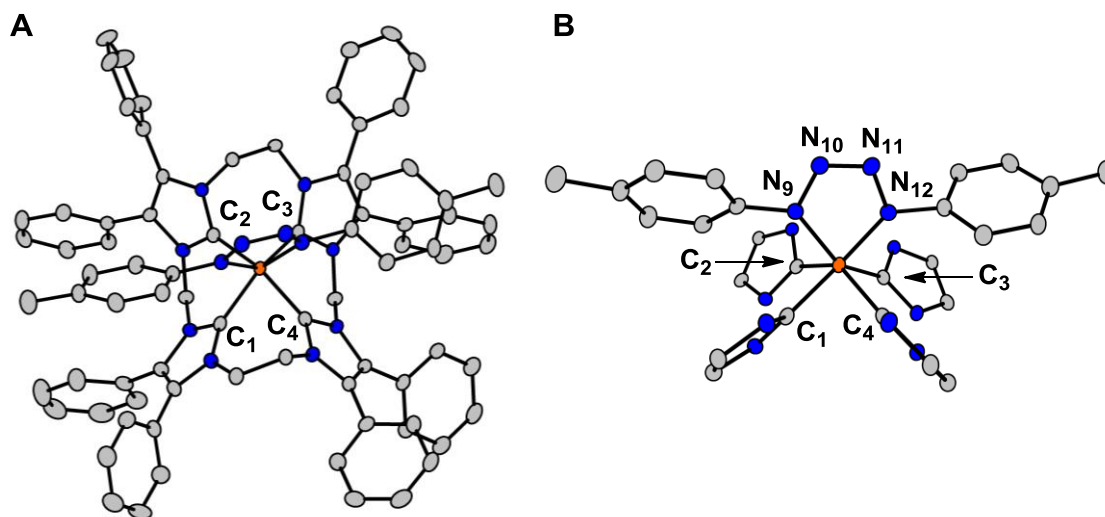


Figure 5.2. X-ray crystal structure of $[(^{\text{Me,Et}}\text{TC}^{\text{Ph}})\text{Fe}(\text{ArN}_4\text{Ar})](\text{PF}_6)_2$ (**2**). Structure shown as labeled crystal structure (A) and with selected parts of the macrocycle omitted for clarity (B). Orange, blue and grey ellipsoids (50% probability) represent Fe, N and C, respectively. Solvent molecules and H atoms have been omitted for clarity. Selected bond distances (Å) and angles (deg.) are as follows: Fe-C₁, 1.953(4) ; Fe-C₂, 1.986(4); Fe-C₃, 1.951(4); Fe-C₄, 2.008(4); Fe-N₉, 1.894(3); N₉-N₁₀, 1.350(4); N₁₀-N₁₁, 1.286(5); N₁₁-N₁₂, 1.343(5); C₁-Fe-N₉, 88.4(2); C₁-Fe-C₄, 85.8(2); N₉-Fe-N₁₂, 77.2(1).

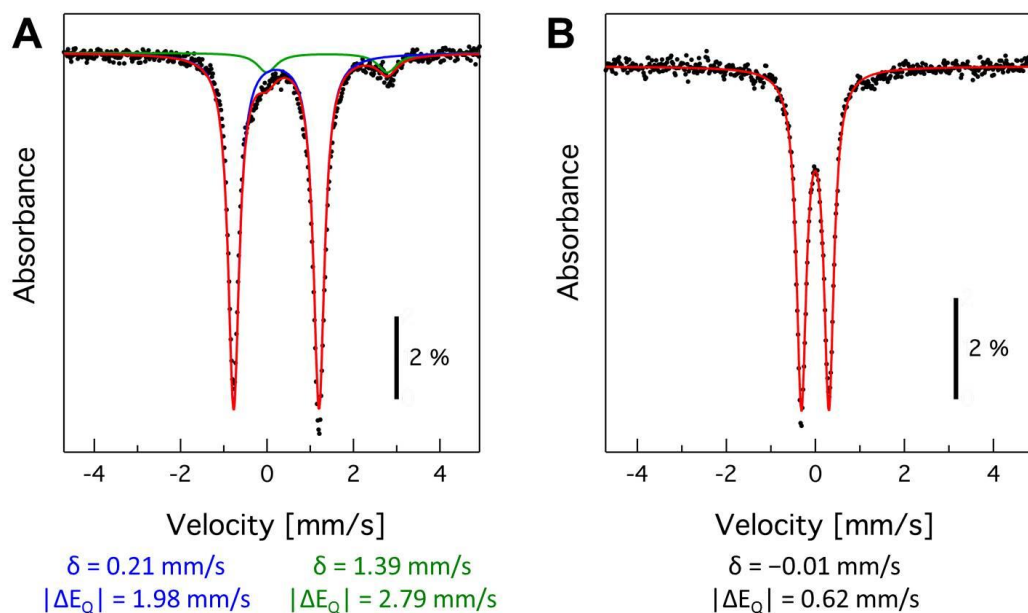


Figure 5.3. Mössbauer spectra of complexes $[(^{\text{Me,Et}}\text{TC}^{\text{Ph}})\text{Fe}(\text{CH}_3\text{CN})_2](\text{PF}_6)_2$ (left) and $[(^{\text{Me,Et}}\text{TC}^{\text{Ph}})\text{Fe}(\text{ArN}_4\text{Ar})](\text{PF}_6)_2$ (right). Spectra Collected by Raul Sanchez in Dr. Theodore Betley's lab at Harvard University.

complex is a side product or also an intermediate in the original aziridination catalytic cycle. In order to determine this, the tetrazene complex was added to cyclooctene, and heated while stirring overnight. Removal of volatiles followed by ^1H NMR and DART/MS analysis revealed the presence of both dimethylazobenzene and the aziridine product in approximately a 2:1 ratio, respectively. Not only is the formation of **2** not an end point in the catalytic cycle, but it too acts as an aziridination intermediate in the updated catalytic cycle (Figure 5.4).

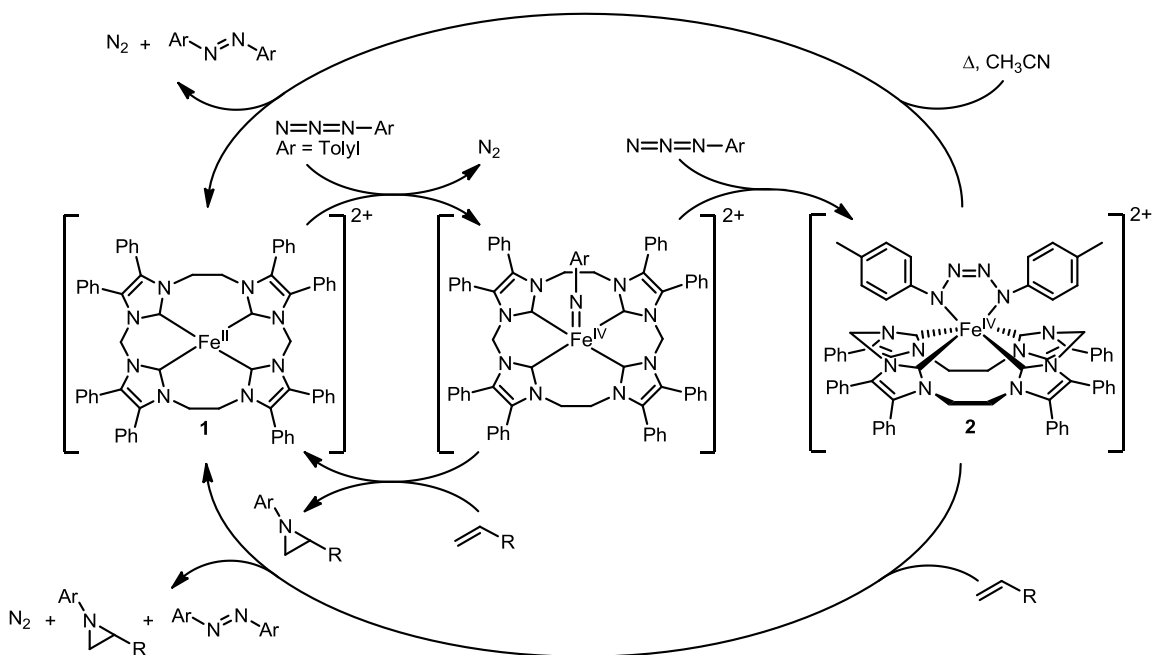


Figure 5.4. Modified proposed aziridination mechanism with catalyst $[(^{\text{Me,Et}}\text{TC}^{\text{Ph}})\text{Fe}(\text{CH}_3\text{CN})_2](\text{PF}_6)_2$.

Conclusion

In conclusion, we have synthesized the first 6-coordinate low spin ($S = 0$) iron(IV) complex, $[(^{\text{Me,Et}}\text{TC}^{\text{Ph}})\text{Fe}(\text{ArN}_4\text{Ar})](\text{PF}_6)_2$, supported by both a tetrazene and tetracarbenes ligand. The complex was synthesized by addition of excess tolyl azide to aziridination catalyst, $[(^{\text{Me,Et}}\text{TC}^{\text{Ph}})\text{Fe}(\text{CH}_3\text{CN})_2](\text{PF}_6)_2$. The clean conversion of $[(^{\text{Me,Et}}\text{TC}^{\text{Ph}})\text{Fe}(\text{ArN}_4\text{Ar})](\text{PF}_6)_2$ to $[(^{\text{Me,Et}}\text{TC}^{\text{Ph}})\text{Fe}(\text{CH}_3\text{CN})_2](\text{PF}_6)_2$ was confirmed by NMR spectroscopy and mass spectrometry. ^{13}C NMR shows a significant upfield chemical shift compared to $(^{\text{Me,Et}}\text{TC}^{\text{Ph}})\text{Fe}(\text{CH}_3\text{CN})_2](\text{PF}_6)_2$, and notably it is the first reported ^{13}C NMR Fe^{IV} -NHC chemical shift. Single-crystal X-

ray diffraction confirmed the addition of the tetrazene ligand and that $[(^{\text{Me,Et}}\text{TC}^{\text{Ph}})\text{Fe}(\text{ArN}_4\text{Ar})](\text{PF}_6)_2$ was in a distorted trigonal prismatic geometry. The crystal structure suggests the tetrazene ligand was bonded in a dianionic manner based which is indicative of an iron(IV) metal center. The metal center was confirmed an iron(IV) ($S = 0$) by Mössbauer spectroscopy. Finally, reactivity studies suggest that $[(^{\text{Me,Et}}\text{TC}^{\text{Ph}})\text{Fe}(\text{ArN}_4\text{Ar})](\text{PF}_6)_2$ decomposes to form 4,4'-dimethylazobenzene and 1-methyl-7-(*p*-tolyl)-7-azabicyclo[4.1.0]heptane in neat cyclooctene which shows $[(^{\text{Me,Et}}\text{TC}^{\text{Ph}})\text{Fe}(\text{ArN}_4\text{Ar})](\text{PF}_6)_2$ is also an acceptable nitrene transfer source for aziridination.

Experimental

All reactions were performed under a dry nitrogen atmosphere with the use of either a drybox or standard Schlenk techniques. Solvents were dried on an Innovative Technologies(Newburgport, MA) Pure Solv MD-7 Solvent Purification System and degassed by three freeze-pump-thaw cycles on a Schlenk line to remove O_2 prior to use. Acetonitrile- d_3 , and chloroform- d were degassed by three freeze-pump-thaw cycles prior to drying over activated molecular sieves. These NMR solvents were then stored under N_2 in a glovebox. $[(^{\text{Me,Et}}\text{TC}^{\text{Ph}})\text{Fe}(\text{CH}_3\text{CN})_2](\text{PF}_6)_2$ and tolyl azide were prepared as described previously.^{46, 66} All reagents were purchased from commercial vendors and used without purification. ^1H , $^{13}\text{C}\{^1\text{H}\}$, and ^{19}F NMR spectra were recorded at ambient temperature on a Varian VNMRs 500 MHz narrow-bore broadband system. ^1H and ^{13}C NMR chemical shifts were referenced to the residual solvent. ^{19}F NMR

chemical shifts are reported relative to an external standard of neat CFCl_3 . ^{57}Fe Mössbauer spectra were measured with a constant acceleration spectrometer (SEE Co., Minneapolis, MN). Isomer shifts are quoted relative to Fe foil at room temperature. Data was analyzed and simulated with Igor Pro 6 software (WaveMetrics, Portland, OR) using Lorentzian Fitting function. Thermogravimetric analysis data was collected on a TA instruments TGA Q50 under N_2 . All mass spectrometry analyses were conducted at the Mass Spectrometry Center located in the Department of Chemistry at the University of Tennessee. The DART analyses were performed using a JEOL AccuTOF-D time-of-flight (TOF) mass spectrometer with a DART (direct analysis in real time) ionization source from JEOL USA, Inc. (Peabody, MA). The ESI/MS analyses were performed using a QSTAR Elite quadrupole time-of-flight (QTOF) mass spectrometer with an electrospray ionization source from AB Sciex (Concord, Ontario, Canada). Mass spectrometry sample solutions of metal complexes were prepared in acetonitrile. Infrared spectra were collected on a Thermo Scientific Nicolet iS10 with a Smart iTR accessory for attenuated total reflectance. UV-vis measurements were taken inside a dry glovebox on an Ocean Optics USB4000 UV-Vis system with 1 cm path length quartz crystal cell. Cyclic voltammetry measurements were made inside a dry glovebox using a BAS Epsilon electrochemical analyzer with a platinum working electrode, platinum wire counter electrode, and Ag/AgNO_3 reference electrode. All potentials were

measured versus an external standard of ferrocene. Carbon, hydrogen, and nitrogen analyses were obtained from Atlantic Microlab, Norcross, GA.

Synthesis of $[(^{\text{Me,Et}}\text{TC}^{\text{Ph}})\text{Fe}(\text{ArN}_4\text{Ar})](\text{PF}_6)_2$, (2). $[(^{\text{Me,Et}}\text{TC}^{\text{Ph}})\text{Fe}(\text{CH}_3\text{CN})_2](\text{PF}_6)_2$ (0.0154 g, 0.0112 mmol) was added to a 20-mL vial with acetonitrile (10 mL) and stirred (450 rpm) with heating at 40 °C for 20 minutes. Toly azide (50 μL) was then added to the reaction mixture and continued to be heated and stirred overnight. The volatiles were then removed *en vacuo*. The sample was then washed with diethyl ether (3x10 mL) and residual solvent was removed under reduced pressure. The sample was dissolved in acetonitrile (4 mL) and filtered over Celite. The filtrate was collected. The pure product was collected as red crystals by vapor diffusion of diethyl ether into the acetonitrile solution (0.0127g, 74.1%). ^1H NMR (CD_3CN , 499.74 MHz): δ 7.35 (m, 28H), 7.16 (m, 12H), 6.97 (d, $J = 7.4$ Hz, 8H), 6.06 (d, $J = 12.6$ Hz, 2H), 5.15 (d, $J = 13.4$ Hz, 2H), 3.52 (q, $J = 6.2$ Hz, 4H), 2.41 (d, $J = 12.6$ Hz, 4H), 2.40 (s, 6H). ^{13}C NMR (CD_3CN , 125.66 MHz): δ 169.79, 154.89, 139.16, 136.41, 134.35, 131.09, 131.00, 130.72, 130.70, 130.67, 129.76, 129.56, 126.52, 125.95, 124.56, 57.56, 44.85, 20.61. ^{19}F NMR(CD_3CN , 470.23 MHz): δ -72.42 (d, $J = 706.6$ Hz). IR (neat): 3061, 1594, 1500, 1489, 1444, 1414, 1375, 1338, 1225, 1184, 1100, 177, 1008, 926, 829, 788, 764, 696 cm^{-1} . UV-vis (CH_3CN) λ_{max} , nm (ϵ): 420 (9300). ESI/MS (m/z): $[\text{M}-\text{PF}_6]^+$ 1395.43, $[\text{M}-2\text{PF}_6]^{2+}$ 625.68. Electrochemistry (vs ferrocene in CH_3CN with $[\text{TBA}][\text{PF}_6]$ as supporting electrolyte): $\text{Fe}^{\text{IV}}/\text{Fe}^{\text{III}}$, -1055 mV. Anal. Calcd for

$\text{C}_{80}\text{H}_{66}\text{F}_{12}\text{FeN}_{12}\text{P}_2$: C, 62.34; H, 4.32; N, 10.91. Found: C, 61.43; H, 4.67; N, 11.62.

Decomposition Experiment. Complex **2** was dissolved in CD_3CN and placed into an NMR tube which was sealed with Parafilm. ^1H NMR was taken initially and then heated to 75°C overnight. ^1H NMR was then taken at 12 hour intervals at which time the heat was raised by 5°C until all **2** was converted back to complex **1** (Figure 5.5). At 85°C all of **2** had been converted back to **1** and both ^1H NMR and DART/MS confirmed the presence of 4,4'-dimethylazobenzene as compared to an external standard. Thermogravimetric analysis of pure crystals of **2** corroborated this result with a 4.3% weight loss at 90°C as compared to the expected 4.4% weight loss (**2** - CH_3CN - N_2). DART/MS (m/z): $[\text{M}+\text{H}]^+$ 211.1.

Nitrene transfer experiment. Complex **2** was added to a 20-mL vial and 5 mL of cyclooctene was added, heated to 90°C and stirred for 12 hours. After 12 hours the reaction was cooled to room temperature and all volatiles were removed under reduced pressure. Benzene was then added to the vial (4 mL), stirred for ten minutes, and filtered over Celite. The volatiles of the filtrate were again removed and dissolved in CDCl_3 . The chemical shifts of 9-(p-tolyl)-9-azabicyclo[6.1.0]nonane were previously reported and an external standard revealed the shifts of 4,4'-dimethylazobenzene in CDCl_3 . Direct integration of the

doublets in the 'aryl region' of the ^1H NMR spectra determined a 2.3:1 ratio of 4,4'-dimethylazobenzene to 9-(p-tolyl)-9-azabicyclo[6.1.0]nonane (Figure 5.6).

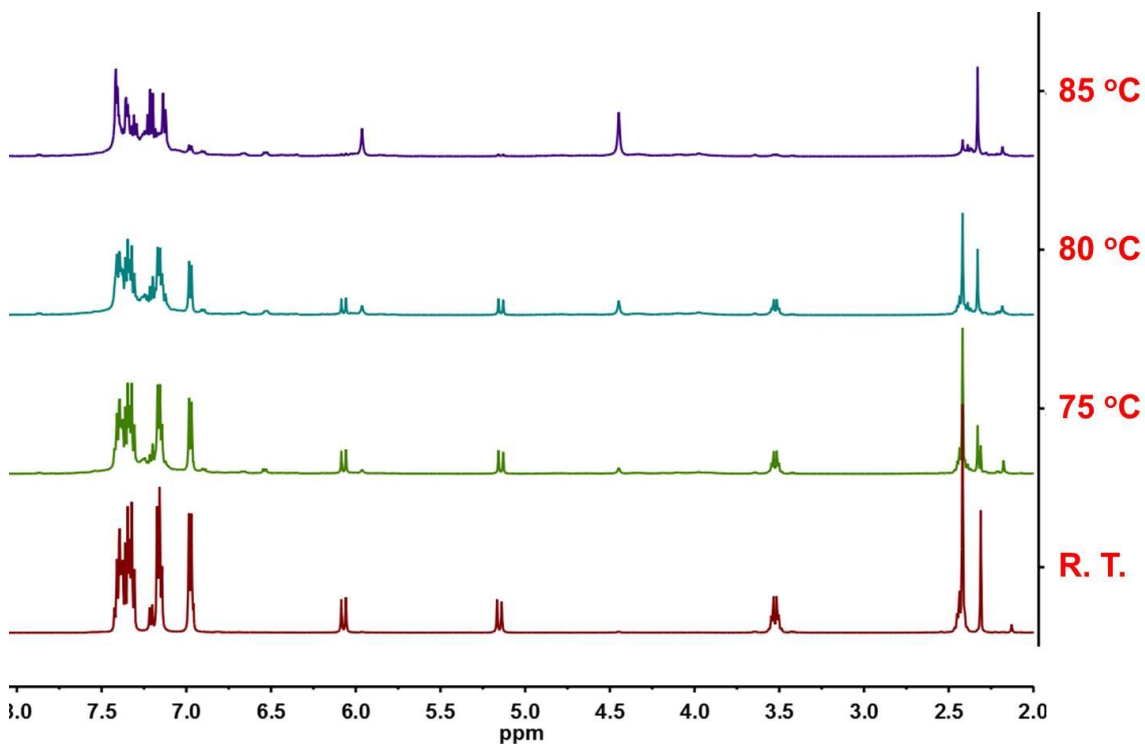


Figure 5.5. Decomposition of **2** as followed by ^1H NMR at room temperature (red), 75 °C (green), 80 °C (blue), and 85 °C (purple).

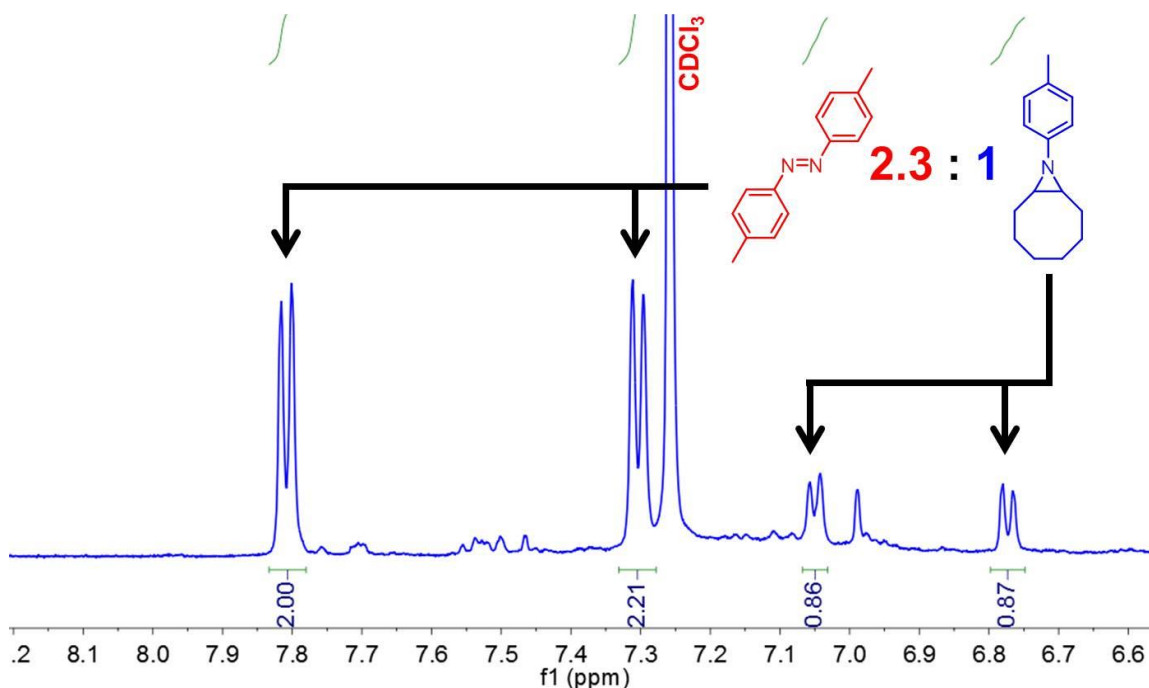


Figure 5.6. ^1H NMR of the extracted organic products from the decomposition of $[(^{\text{Me,Et}}\text{TC}^{\text{Ph}})\text{Fe}(\text{ArN}_4\text{Ar})](\text{PF}_6)_2$ in the presence of excess cyclooctene.

X-ray Structure Determinations. X-ray diffraction measurements were performed on single-crystals coated with Paratone oil and mounted on glass fibers. Each crystal was frozen under a stream of N_2 while data were collected on a Bruker APEX diffractometer. A matrix scan using at least 12 centered reflections was used to determine initial lattice parameters. Reflections were merged and corrected for Lorenz and polarization effects, scan speed, and background using SAINT 4.05. Absorption corrections, including odd and even ordered spherical harmonics were performed using SADABS, if necessary.

Space group assignments were based upon systematic absences, E statistics, and successful refinement of the structure. The structures were solved by direct methods with the aid of successive difference Fourier maps, and were refined against all data using the SHELXTL 5.0 software package.

Chapter 6

Overcoming NHCs Neutrality: Installing Tetracarbenes on Group 13 and 14 Metals

Abstract

The first tetracarbene complexes of Group 13 and 14 metals have been synthesized by employing dianionic macrocyclic tetracarbene ligands. The tin, indium, and aluminium tetracarbene complexes are structurally analogous to their porphyrin or salen analogues. The aluminium complex is the first example of multiple NHCs bound to this metal centre.

Introduction

Tetradentate ligands that bind in an equatorial manner about the metal centre are a mainstay for developing successful main group catalysts.⁸⁶ Although a plethora of examples abound, perhaps the most important auxiliary ligands of this type are salen and porphyrin derivatives (Figure 6.1A).^{86b-e} Aluminium complexes that feature both of these classes of ligands are highly reactive Lewis acids that can efficiently perform ring opening polymerization and phospho-transfer catalysis.^{86c, 87} In a similar manner, gallium and indium salen complexes have been used for ring opening polymerization of cyclic esters.^{86b,88} Finally, although tin porphyrin complexes are primarily used for scaffolding,⁸⁹ due to increased durability, tin salen complexes have found utility as catalysts for propylene carbonate formation⁹⁰ and for ring opening polymerization.⁹¹ Consequently, the establishment of a new electron-rich tetradentate equatorial framework would be a significant development that may allow for enhanced catalytic activity on main group complexes.

Despite the fact that *N*-heterocyclic carbene (NHC) ligands have been key auxiliary ligands for the discovery of new main group multiple bonds on B,⁹² Si,⁹³ and P,⁹⁴ only four examples of main group metal complexes have been synthesized with more than two NHCs.⁹⁵ Each of these four complexes produced cationic main group complexes. With the exception of two cationic tricarbene complexes, group 13 and 14 metals, have been limited to a maximum of two NHCs per metal centre (Figure 6.1B-C). One rationalisation for this deficiency of polydentate NHC complexes is the cationic charge on the resulting complex, which is not the case for porphyrin and salen complexes.

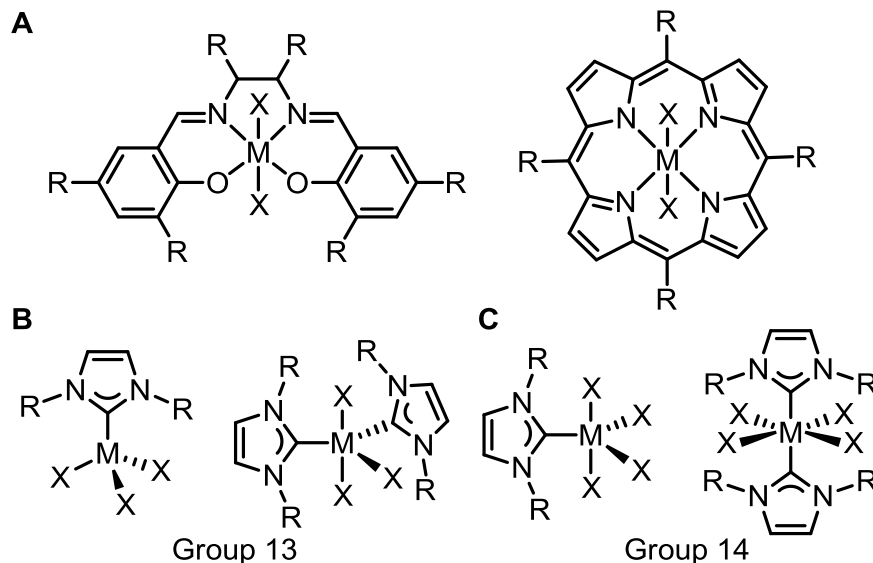


Figure 6.1. Contrasting Group 13 and 14 metal complexes. Tetradentate salen and porphyrin ligands (A) versus typical complex geometries with NHC ligands on group 13 metals (B) and group 14 metals (C).

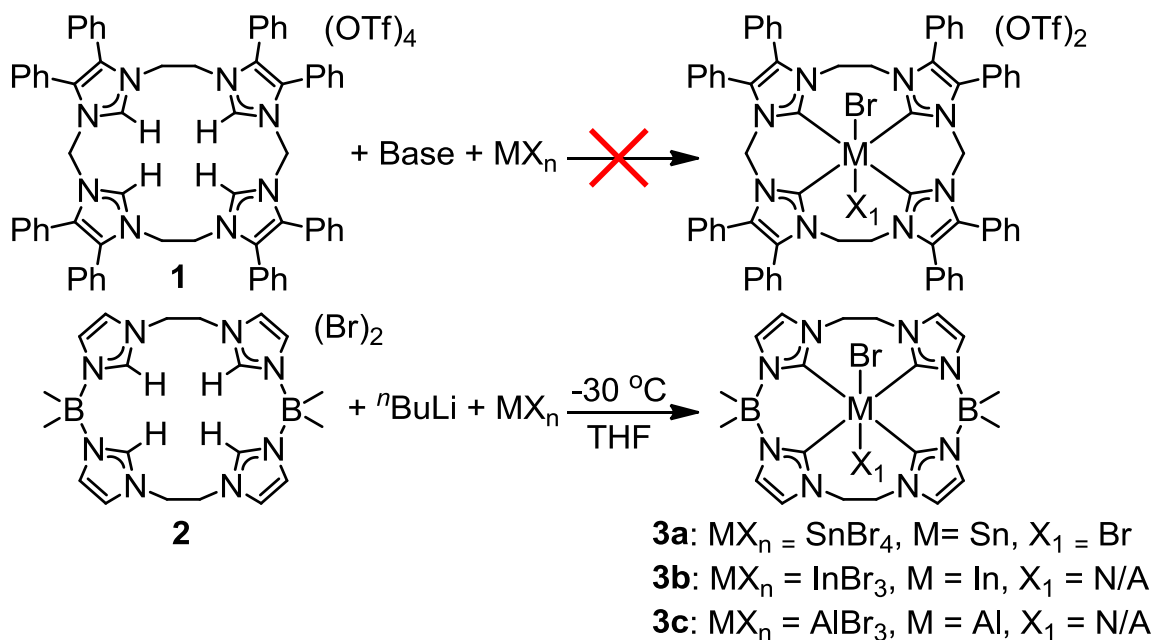
One approach to mitigating the problem of excess charge is to develop polydentate NHC ligands that are anionic. Smith has previously reported anionic bidentate and tridentate NHC ligands with borates in the backbone, but he has not reported any main group complexes with these ligands.⁹⁶ Our group recently reported the first borate-containing macrocyclic tetracarbene ligand and its associated nickel and palladium complexes.⁹⁷ In this communication, we describe the first examples of main group complexes with anionic polydentate NHC ligands. Our synthetic strategy is viable for a variety of coordination geometries and main group metals from groups 13 and 14. These tetracarbene complexes are isostructural to complexes with salen and porphyrin as the tetradentate auxiliary ligand.

Synthesis and Characterization of Tetracarbene Main Group Complexes

We initially tested the macrocyclic tetraimidazolium (^{Me,Et}TC^{Ph})(OTf)₄ (**1**) in our efforts to prepare group 13 and 14 tetracarbene complexes (Scheme 6.1). Ligand precursor **1**, which yields neutral NHCs when deprotonated, has been effectively ligated to a wide variety of transition metals either through direct deprotonation or via transmetallation from its dimeric silver complex.⁹⁸ Although these methods are effective for preparing transition metal complexes from Cr to Au, we were unsuccessful in synthesizing a group 13 or 14 metal complex with **1** (Scheme 6.1).

Since ligand precursor **1** was ineffective, we turned to the recently reported dianionic tetraimidazolium (^{BMe₂,Et}TC^H)Br₂ (**2**) (Scheme 6.1) that yielded mononuclear square planar metal complexes with Ni and Pd.⁹⁷ In situ deprotonation of **2** with *N*-butyllithium at -30 °C followed by the addition of the a main group metal bromide salt was successful for the synthesis of (^{BMe₂,Et}TC^H)SnBr₂ (**3a**), (^{BMe₂,Et}TC^H)InBr (**3b**), and (^{BMe₂,Et}TC^H)AlBr (**3c**). All three complexes bind the ligand to form an equatorial plane around the metal ion and are air sensitive in both solution and the solid state. In addition, **3b** degrades in organic solvents over a course of several hours.

Scheme 6.1. Synthesis of tetracarbene main group metal complexes.



All three metal complexes were characterized with ESI/MS, multi-nuclear NMR, and single-crystal X-ray crystallography. Even though the complexes are all neutral, high quality ESI/MS could be collected for each one. ESI/MS data for **3a** shows a peak at m/z 608.09 associated with $\{({}^{\text{BMe}_2,\text{Et}}\text{TC}^H)\text{SnBr}\}^+$ with the correct isotopic distribution. Similarly **3b** and **3c** show peaks attributed to the loss of one bromide at m/z 517.11 and 429.20 associated with $\{({}^{\text{BMe}_2,\text{Et}}\text{TC}^H)\text{In}\}^+$ and $\{({}^{\text{BMe}_2,\text{Et}}\text{TC}^H)\text{Al}\}^+$, respectively.

Since all of the main group complexes were diamagnetic, NMR data was collected for each complex. ^1H NMR of **3a** indicates that the 6-coordinate complex exhibits fluxional behaviour in solution, which is in direct contrast to **3b** and **3c** that show diastereotopic proton splitting for the ethyl protons. The fluxional behaviour is consistent with other octahedral complexes that our group has prepared,^{98b, 98c} while the more rigid **3b** and **3c** are consistent with square planar examples.^{97-98, 98c} Since these complexes are the first examples of tetracarbenes on these metals, the carbene peak position is of great interest. Although ^{13}C NMR data was collected for **3c**, the carbene carbon could not be resolved. This result was not unexpected since few carbene resonances have been previously reported for Al-NHCs resonances and they are often broad.⁹⁹ This lack of reported resonances is presumably due to the high quadrupole moment of ^{27}Al {99%, $I = 5/2$ }. More encouragingly, a ^{13}C NMR spectra of **3a** shows a resonance for the carbene carbon at 166.86 ppm that is consistent with

a tin(IV) dicarbene complex.¹⁰⁰ To probe the electronic effect of having four NHCs bound to the tin centre, we collected a ^{119}Sn NMR spectra, which showed a chemical shift of -1099.35 ppm. This resonance is shifted drastically upfield when compared to a previously prepared octahedral Sn(IV) dicarbene complex that has a chemical shift of -662.99 ppm.¹⁰⁰ The large upfield chemical shift may be attributed to increased shielding effects from the additional strong σ -donor NHCs.¹⁰¹

The X-ray crystal structure of **3a** (Figure 6.2) provided a potential clue for the observed ^1H NMR fluxional behaviour, as two conformations of the ligand around the Sn metal centre were found in the unit cell. The first conformation shows significant bending of one of the bromide ligands from an ideal octahedral geometry due to the steric repulsion from the borate methyl substituents (Figure 6.2A). In order to accommodate both borate moieties below the ligand plane, two of the carbene ligands (C2 and C3) are planar with the Sn. The second conformation of **3a** shows an almost undistorted octahedral geometry (Figure 6.2B). In this conformation, the borate moieties are on opposite sides of the macrocyclic plane. Both conformations have Sn-C bond lengths that are slightly longer than a previously published octahedral Sn dicarbene.¹⁰⁰ To our knowledge, **3a** is the first structurally confirmed polydentate NHC on Sn.

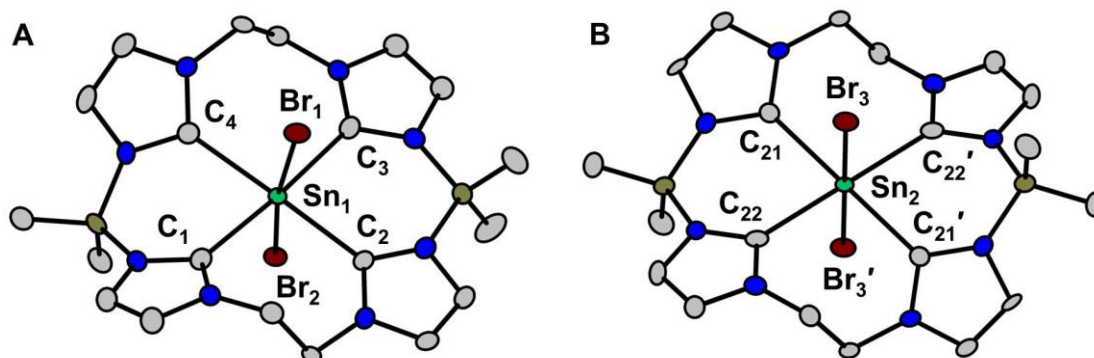


Figure 6.2. X-ray crystal structure of $(^{\text{BMe}_2, \text{Et}}\text{TC}^{\text{H}})\text{SnBr}_2$ (**3a**, shown in two different conformations). Green, burgundy, olive, blue, and grey ellipsoids (50% probability) represent Sn, Br, B, N, and C, respectively. H atoms and solvent molecules have been omitted for clarity. Selected bond distances (Å) and angles (deg.) are as follows: $\text{Sn}_1\text{-C}_1$, 2.295(4); $\text{Sn}_1\text{-C}_2$, 2.276(4); $\text{Sn}_1\text{-C}_3$, 2.284(5); $\text{Sn}_1\text{-C}_4$, 2.282(4); $\text{Sn}_1\text{-Br}_1$, 2.6643(5); $\text{Sn}_1\text{-Br}_2$, 2.6255(5); $\text{Sn}_2\text{-C}_{21}$, 2.307(4); $\text{Sn}_2\text{-C}_{22}$, 2.293(4); $\text{Sn}_2\text{-Br}_3$, 2.6074(5); $\text{C}_1\text{-Sn}_1\text{-C}_3$, 176.2(2); $\text{C}_2\text{-Sn}_1\text{-C}_4$, 175.9(2); $\text{Br}_1\text{-Sn}_1\text{-Br}_2$, 172.11(2); $\text{C}_1\text{-Sn}_1\text{-C}_2$, 96.1(2); $\text{C}_1\text{-Sn}_1\text{-C}_4$, 80.8(2); $\text{C}_{21}\text{-Sn}_2\text{-C}_{21}'$, 180.0; $\text{C}_{22}\text{-Sn}_2\text{-C}_{22}'$, 180.0; $\text{Br}_3\text{-Sn}_2\text{-Br}_3'$, 180.0; $\text{C}_{21}\text{-Sn}_2\text{-Br}_3$, 92.3(1); $\text{C}_{22}\text{-Sn}_2\text{-Br}_3$, 91.4(1); $\text{C}_{21}'\text{-Sn}_2\text{-Br}_3$, 87.8(1); $\text{C}_{22}'\text{-Sn}_2\text{-Br}_3$, 88.6(1).

The group 13 metal complexes were also structurally characterized with single-crystal X-ray diffraction, which revealed five coordinate complexes. The X-ray crystal structure of **3b** (Figure 6.3A) indicates a distorted square pyramidal geometry ($\tau = 0.37$).¹⁰² The *trans* C-In-C bond angles are highly divergent with $\text{C}_1\text{-In-C}_3$ at $151.7(4)^\circ$ and $\text{C}_2\text{-In-C}_4$ at $173.7(4)^\circ$. Likewise, the In-C_2 and In-C_4

bond distances are approximately 0.05 Å shorter than In-C₁ and In C₃. **3b** is a rare example of a polydentate NHC ligand bound to In and the first example of a tetracarbene on indium.¹⁰³

Despite several attempts to obtain high quality crystals of **3c**, we were only able to obtain a disordered X-ray structure that allowed us to determine connectivity about the Al centre (see experimental section below, Figure 6.4). In order to crystallographically characterize an Al tetracarbene complex, we modified the synthesis by substituting AlCl₃ for AlBr₃. Unfortunately, this change led to a mixture of **3c** and (^{BMe₂,Et}TC^H)AlCl (**3d**). Nonetheless, a single-crystal of **3d** was isolated for single-crystal X-ray diffraction (Figure 6.3B). The crystal structure of **3d** reveals it is isostructural to both **3b** and **3c** and also has a distorted square pyramidal geometry ($\tau = 0.32$). The distortion of the *trans* C-Al-C bond angles is similar to what is observed for **3b**. Complex **3d** has similar bond lengths to previously published Al carbene complexes.¹⁰⁴ The Al complexes **3c** and **3d** are particularly novel complexes as they are the first examples with more than one NHC ligand on Al and the first example of a 5-coordinate Al complex with an NHC ligand. Complex **3c** and **3d** clearly exemplify the need for an anionic ligand in order to easily prepare polydentate NHC Al complexes.

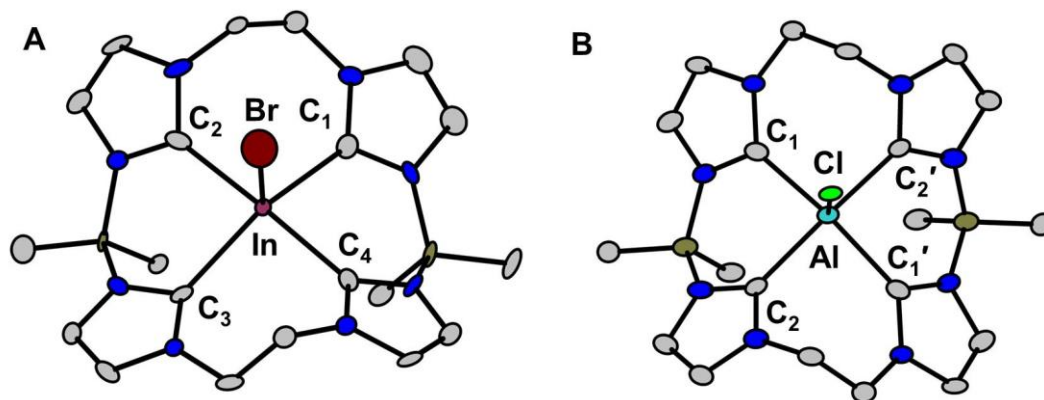


Figure 6.3. X-ray crystal structure of (A) $(^{\text{BMe}_2,\text{Et}}\text{TC}^{\text{H}})\text{InBr}$ (3b) and (B) $(^{\text{BMe}_2,\text{Et}}\text{TC}^{\text{H}})\text{AlCl}$ (3d). Pink, burgundy, teal, lime green, olive, blue, and grey ellipsoids (50% probability) represent In, Br, Al, Cl, B, N, and C, respectively. H atoms have been omitted for clarity. Selected bond distances (Å) and angles (deg.) are as follows. For 3b: In-C₁, 2.28(1); In-C₂, 2.22(1); In-C₃, 2.28(1); In-C₄, 2.23(1); In-Br, 1.594(2); C₁-In-C₃, 151.7(4); C₂-In-C₄, 173.7(4); C₁-In-C₂, 92.4(4); C₁-In-C₄, 86.2(4). For 3d: Al-C₁, 2.130(5); Al-C₂, 2.080(5); Al-Cl, 2.275(3); C₁-Al-C_{1'}, 146.1(3); C₂-Al-C_{2'}, 165.1(3); C₁-Al-C₂, 87.0(2); C₁-Al-C_{2'}, 88.6(2); C₁-Al-Cl, 107.0(1); C₂-Al-Cl, 97.5(1).

Conclusion

In conclusion, we have synthesized the first tetracarbene complexes on group 13 and 14 metals. The aluminium example is the first example of a poly-NHC ligand on this metal. Employing an anionic macrocycle proved crucial since a neutral variation of our ligand was unsuccessful in complexing main group metals. The dianionic macrocyclic tetracarbene ligand binds to the metal centres forming a distorted equatorial plane. Proton NMR demonstrated that the Sn complex is fluxional in solution, while the In and Al complexes are rigid. ^{119}Sn NMR suggests a high degree of shielding from the tetracarbene ligand. Future research will focus on catalytic reactions with the aluminium complex.

Experimental

All reactions were performed under a dry nitrogen atmosphere with the use of either a drybox or standard Schlenk techniques. Solvents were dried on an Innovative Technologies (Newburgport, MA) Pure Solv MD-7 Solvent Purification System and degassed by three freeze-pump-thaw cycles on a Schlenk line to remove O_2 prior to use. Acetonitrile- d_3 , benzene- d_6 , and tetrahydrofuran- d_8 were degassed by three freeze-pump-thaw cycles prior to drying over activated molecular sieves. These NMR solvents were then stored under N_2 in a glovebox. $(^{\text{B(Me)2,EtTC}^H})(\text{Br})_2$ was prepared as described previously.⁹⁷ All reagents were purchased from commercial vendors and used without purification. ^1H and $^{13}\text{C}\{^1\text{H}\}$ were recorded at ambient temperature on a

Varian VNMRS 500 MHz narrow-bore broadband system. ^{119}Sn NMR spectra was recorded at ambient temperature on a Bruker Avance 400 MHz NMR. ^1H and ^{13}C NMR chemical shifts were referenced to the residual solvent. ^{119}Sn NMR chemical shifts are reported relative to an external standard of $\text{Sn}(\text{Me})_4$ in acetonitrile- d_3 . All mass spectrometry analyses were conducted at the Mass Spectrometry Center located in the Department of Chemistry at the University of Tennessee. The ESI/MS analyses were performed using a QSTAR Elite quadrupole time-of-flight (QTOF) mass spectrometer with an electrospray ionization source from AB Sciex (Concord, Ontario, Canada). Mass spectrometry sample solutions of metal complexes were prepared in acetonitrile. Infrared spectra were collected on a Thermo Scientific Nicolet iS10 with a Smart iTR accessory for attenuated total reflectance. Carbon, hydrogen, and nitrogen analyses were obtained from Atlantic Microlab, Norcross, GA.

Synthesis of $(^{\text{B}(\text{Me})_2\text{EtTC}^H})\text{SnBr}_2$ (3a). $(^{\text{B}(\text{Me})_2\text{EtTC}^H})(\text{Br})_2$ (0.300 g, 0.530 mmol) was added to a 20-mL vial with tetrahydrofuran (10 mL) and stirred at room temperature (450 rpm) for 5 min. The resulting slurry was cooled to $-30\text{ }^\circ\text{C}$. $^n\text{BuLi}$ (2.50 M, 0.849 mL, 2.12 mmol) was added to the slurry and allowed to stir until the white slurry became an orange-yellow solution (~15 min.). Tin(IV) bromide (0.232 g, 0.530 mmol) was then added to the resulting solution and allowed to stir at room temperature overnight. The reaction mixture was then filtered over Celite and the resulting solution was concentrated to 3 mL under

reduced pressure. The colorless product was crystallized by vapor diffusion of pentane into this solution (0.026 g, 7.2% yield). ^1H NMR (CD_3CN , 499.74 MHz): δ 7.29 (d, $J = 1.8$ Hz, 4H), 7.16 (d, $J = 1.7$ Hz, 4H), 4.78 (s, 8H), 0.25 (s, 12H). ^{13}C NMR (CD_3CN , 125.66 MHz): δ 166.86, 124.86, 122.89, 51.24, 23.04, 14.32. ^{119}Sn NMR (CD_3CN , SnMe_4 ext., 149.16 MHz): δ -1099.35. IR (neat): 3378, 3132, 3008, 2943, 2932, 1631, 1545, 1418, 1400, 1299, 1288, 1206, 1155, 1119, 1071, 1031, 942, 828, 798, 743, 708, 669 cm^{-1} . ESI/MS (m/z): $[\text{M}-\text{Br}]^+$ 608.09. Anal. Calcd for $\text{C}_{22.5}\text{H}_{34}\text{B}_2\text{Br}_2\text{N}_8\text{Sn}_1$ ($3\text{a} \cdot \frac{1}{2}\text{C}_5\text{H}_{12}$): C, 37.71; H, 4.78; N, 15.63. Found: C, 37.03; H, 4.51; N, 15.31.

Synthesis of $(^{\text{B}(\text{Me})_2\text{EtTC}^H})\text{InBr}$ (3b**).** $(^{\text{B}(\text{Me})_2\text{EtTC}^H})(\text{Br})_2$ (0.214 g, 0.377 mmol) was added to a 20-mL vial with tetrahydrofuran (10 mL) and stirred at room temperature (450 rpm) for 5 min. The resulting slurry was cooled to -30 $^\circ\text{C}$. $n\text{BuLi}$ (2.50 M, 0.604 mL, 1.5 mmol) was added to the slurry and allowed to stir until the white slurry became an orange-yellow solution (~15 min.). Indium(III) bromide (0.134 g, 0.377 mmol) was then added to the resulting solution and allowed to stir at room temperature overnight. The reaction mixture was then filtered over Celite and the resulting solution was concentrated to 3 mL under reduced pressure. The colorless product was isolated by vapor diffusion of pentane into this solution. Due to decomposition of the product in most solvents, full characterization was not possible within the time constraints of **3b** degrading. A single-crystal suitable for X-ray diffraction was obtained by vapor diffusion of

pentane into a concentrated benzene solution containing **3b**. ^1H NMR (C_6D_6 , 499.74 MHz): δ 7.14 (d, $J = 1.6$ Hz, 4H), 5.96 (d, $J = 1.6$ Hz, 4H), 4.66-4.59 (m, 4H), 3.13-3.07 (m, 4H), 0.82 (s, 6H), 0.59 (s, 6H). IR (neat): 3390, 3115, 2929, 1630, 1546, 1455, 1415, 1394, 1371, 1291, 1260, 1217, 1150, 1109, 1078, 1038, 1019, 966, 946, 839, 797, 750, 736, 727, 697, 670, 635 cm^{-1} . ESI/MS (m/z): $[\text{M}-\text{Br}]^+$ 517.11.

Synthesis of $(^{\text{B}(\text{Me})_2\text{EtTC}^H})\text{AlBr}$ (3c**).** $(^{\text{B}(\text{Me})_2\text{EtTC}^H})(\text{Br})_2$ (0.146 g, 0.259 mmol) was added to a 20-mL vial with tetrahydrofuran (10 mL) and stirred at room temperature (450 rpm) for 5 min. The resulting slurry was cooled to -30 $^\circ\text{C}$. $^n\text{BuLi}$ (2.50 M, 0.413 mL, 1.03 mmol) was added to the slurry and allowed to stir until the white slurry became an orange-yellow solution (~15 min.). Aluminum(III) bromide (68.9 mg, 0.259 mmol) was then added to the resulting solution and allowed to stir at room temperature overnight. The reaction mixture was then filtered over Celite and the volatiles were removed under reduced pressure resulting in a white powder. The powder was extracted with benzene (10 mL), filtered over Celite and the volatiles were again removed under reduced pressure yielding the pure white powder product (0.0221 g, 16.8% yield). Crystals suitable for single-crystal X-ray diffraction were grown by vapor diffusion of pentane into a concentrated solution of **3c** in tetrahydrofuran. ^1H NMR (CD_3CN , 499.74 MHz): δ 7.13 (d, $J = 1.6$ Hz, 4H), 7.03 (d, $J = 1.6$ Hz, 4H), 5.53-5.43 (m, 4H), 4.37-4.31 (m, 4H), 0.25 (s, 6H), -0.20 (s, 6H). ^{13}C NMR (CD_3CN , 125.66 MHz): δ 123.04,

121.78, 48.79, 15.63, 14.32. IR (neat): 3379, 3132, 2932, 1631, 1545, 1467, 1418, 1399, 1375, 1288, 1244, 1206, 1155, 1119, 1032, 971, 958, 942, 848, 797, 742, 730, 708, 669 cm^{-1} . ESI/MS (m/z): $[\text{M-Br}]^+$ 429.20. Anal. Calcd for $\text{C}_{20}\text{H}_{28}\text{Al}_1\text{B}_2\text{Br}_1\text{N}_8$: C, 47.19; H, 5.54; N, 22.01. Found: C, 46.45; H, 6.18; N, 21.05.

Synthesis of $(^{\text{B}(\text{Me})_2\text{EtTC}^H})\text{AlCl}$ (3d**).** $(^{\text{B}(\text{Me})_2\text{EtTC}^H})(\text{Br})_2$ (0.294 g, 0.520 mmol) was added to a 20-mL vial with tetrahydrofuran (10 mL) and stirred at room temperature (450 rpm) for 5 min. The resulting slurry was cooled to $-30\text{ }^\circ\text{C}$. $^n\text{BuLi}$ (2.50 M, 0.832 mL, 2.08 mmol) was added to the slurry and allowed to stir until the white slurry became an orange-yellow solution (~15 min.). Aluminum(III) chloride (69.3 mg, 0.520 mmol) was then added to the resulting solution and allowed to stir at room temperature overnight. The reaction mixture was then filtered over Celite and the volatiles were removed under reduced pressure resulting in a white powder. The powder was extracted with benzene (10 mL) and filtered over Celite. Crystals suitable for single-crystal X-ray diffraction were grown by vapor diffusion of pentane into a concentrated solution of **3d** in benzene.

X-ray Structure Determinations. X-ray diffraction measurements were performed on single-crystals coated with Paratone oil and mounted on glass fibers. Each crystal was frozen under a stream of N_2 while data were collected

on a Bruker APEX diffractometer. A matrix scan using at least 12 centered reflections was used to determine initial lattice parameters. Reflections were merged and corrected for Lorentz and polarization effects, scan speed, and background using SAINT 4.05. Absorption corrections, including odd and even ordered spherical harmonics were performed using SADABS, if necessary. Space group assignments were based upon systematic absences, *E* statistics, and successful refinement of the structure. The structures were solved by direct methods with the aid of successive difference Fourier maps, and were refined against all data using the SHELXTL 5.0 software package.

Structure **3c** exhibited positional disorder on the macrocyclic ligand. The macrocycle was refined using the PART instruction by splitting the macrocycle over two positions. Poor data prevented the anisotropic refinement of all atoms. Structure **3a** contains a half equivalent of pentane which was modeled at half occupancy.

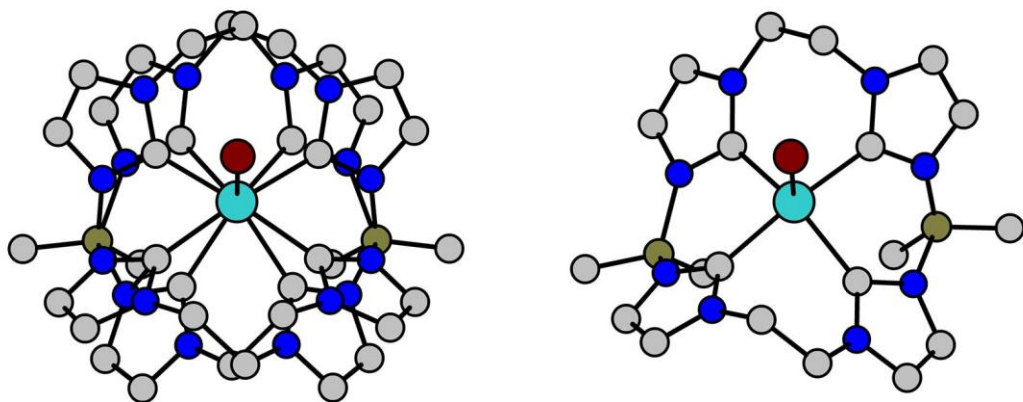


Figure 6.4. Graphical representation of $(^{B(Me)_2,Et}TC^H)AlBr$ (3c). Both the disordered structure (left) and with only one representative macrocycle (right) based on X-ray analysis are shown. Teal, burgundy, olive, blue, and grey spheres represent Al, Br, B, N, and C. H atoms have been removed for clarity.

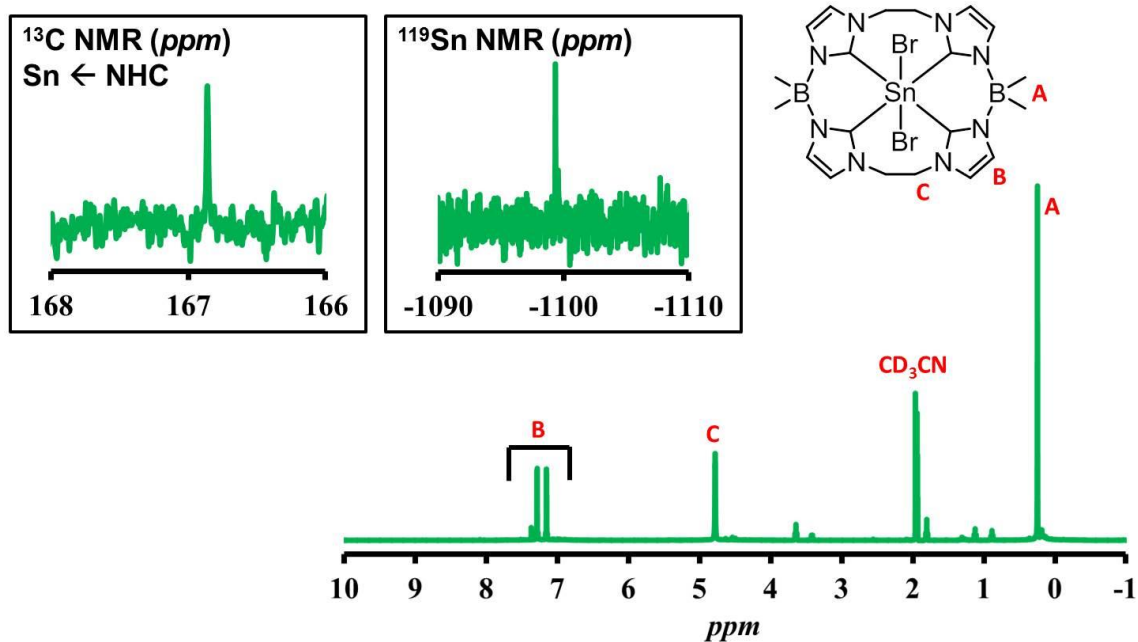


Figure 6.5. NMR data for $(^{B(Me)_2,Et}TC^H)SnBr_2$ (3a). Labeled 1H NMR of 3a with highlights of both NHC-SN chemical shift in ^{13}C NMR and the ^{119}Sn NMR chemical shift.

Chapter 7

Conclusion

Prior to this work only a few examples of macrocyclic tetracarbenes ligands had been prepared. Furthermore, each of these tetracarbene complexes were either electronically saturated or the ligand was too large to allow other ligands access to the metal center for potential catalytic transformations. We have found that in order to prepare a variety potential catalysts supported by a macrocyclic tetracarbene two characteristics are necessary: the macrocycle must have a small ring size of no more than 18 atoms and the ligand needs to be prepared from a free tetraimidazolium ligand precursor.

First, we demonstrated a facile, two step synthesis of an 18-atom ringed tetra-imidazolium ligand that employed 1,2-bis-(trifoxy)ethane as the key dielectrophile to close the macrocycle. The ligand precursor was prepared on a multi-gram scale quickly and cleanly without the use of dilute solvent conditions. Ligand precursor ($(^{\text{Me,Et}}\text{TC}^{\text{Ph}})(\text{OTf})_4$) can be installed on platinum by a weak base deprotonation strategy to form $[(^{\text{Me,Et}}\text{TC}^{\text{Ph}})\text{Pt}](\text{PF}_6)_2$. Both the $(^{\text{Me,Et}}\text{TC}^{\text{Ph}})(\text{OTf})_4$ and $[(^{\text{Me,Et}}\text{TC}^{\text{Ph}})\text{Pt}](\text{PF}_6)_2$ can be characterized by multi-nuclear NMR, mass spectrometry, single-crystal X-ray diffraction, and other spectroscopic techniques.

The tetracarbene ligand was installed on iron and was found to be a particularly effective aziridination catalyst. The tetra-carbene iron complex, $[(^{\text{Me,Et}}\text{TC}^{\text{Ph}})\text{Fe}(\text{NCCH}_3)_2](\text{PF}_6)_2$, was synthesized from the tetra-imidazolium

precursor, $(^{Me,Et}TC^{Ph})(I)_4$, via an in situ strong base deprotonation strategy. $[(^{Me,Et}TC^{Ph})Fe(NCCH_3)_2](PF_6)_2$ was characterized by multi-nuclear NMR spectroscopy and single-crystal X-ray diffraction. This catalyst reacts with aryl azides and a wide variety of substituted aliphatic alkenes to give aziridines in a “C₂ + N₁” addition reaction. We were even able to form 9-(*p*-tolyl)-9-azabicyclo-[6.1.0]nonane in nearly quantitative yield from *cis*-cyclooctene and tolyl-azide. In addition, we were able to synthesize aziridines with 2,3-dimethyl-butene, a tetra-substituted alkene. These aliphatic alkenes are generally considered more challenging reagents than styrene variants which have been previously studied. $[(^{Me,Et}TC^{Ph})Fe(NCCH_3)_2](PF_6)_2$ also shows exceptional functional group tolerance with functionalized aryl azides and 1-decene, only decomposing when protic functional groups are present. The catalyst can also be recovered and re-used up to three additional times with only a nominal reduction in yield. This new aziridination catalyst showcases a ‘green’ approach to prepare aziridines, while also performing examples of aziridination never possible before.

Although the aziridination intermediate could not be isolated, mass spectrometry data suggested an Fe(IV) imide, $[(^{Me,Et}TC^{Ph})Fe=NAr](PF_6)_2$, is the likely intermediate. By adding excess aryl azide we have synthesized an iron(IV) complex, $[(^{Me,Et}TC^{Ph})Fe(ArN_4Ar)](PF_6)_2$, supported by both a tetrazene and tetracarbene ligand. The clean conversion of $[(^{Me,Et}TC^{Ph})Fe(ArN_4Ar)](PF_6)_2$ to $[(^{Me,Et}TC^{Ph})Fe(CH_3CN)_2](PF_6)_2$ was confirmed by NMR spectroscopy and mass spectrometry. ¹³C NMR shows a significant upfield chemical shift of the

tetrazene complex compared to $[(^{\text{Me,Et}}\text{TC}^{\text{Ph}})\text{Fe}(\text{CH}_3\text{CN})_2](\text{PF}_6)_2$. The $\text{Fe}^{\text{IV}}\text{-NHC}$ ^{13}C NMR chemical shift is the first reported example. Single-crystal X-ray diffraction confirmed the addition of the tetrazene ligand and that $[(^{\text{Me,Et}}\text{TC}^{\text{Ph}})\text{Fe}(\text{ArN}_4\text{Ar})](\text{PF}_6)_2$ was in a distorted trigonal prismatic geometry. The metal center of $[(^{\text{Me,Et}}\text{TC}^{\text{Ph}})\text{Fe}(\text{ArN}_4\text{Ar})](\text{PF}_6)_2$ was confirmed to be an iron(IV) ($S = 0$) by Mössbauer spectroscopy. Finally, reactivity studies suggest that $[(^{\text{Me,Et}}\text{TC}^{\text{Ph}})\text{Fe}(\text{ArN}_4\text{Ar})](\text{PF}_6)_2$ decomposes to form 4,4'-dimethylazobenzene and to 9-(p-tolyl)-9-azabicyclo[6.1.0]nonane in neat cyclooctene indicating $[(^{\text{Me,Et}}\text{TC}^{\text{Ph}})\text{Fe}(\text{ArN}_4\text{Ar})](\text{PF}_6)_2$ is also an acceptable nitrene transfer source for aziridination.

In order to institute a general synthetic method to prepare tetracarbene complexes with several transition metals and improve upon poor tetracarbene yields, we have synthesized a dimeric silver NHC transmetallating reagent, $[(^{\text{Me,Et}}\text{TC}^{\text{Ph}})\text{Ag}]_2\text{Ag}_2(\text{PF}_6)_4$. This reagent reacts with a wide variety of di- and trivalent metal halides to give mononuclear tetracarbene complexes. These silver complexes were characterized by multi-nuclear NMR spectroscopy, mass spectrometry, single-crystal X-ray diffraction as well as other spectroscopic techniques. The silver reagents transmetallate the tetracarbene ligands to nine different metal halides from the first to third row on the periodic table in moderate to high yield. All of the metal tetracarbene complexes were characterized similarly to $[(^{\text{Me,Et}}\text{TC}^{\text{Ph}})\text{Ag}]_2\text{Ag}_2(\text{PF}_6)_2$. The complexes formed for the three first row metals, chromium, iron and cobalt, are rare examples of silver NHC

transmetallation to these metals. The redox active transmetallation to chromium is particularly significant since early metal NHC chemistry is underdeveloped and this complex is the first tetracarbene on this metal. Given the importance of the few macrocyclic tetracarbenes that have been previously synthesized, this transmetallation strategy demonstrates that macrocyclic tetracarbenes can be prepared on metals across the periodic table

In an attempt to move toward improving solubility of the tetracarbene catalysts, a second generation tetracarbene ligand with two borate moieties in the ligand backbone was prepared. Utilizing $(^{B(Me)_2,Et}TC^H)(Br)_2$, the first tetracarbene complexes of Group 13 and 14 metals were synthesized. The aluminium example, $(^{B(Me)_2,Et}TC^H)AlBr$, is the first example of a poly-NHC complex on this metal. Employing an anionic macrocycle proved crucial since the neutral tetracarbene ligand, $(^{Me,Et}TC^{Ph})(OTf)_4$, was unsuccessful in complexing main group metals. Proton NMR demonstrated that the Sn complex, $(^{B(Me)_2,Et}TC^H)Sn(Br)_2$, is fluxional in solution, while the In and Al complexes are rigid. ^{119}Sn NMR suggests a high degree of shielding from the tetracarbene ligand.

References

1. Yudin, A.; Editor, *Aziridines and Epoxides in Organic Synthesis*. 2006; p 492 pp.
2. (a) Makiguchi, K.; Kakuchi, T.; Satoh, T., Organocatalytic ring-opening polymerization of cyclic esters, cyclic carbonates, and epoxides. *Yuki Gosei Kagaku Kyokaishi* **2013**, *71*, 706-715; (b) Qin, G.; Fan, L.; Cao, S.; Bu, Z.; Chen, T.; Yi, K., Research progress on catalysts for copolymerization of CO₂ and epoxides. *Huagong Jinzhan* **2013**, *32*, 327-332, 358.
3. Thibodeaux, C. J.; Chang, W.-c.; Liu, H.-w., Enzymatic Chemistry of Cyclopropane, Epoxide, and Aziridine Biosynthesis. *Chem. Rev.* **2012**, *112*, 1681-1709.
4. (a) Hu, X. E., Nucleophilic ring opening of aziridines. *Tetrahedron* **2004**, *60*, 2701-2743; (b) Lu, P., Recent developments in regioselective ring opening of aziridines. *Tetrahedron* **2010**, *66*, 2549-2560; (c) Schneider, C., Catalytic, enantioselective ring opening of aziridines. *Angew. Chem., Int. Ed.* **2009**, *48*, 2082-2084.
5. (a) Dauban, P.; Malik, G., A Masked 1,3-Dipole Revealed from Aziridines. *Angew. Chem., Int. Ed.* **2009**, *48*, 9026-9029; (b) Krake, S. H.; Bergmeier, S. C., Inter- and intramolecular reactions of epoxides and aziridines with π -nucleophiles. *Tetrahedron* **2010**, *66*, 7337-7360.
6. (a) Chang, J. W. W.; Ton, T. M. U.; Chan, P. W. H., Transition metal catalyzed aminations and aziridinations of C-H and C-C bonds with iminoiodinanes. *Chem. Rec.* **2011**, *11*, 331-357; (b) Driver, T. G., Recent

advances in transition metal-catalyzed N-atom transfer reactions of azides. *Org. Biomol. Chem.* **2010**, *8*, 3831-3846; (c) Karila, D.; Dodd, R. H., Recent progress in iminoiodane-mediated aziridination of olefins. *Curr. Org. Chem.* **2011**, *15*, 1507-1538; (d) Minakata, S., Utilization of *N*-X Bonds in The Synthesis of *N*-Heterocycles. *Acc. Chem. Res.* **2009**, *42*, 1172-1182.

7. Jenkins, D. M., Atom-economical C₂ + N₁ aziridination: progress towards catalytic intermolecular reactions using alkenes and aryl azides. *Synlett* **2012**, *23*, 1267-1270.

8. Pellissier, H., Recent developments in asymmetric aziridination. *Tetrahedron* **2010**, *66*, 1509-1555.

9. Cenini, S.; Tollari, S.; Penoni, A.; Cereda, C., Catalytic amination of unsaturated hydrocarbons: reactions of *p*-nitrophenyl azide with alkenes catalyzed by metalloporphyrins. *J. Mol. Catal. A: Chem.* **1999**, *137*, 135-146.

10. (a) Fantauzzi, S.; Gallo, E.; Caselli, A.; Piangiolino, C.; Ragaini, F.; Cenini, S., The (porphyrin)ruthenium-catalyzed aziridination of olefins using aryl azides as nitrogen sources. *Eur. J. Org. Chem.* **2007**, 6053-6059; (b) Fantauzzi, S.; Gallo, E.; Caselli, A.; Ragaini, F.; Macchi, P.; Casati, N.; Cenini, S., Origin of the Deactivation in Styrene Aziridination by Aryl Azides, Catalyzed by Ruthenium Porphyrin Complexes. Structural Characterization of a Δ^2 -1,2,3-Triazoline Ru^{II}(TPP)CO Complex. *Organometallics* **2005**, *24*, 4710-4713.

11. (a) Brown, S. D.; Betley, T. A.; Peters, J. C., A Low-Spin d⁵ Iron Imide: Nitrene Capture by Low-Coordinate Iron(I) Provides the 4-Coordinate Fe(III)

Complex $[\text{PhB}(\text{CH}_2\text{PPh}_2)_3]\text{FeobN-p-tolyl}$. *J. Am. Chem. Soc.* **2003**, *125*, 322-323;
(b) Laskowski, C. A.; Miller, A. J. M.; Hillhouse, G. L.; Cundari, T. R., A Two-Coordinate Nickel Imido Complex That Effects C-H Amination. *J. Am. Chem. Soc.* **2011**, *133*, 771-773; (c) Mindiola, D. J.; Hillhouse, G. L., Terminal amido and imido complexes of three-coordinate nickel. *J. Am. Chem. Soc.* **2001**, *123*, 4623-4624.

12. (a) Kyba, E. P.; Davis, R. E.; Hudson, C. W.; John, A. M.; Brown, S. B.; McPhaul, M. J.; Liu, L.-K.; Glover, A. C., Tetradentate 14-membered tert-phosphino-containing macrocycles. *J. Am. Chem. Soc.* **1981**, *103*, 3868-75; (b) Kyba, E. P.; Hudson, C. W.; McPhaul, M. J.; John, A. M., Polyphosphino macrocyclic ligand systems. *J. Am. Chem. Soc.* **1977**, *99*, 8053-4; (c) Mizuta, T.; Okano, A.; Sasaki, T.; Nakazawa, H.; Miyoshi, K., Palladium(II) and Platinum(II) Complexes of Tetraphosphamacrocyclic. X-ray Crystal Structures of Phosphorus Analogs of a (Tetramethylcyclam)metal Complex. *Inorg. Chem.* **1997**, *36*, 200-203; (d) Strassner, T., The role of NHC ligands in oxidation catalysis. *Top. Organomet. Chem.* **2007**, *22*, 125-148.

13. Poyatos, M.; Mata, J. A.; Peris, E., Complexes with Poly(*N*-heterocyclic carbene) Ligands: Structural Features and Catalytic Applications. *Chem. Rev.* **2009**, *109*, 3677-3707.

14. Hahn, F. E.; Langenhahn, V.; Luegger, T.; Pape, T.; Le Van, D., Template synthesis of a coordinated tetracarbene ligand with crown ether topology. *Angew. Chem., Int. Ed.* **2005**, *44*, 3759-3763.

15. (a) Findlay, N. J.; Park, S. R.; Schoenebeck, F.; Cahard, E.; Zhou, S.-z.; Berlouis, L. E. A.; Spicer, M. D.; Tuttle, T.; Murphy, J. A., Reductions of Challenging Organic Substrates by a Nickel Complex of a Noninnocent Crown Carbene Ligand. *J. Am. Chem. Soc.* **2010**, *132*, 15462-15464; (b) McKie, R.; Murphy, J. A.; Park, S. R.; Spicer, M. D.; Zhou, S.-z., Homoleptic crown *N*-heterocyclic carbene complexes. *Angew. Chem., Int. Ed.* **2007**, *46*, 6525-6528; (c) Park, S. R.; Findlay, N. J.; Garnier, J.; Zhou, S.; Spicer, M. D.; Murphy, J. A., Electron transfer activity of a cobalt crown carbene complex. *Tetrahedron* **2009**, *65*, 10756-10761.
16. (a) Nugent, W. A.; Mayer, J. M., *Metal-ligand multiple bonds : the chemistry of transition metal complexes containing oxo, nitrido, imido, alkylidene, or alkylidyne ligands*. Wiley: New York, 1988; p xi, 334 p; (b) Lin, Z.; Hall, M. B., A group theoretical analysis on transition-metal complexes with metal-ligand multiple bonds. *Coord. Chem. Rev.* **1993**, *123*, 149-67.
17. (a) Rohde, J.-U.; In, J.-H.; Lim, M. H.; Brennessel, W. W.; Bukowski, M. R.; Stubna, A.; Muenck, E.; Nam, W.; Que, L., Jr., Crystallographic and Spectroscopic Characterization of a Nonheme Fe(IV)=O complex. *Science* **2003**, *299* (5609), 1037-1039; (b) Li, F.; England, J.; Que, L., Near-Stoichiometric Conversion of H₂O₂ to Fe^{IV}=O at a Nonheme Iron(II) Center. Insights into the O-O Bond Cleavage Step. *J. Am. Chem. Soc.* **2010**, *132*, 2134-2135; (c) Meyer, K.; Bill, E.; Mienert, B.; Weyhermueller, T.; Wieghardt, K., Photolysis of *cis*- and *trans*-[Fe^{III}(cyclam)(N₃)₂]⁺ Complexes: Spectroscopic Characterization of a

Nitridoiron(V) Species. *J. Am. Chem. Soc.* **1999**, *121*, 4859-4876; (d) Berry, J. F.; Bill, E.; Bothe, E.; DeBeer George, S.; Mienert, B.; Neese, F.; Wieghardt, K., An Octahedral Coordination Complex of Iron(VI). *Science* **2006**, *312* (5782), 1937-1941.

18. (a) Scepianiak, J. J.; Fulton, M. D.; Bontchev, R. P.; Duesler, E. N.; Kirk, M. L.; Smith, J. M., Structural and spectroscopic characterization of an electrophilic iron nitrido complex. *J. Am. Chem. Soc.* **2008**, *130*, 10515-10517; (b) Vogel, C.; Heinemann, F. W.; Sutter, J.; Anthon, C.; Meyer, K., An iron nitride complex. *Angew. Chem., Int. Ed.* **2008**, *47*, 2681-2684; (c) Betley, T. A.; Peters, J. C., A Tetrahedrally Coordinated L_3Fe-N_x Platform that Accommodates Terminal Nitride ($Fe^{IV}\equiv N$) and Dinitrogen ($FeI-N_2-FeI$) Ligands. *J. Am. Chem. Soc.* **2004**, *126*, 6252-6254.

19. (a) Jenkins, D. M.; Betley, T. A.; Peters, J. C., Oxidative Group Transfer to Co(I) Affords a Terminal Co(III) Imido Complex. *J. Am. Chem. Soc.* **2002**, *124*, 11238-11239; (b) Hu, X.; Meyer, K., Terminal Cobalt(III) Imido Complexes Supported by Tris(Carbene) Ligands: Imido Insertion into the Cobalt-Carbene Bond. *J. Am. Chem. Soc.* **2004**, *126*, 16322-16323; (c) Shay, D. T.; Yap, G. P. A.; Zakharov, L. N.; Rheingold, A. L.; Theopold, K. H., Intramolecular C-H activation by an open-shell cobalt(III) imido complex. *Angew. Chem., Int. Ed.* **2005**, *44*, 1508-1510.

20. (a) Herrmann, W. A., *N*-heterocyclic carbenes. *N*-heterocyclic carbenes: A new concept in organometallic catalysis. *Angew. Chem., Int. Ed.* **2002**, *41*,

1290-1309; (b) Diez-Gonzalez, S.; Marion, N.; Nolan Steven, P., *N*-heterocyclic carbenes in late transition metal catalysis. *Chem. Rev.* **2009**, *109*, 3612-76.

21. (a) Unger, Y.; Zeller, A.; Taige, M. A.; Strassner, T., Near-UV phosphorescent emitters: *N*-heterocyclic platinum(II) tetracarbene complexes. *Dalton Trans.* **2009**, 4786-4794; (b) Unger, Y.; Zeller, A.; Ahrens, S.; Strassner, T., Blue phosphorescent emitters: new *N*-heterocyclic platinum(II) tetracarbene complexes. *Chem. Commun.* **2008**, 3263-3265.

22. Quezada, C. A.; Garrison, J. C.; Tessier, C. A.; Youngs, W. J., Synthesis and structural characterization of two bis(imidazol-2-ylidene) complexes of Pt(II). *J. Organomet. Chem.* **2003**, *671*, 183-186.

23. Lee, C.-S.; Pal, S.; Yang, W.-S.; Hwang, W.-S.; Lin, I. J. B., Bis-chelate tetracarbene palladium(II) complex as an efficient and recyclable catalyst precursor for Heck reaction. *J. Mol. Catal. A Chem.* **2008**, *280*, 115-121.

24. (a) Sato, K.; Onitake, T.; Arai, S.; Yamagishi, T., Size selective recognition of anions by a tetracationic imidazoliophane. *Heterocycles* **2003**, *60*, 779-784; (b) Shi, Z.; Thummel, R. P., N,N'-Bridged Derivatives of 2,2'-Bibenzimidazole. *J. Org. Chem.* **1995**, *60*, 5935-45; (c) Wong, W. W. H.; Vickers, M. S.; Cowley, A. R.; Paul, R. L.; Beer, P. D., Tetrakis(imidazolium) macrocyclic receptors for anion binding. *Org. Biomol. Chem.* **2005**, *3*, 4201-4208.

25. Lindner, E.; Von Au, G.; Eberle, H. J., Preparation and properties of and reactions with metal-containing heterocycles. Preparation and properties of

ethanediyl, propanediyl, pentanediyl and decanediyl bis(trifluoromethanesulfonate). *Chem. Ber.* **1981**, 114, 810-13.

26. Tapu, D.; Dixon, D. A.; Roe, C., ^{13}C NMR Spectroscopy of "Arduengo-type" Carbenes and Their Derivatives. *Chem. Rev.* **2009**, 109 (8), 3385-3407.

27. (a) Fehlhammer, W. P.; Bliss, T.; Kernbach, U.; Bruedgam, I., Homoleptic carbene complexes. VI. Bis{1,1'-methylene-3,3'-dialkyl-diimidazolin-2,2'-diylidene}palladium chelate complexes by the free carbene route. *J. Organomet. Chem.* **1995**, 490, 149-53; (b) Herrmann, W. A.; Schwarz, J.; Gardiner, M. G.; Spiegler, M., *N*-heterocyclic carbenes. Homoleptic chelating *N*-heterocyclic carbene complexes of palladium and nickel. *J. Organomet. Chem.* **1999**, 575, 80-86.

28. Abu-Omar, M. M., High-valent iron and manganese complexes of corrole and porphyrin in atom transfer and dioxygen evolving catalysis. *Dalton Trans.* **2011**, 40, 3435-3444.

29. (a) Kasai, M.; Kono, M., Studies on the chemistry of mitomycins. *Synlett* **1992**, 778-90; (b) Colandrea, V. J.; Rajaraman, S.; Jimenez, L. S., Synthesis of the Mitomycin and FR900482 Ring Systems via Dimethyldioxirane Oxidation. *Org. Lett.* **2003**, 5, 785-787; (c) Liu, R.; Herron, S. R.; Fleming, S. A., Copper-Catalyzed Tethered Aziridination of Unsaturated *N*-Tosyloxy Carbamates. *J. Org. Chem.* **2007**, 72, 5587-5591.

30. (a) Loncaric, C.; Wulff, W. D., An efficient synthesis of (-)-chloramphenicol via asymmetric catalytic aziridination: a comparison of catalysts prepared from

triphenylborate and various linear and vaulted biaryls. *Org. Lett.* **2001**, 3, 3675-3678; (b) Sharma, P.; Kumar, A.; Upadhyay, S.; Sahu, V.; Singh, J., Synthesis and QSAR modeling of 2-acetyl-2-ethoxycarbonyl-1-[4(4'-arylazo)-phenyl]-N,N-dimethylaminophenyl aziridines as potential antibacterial agents. *Eur. J. Med. Chem.* **2009**, 44, 251-259; (c) Nemeikaite-Ceniene, A.; Sarlauskas, J.; Anusevicius, Z.; Nivinskas, H.; Cenas, N., Cytotoxicity of RH1 and related aziridinylbenzoquinones: involvement of activation by NAD(P)H:quinone oxidoreductase (NQO1) and oxidative stress. *Arch. Biochem. Biophys.* **2003**, 416, 110-118.

31. Fantauzzi, S.; Caselli, A.; Gallo, E., Nitrene transfer reactions mediated by metallo-porphyrin complexes. *Dalton Trans.* **2009**, 5434-5443.

32. Aviv, I.; Gross, Z., Corrole-based applications. *Chem. Commun.* **2007**, 1987-1999.

33. (a) Omura, K.; Murakami, M.; Uchida, T.; Irie, R.; Katsuki, T., Enantioselective aziridination and amination using p-toluenesulfonyl azide in the presence of Ru(salen)(CO) complex. *Chem. Lett.* **2003**, 32 (4), 354-355; (b) Leung, S. K.-Y.; Tsui, W.-M.; Huang, J.-S.; Che, C.-M.; Liang, J.-L.; Zhu, N., Imido Transfer from Bis(imido)ruthenium(VI) Porphyrins to Hydrocarbons: Effect of Imido Substituents, C-H Bond Dissociation Energies, and Ru^{VI/V} Reduction Potentials. *J. Am. Chem. Soc.* **2005**, 127, 16629-16640; (c) Liu, Y.; Che, C.-M., [Fe^{III}(F20-tpc)Cl] Is an Effective Catalyst for Nitrene Transfer Reactions and Amination of Saturated Hydrocarbons with Sulfonyl and Aryl Azides as Nitrogen

Source under Thermal and Microwave-Assisted Conditions. *Chem.--Eur. J.* **2010**, *16*, 10494-10501.

34. Smith, P. A. S.; Brown, B. B., The reaction of aryl azides with hydrogen halides. *J. Am. Chem. Soc.* **1951**, *73*, 2438-41.

35. Li, Y.; Gao, L.-X.; Han, F.-S., Reliable and Diverse Synthesis of Aryl Azides through Copper-Catalyzed Coupling of Boronic Acids or Esters with TMSN₃. *Chem.--Eur. J.* **2010**, *16*, 7969-7972.

36. Bräse, S.; Gil, C.; Knepper, K.; Zimmermann, V., Organic Azides: An Exploding Diversity of a Unique Class of Compounds. *Angew. Chem. Int. Ed.* **2005**, *44*, 5188-5240.

37. (a) Cenini, S.; Tollari, S.; Penoni, A.; Cereda, C., Catalytic amination of unsaturated hydrocarbons: reactions of p-nitrophenyl azide with alkenes catalyzed by metalloporphyrins. *J. Mol. Catal. A: Chem.* **1999**, *137*, 135-146; (b) Piangiolino, C.; Gallo, E.; Caselli, A.; Fantauzzi, S.; Ragaini, F.; Cenini, S., The [Ru(CO)(porphyrin)]-catalyzed synthesis of *N*-aryl-2-vinylaziridines. *Eur. J. Org. Chem.* **2007**, 743-750.

38. Bass, H. M.; Cramer, S. A.; Price, J. L.; Jenkins, D. M., 18-Atom-Ringed Macrocyclic Tetra-imidazoliums for Preparation of Monomeric Tetra-carbene Complexes. *Organometallics* **2010**, *29*, 3235-3238.

39. Peris, E., Routes to *N*-heterocyclic carbene complexes. *Top. Organomet. Chem.* **2007**, *21*, 83-116.

40. McGuinness, D. S.; Gibson, V. C.; Steed, J. W., Bis(carbene)pyridine Complexes of the Early to Middle Transition Metals: Survey of Ethylene Oligomerization and Polymerization Capability. *Organometallics* **2004**, *23*, 6288-6292.
41. Kaufhold, O.; Hahn, F. E.; Pape, T.; Hepp, A., Ruthenium(II) and iron(II) complexes of *N*-pyridyl substituted imidazoli*N*-2-ylidenes. *J. Organomet. Chem.* **2008**, *693*, 3435-3440.
42. (a) Soundararajan, N.; Platz, M. S., Descriptive photochemistry of polyfluorinated azide derivatives of methyl benzoate. *J. Org. Chem.* **1990**, *55*, 2034-44; (b) Poe, R.; Schnapp, K.; Young, M. J. T.; Grayzar, J.; Platz, M. S., Chemistry and kinetics of singlet pentafluorophenylnitrene. *J. Am. Chem. Soc.* **1992**, *114*, 5054-67.
43. Brown, S. D.; Peters, J. C., Ground-State Singlet $L_3Fe-(\mu-N)-FeL_3$ and $L_3Fe(NR)$ Complexes Featuring Pseudotetrahedral Fe(II) Centers. *J. Am. Chem. Soc.* **2005**, *127*, 1913-1923.
44. (a) Betley, T. A.; Peters, J. C., Dinitrogen Chemistry from Trigonally Coordinated Iron and Cobalt Platforms. *J. Am. Chem. Soc.* **2003**, *125*, 10782-10783; (b) Mehn, M. P.; Brown, S. D.; Jenkins, D. M.; Peters, J. C.; Que, L., Jr., Vibrational Spectroscopy and Analysis of Pseudo-tetrahedral Complexes with Metal Imido Bonds. *Inorg. Chem.* **2006**, *45*, 7417-7427; (c) Lu, C. C.; Saouma, C. T.; Day, M. W.; Peters, J. C., Fe(I)-Mediated Reductive Cleavage and Coupling of CO₂: An $Fe^{II}(\mu-O, \mu-CO)Fe^{II}$ Core. *J. Am. Chem. Soc.* **2007**, *129*, 4-5; (d)

- Scepaniak, J. J.; Young, J. A.; Bontchev, R. P.; Smith, J. M., Formation of Ammonia from an Iron Nitrido Complex. *Angew. Chem. Int. Ed.* **2009**, *48*, 3158-3160.
45. (a) Thomas, C. M.; Mankad, N. P.; Peters, J. C., Characterization of the Terminal Iron(IV) Imides {[PhBPtBu₂(pz')] $\text{Fe}^{\text{IV}}\equiv\text{NAd}\}^+$. *J. Am. Chem. Soc.* **2006**, *128*, 4956-4957; (b) Nieto, I.; Ding, F.; Bontchev, R. P.; Wang, H.; Smith, J. M., Thermodynamics of Hydrogen Atom Transfer to a High-Valent Iron Imido Complex. *J. Am. Chem. Soc.* **2008**, *130*, 2716-2717.
46. Huber, M. L.; Pinhey, J. T., Reaction of aryllead triacetates with sodium azide in dimethyl sulfoxide: a new route to aryl azides. *J. Chem. Soc., Perkin Trans. 1* **1990**, 721-2.
47. Abramovitch, R. A.; Challand, S. R.; Scriven, E. F. V., Intermolecular aromatic substitution by aryl nitrenes. *J. Org. Chem.* **1972**, *37*, 2705-10.
48. Butler, R. N.; Collier, S.; Fleming, A. F. M., Pentazoles: proton and carbo N -13 NMR spectra of some 1-arylpentazoles: kinetics and mechanism of degradation of the arylpentazole system. *J. Chem. Soc., Perkin Trans. 2* **1996**, 801-803.
49. Baron, A.; Herrero, C.; Quaranta, A.; Charlot, M.-F.; Leibl, W.; Vauzeilles, B.; Aukauloo, A., Click Chemistry on a Ruthenium Polypyridine Complex. An Efficient and Versatile Synthetic Route for the Synthesis of Photoactive Modular Assemblies. *Inorg. Chem.* **2012**, *51*, 5985-5987.

50. Liu, Q.; Tor, Y., Simple Conversion of Aromatic Amines into Azides. *Org. Lett.* **2003**, *5*, 2571-2572.
51. Tomioka, H.; Sawai, S., Photolysis of regioisomeric diazides of 1,2-diphenylacetylenes studied by matrix-isolation spectroscopy and DFT calculations. *Org. Biomol. Chem.* **2003**, *1*, 4441-4450.
52. Pelletier, G.; Bechara, W. S.; Charette, A. B., Controlled and Chemoselective Reduction of Secondary Amides. *J. Am. Chem. Soc.* **2010**, *132*, 12817-12819.
53. Morawietz, J.; Sander, W.; Traeubel, M., Intramolecular Hydrogen Transfer in (2-Aminophenyl)carbene and 2-Tolylnitrene. Matrix Isolation of 6-Methylene-2,4-cyclohexadiene-1-imine. *J. Org. Chem.* **1995**, *60*, 6368-78.
54. Lo, C.-N.; Hsu, C.-S., Synthesis and electroluminescence properties of white-light single polyfluorenes with high-molecular weight by click reaction. *J. Polym. Sci., Part A: Polym. Chem.* **2011**, *49*, 3355-3365.
55. Wollman, E. W.; Kang, D.; Frisbie, C. D.; Lorkovic, I. M.; Wrighton, M. S., Photosensitive Self-Assembled Monolayers on Gold: Photochemistry of Surface-Confined Aryl Azide and Cyclopentadienylmanganese Tricarbonyl. *J. Am. Chem. Soc.* **1994**, *116*, 4395-404.
56. Nicolaides, A.; Enyo, T.; Miura, D.; Tomioka, H., p-Phenylenecarbenonitrene and Its Halogen Derivatives: How Does Resonance Interaction between a Nitrene and a Carbene Center Affect the Overall Electronic Configuration? *J. Am. Chem. Soc.* **2001**, *123*, 2628-2636.

57. Lieber, E.; Rao, C. N. R.; Chao, T. S.; Hoffman, C. W. W., Infrared spectra of organic azides. *Anal. Chem.* **1957**, 29, 916-918.
58. Corberan, R.; Mas-Marza, E.; Peris, E., Mono-, Bi- and Tridentate *N*-Heterocyclic Carbene Ligands for the Preparation of Transition-Metal-Based Homogeneous Catalysts. *Eur. J. Inorg. Chem.* **2009**, 1700-1716.
59. Hu, X.; Meyer, K., New tripodal *N*-heterocyclic carbene chelators for small molecule activation. *J. Organomet. Chem.* **2005**, 690, 5474-5484.
60. (a) Fortman, G. C.; Nolan, S. P., *N*-Heterocyclic carbene (NHC) ligands and palladium in homogeneous cross-coupling catalysis: a perfect union. *Chem. Soc. Rev.* **2011**, 40, 5151-5169; (b) Shigeng, G.; Tang, J.; Zhang, D.; Wang, Q.; Chen, Z.; Weng, L., Synthesis, structure, and catalytic activity of palladium complexes with new chiral cyclohexane-1,2-based di-NHC-ligands. *J. Organomet. Chem.* **2012**, 700, 223-229.
61. Lund, C. L.; Sgro, M. J.; Cariou, R.; Stephan, D. W., A *Cis*-Bis-Mixed-Carbene Ruthenium Hydride Complex: An Olefin-Selective Hydrogenation Catalyst. *Organometallics* **2012**, 31, 802-805.
62. Mata, J. A.; Poyatos, M.; Peris, E., Structural and catalytic properties of chelating bis- and tris-*N*-heterocyclic carbenes. *Coord. Chem. Rev.* **2007**, 251, 841-859.
63. Scepaniak, J. J.; Vogel, C. S.; Khusniyarov, M. M.; Heinemann, F. W.; Meyer, K.; Smith, J. M., Synthesis, Structure, and Reactivity of an Iron(V) Nitride. *Science* **2011**, 331, 1049-1052.

64. Edwards, P. G.; Hahn, F. E., Synthesis and coordination chemistry of macrocyclic ligands featuring NHC donor groups. *Dalton Trans.* **2011**, 40, 10278-10288.
65. Nam, W., High-Valent Iron(IV)-Oxo Complexes of Heme and Non-Heme Ligands in Oxygenation Reactions. *Acc. Chem. Res.* **2007**, 40, 522-531.
66. Cramer, S. A.; Jenkins, D. M., Synthesis of Aziridines from Alkenes and Aryl Azides with a Reusable Macrocyclic Tetracarbene Iron Catalyst. *J. Am. Chem. Soc.* **2011**, 133, 19342-19345.
67. Lin, I. J. B.; Vasam, C. S., Preparation and application of *N*-heterocyclic carbene complexes of Ag(I). *Coord. Chem. Rev.* **2007**, 251, 642-670.
68. Wang, H. M. J.; Lin, I. J. B., Facile Synthesis of Silver(I)-Carbene Complexes. Useful Carbene Transfer Agents. *Organometallics* **1998**, 17, 972-975.
69. Bonnet, L. G.; Douthwaite, R. E.; Hodgson, R., Synthesis of Constrained-Geometry Chiral Di-*N*-Heterocyclic Carbene Ligands and Their Silver(I) and Palladium(II) Complexes. *Organometallics* **2003**, 22, 4384-4386.
70. (a) Hu, X.; Tang, Y.; Gantzel, P.; Meyer, K., Silver Complexes of a Novel Tripodal *N*-Heterocyclic Carbene Ligand: Evidence for Significant Metal-Carbene π -Interaction. *Organometallics* **2003**, 22, 612-614; (b) Mas-Marza, E.; Poyatos, M.; Sanau, M.; Peris, E., Carbene Complexes of Rhodium and Iridium from Tripodal *N*-Heterocyclic Carbene Ligands: Synthesis and Catalytic Properties. *Inorg. Chem.* **2004**, 43, 2213-2219.

71. (a) Garrison, J. C.; Youngs, W. J., Ag(I) *N*-Heterocyclic Carbene Complexes: Synthesis, Structure, and Application. *Chem. Rev.* **2005**, *105*, 3978-4008; (b) Hahn, F. E.; Radloff, C.; Pape, T.; Hepp, A., Synthesis of silver (I) and gold (I) complexes with cyclic tetra- and hexacarbene ligands. *Chem.--Eur. J.* **2008**, *14*, 10900-10904; (c) Radloff, C.; Gong, H.-Y.; Schulte, t. B. C.; Pape, T.; Lynch, V. M.; Sessler, J. L.; Hahn, F. E., Metal-Dependent Coordination Modes Displayed by Macrocyclic Polycarbene Ligands. *Chem.--Eur. J.* **2010**, *16*, 13077-13081; (d) Rit, A.; Pape, T.; Hahn, F. E., Self-Assembly of Molecular Cylinders from Polycarbene Ligands and AgI or AuI. *J. Am. Chem. Soc.* **2010**, *132*, 4572-4573; (e) Wang, D.; Zhang, B.; He, C.; Wu, P.; Duan, C., A new chiral *N*-heterocyclic carbene silver(I) cylinder: synthesis, crystal structure and catalytic properties. *Chem. Commun.* **2010**, *46*, 4728-4730.
72. Quezada, C. A.; Garrison, J. C.; Panzner, M. J.; Tessier, C. A.; Youngs, W. J., The Potential Use of Rhodium *N*-Heterocyclic Carbene Complexes as Radiopharmaceuticals: The Transfer of a Carbene from Ag(I) to RhCl₃·3H₂O. *Organometallics* **2004**, *23*, 4846-4848.
73. Smith, J. M.; Long, J. R., First-row transition metal complexes of the strongly donating pentadentate ligand PY₄Im. *Inorg. Chem.* **2010**, *49*, 11223-11230.
74. Mas-Marza, E.; Sanau, M.; Peris, E., Coordination Versatility of Pyridine-Functionalized *N*-Heterocyclic Carbenes: A Detailed Study of the Different

Activation Procedures. Characterization of New Rh and Ir Compounds and Study of Their Catalytic Activity. *Inorg. Chem.* **2005**, *44*, 9961-9967.

75. Arnold, P. L.; Scarisbrick, A. C., Di- and Trivalent Ruthenium Complexes of Chelating, Anionic *N*-Heterocyclic Carbenes. *Organometallics* **2004**, *23*, 2519-2521.

76. Al, T. J.; Lavoie, G. G., Synthesis, Characterization, and Ethylene Polymerization Studies of Chromium, Iron, and Cobalt Complexes Containing 1,3-Bis(imino)-*N*-Heterocyclic Carbene Ligands. *Organometallics* **2012**, *31*, 2463-2469.

77. (a) McGuinness, D. S.; Gibson, V. C.; Wass, D. F.; Steed, J. W., Bis(carbene)pyridine Complexes of Cr(III): Exceptionally Active Catalysts for the Oligomerization of Ethylene. *J. Am. Chem. Soc.* **2003**, *125*, 12716-12717; (b) Kreisel, K. A.; Yap, G. P. A.; Theopold, K. H., A Chelating *N*-Heterocyclic Carbene Ligand in Organochromium Chemistry. *Organometallics* **2006**, *25*, 4670-4679.

78. (a) Berry, J. F., Terminal nitrido and imido complexes of the late transition metals. *Comments Inorg. Chem.* **2009**, *30*, 28-66; (b) Ray, K.; Heims, F.; Pfaff, F. F., Terminal Oxo and Imido Transition-Metal Complexes of Groups 9-11. *Eur. J. Inorg. Chem.* **2013**, *2013*, 3784-3807.

79. Saouma, C. T.; Peters, J. C., $M\equiv E$ and $M=E$ complexes of iron and cobalt that emphasize three-fold symmetry ($E = O, N, NR$). *Coord. Chem. Rev.* **2011**, *255*, 920-937.

80. (a) Trogler, W. C., Synthesis, electronic structure, and reactivity of metallacyclotetraazapentadienes. *Acc. Chem. Res.* **1990**, *23*, 426-31; (b) Cenini, S.; Gallo, E.; Caselli, A.; Ragaini, F.; Fantauzzi, S.; Piangiolino, C., Coordination chemistry of organic azides and amination reactions catalyzed by transition metal complexes. *Coord. Chem. Rev.* **2006**, *250*, 1234-1253; (c) Cowley, R. E.; Bill, E.; Neese, F.; Brennessel, W. W.; Holland, P. L., Iron(II) Complexes with Redox-Active Tetrazene (RNNNNR) Ligands. *Inorg. Chem.* **2009**, *48*, 4828-4836; (d) Danopoulos, A. A.; Wilkinson, G.; Sweet, T. K. N.; Hursthouse, M. B., Reactions of imido complexes of iridium, rhodium and ruthenium. *J. Chem. Soc., Dalton Trans.* **1996**, 3771-3778; (e) Doedens, R. J., Molecular configuration of $\text{Me}_2\text{N}_4\text{Fe}(\text{CO})_3$, a tetrazadiene-tricarbonyliron complex. *Chem. Commun.* **1968**, 1271-2; (f) Michelman, R. I.; Bergman, R. G.; Andersen, R. A., Synthesis, exchange reactions, and metallacycle formation in osmium(II) imido systems: formation and cleavage of osmium-nitrogen bonds. *Organometallics* **1993**, *12*, 2741-51; (g) Mock, M. T.; Popescu, C. V.; Yap, G. P. A.; Dougherty, W. G.; Riordan, C. G., Monovalent iron in a sulfur-rich environment. *Inorg. Chem.* **2008**, *47*, 1889-1891; (h) Overbosch, P.; Van Koten, G.; Grove, D. M.; Spek, A. L.; Duisenberg, A. J. M., (Tetraazabutadiene)platinum complexes. X-ray crystal and molecular structure of the triethylphosphine nucleophilic addition product $[\text{Pt}(1,4-(4\text{-O}_2\text{NC}_6\text{H}_4)_2\text{N}_4)(\text{CHC}(\text{PEt}_3)\text{H}(\text{CH}_2)_2\text{CH}:\text{CHCH}_2\text{CH}_2)(\text{PEt}_3)]$, a novel five-coordinate blue mononuclear platinum species. *Inorg. Chem.* **1982**, *21*, 3253-3260; (i) Overbosch, P.; Van Koten, G.; Spek, A. L.; Roelofsen, G.; Duisenberg,

- A. J. M., Synthesis, reactivity, and crystal structure of [1,4-bis(4-tolyl)tetraazabutadiene](η^5 -cyclopentadienyl)nickel. *Inorg. Chem.* **1982**, 21, 3908-3913; (j) Overbosch, P.; Van Koten, G.; Vrieze, K., Inter- and intramolecular ligand exchange and rearrangement reactions of tetraazadiene complexes of nickel, platinum, and cobalt. *J. Chem. Soc., Dalton Trans.* **1982**, 1541-7.
81. Gehrman, T.; Lloret Fillol, J.; Wadepohl, H.; Gade, L. H., Synthesis, Characterization, and Thermal Rearrangement of Zirconium Tetraazadienyl and Pentaazadienyl Complexes. *Organometallics* **2012**, 31, 4504-4515.
82. (a) Gross, M. E.; Johnson, C. E.; Maroney, M. J.; Trogler, W. C., Photochemistry of cyclopentadienylcobalt 1,4-diaryltetraazadienes. Examples of CH, CF, and CC bond breaking. *Inorg. Chem.* **1984**, 23, 2968-2973; (b) Gross, M. E.; Trogler, W. C., Photochemical loss of dinitrogen from cyclopentadienylcobalt 1,4-diaryltetraazadienes. *J. Organomet. Chem.* **1981**, 209, 407-414.
83. (a) Que, L., Jr.; Tolman, W. B., Biologically inspired oxidation catalysis. *Nature* **2008**, 455, 333-340; (b) McDonald, A. R.; Que, L., High-valent nonheme iron-oxo complexes: Synthesis, structure, and spectroscopy. *Coord. Chem. Rev.* **2013**, 257, 414-428; (c) Abu-Omar, M. M.; Loaiza, A.; Hontzeas, N., Reaction mechanisms of mononuclear non-heme iron oxygenases. *Chem. Rev.* **2005**, 105, 2227-2252; (d) Costas, M.; Mehn, M. P.; Jensen, M. P.; Que, L., Jr., Dioxygen Activation at Mononuclear Nonheme Iron Active Sites: Enzymes, Models, and Intermediates. *Chem. Rev.* **2004**, 104, 939-986; (e) Krebs, C.; Fujimori, D. G.;

Walsh, C. T.; Bollinger, J. M., Jr., Non-Heme Fe(IV)-Oxo Intermediates. *Acc. Chem. Res.* **2007**, *40*, 484-492.

84. (a) Lewis, R. A.; Smiles, D. E.; Darmon, J. M.; Stieber, S. C. E.; Wu, G.; Hayton, T. W., Reactivity and Moessbauer Spectroscopic Characterization of an Fe(IV) Ketimide Complex and Reinvestigation of an Fe(IV) Norbornyl Complex. *Inorg. Chem.* **2013**, *52*, 8218-8227; (b) Meyer, S.; Klawitter, I.; Demeshko, S.; Bill, E.; Meyer, F., A Tetracarbene-Oxoiron(IV) Complex. *Angew. Chem., Int. Ed.* **2013**, *52*, 901-905; (c) Berry, J. F.; Bill, E.; Bothe, E.; Neese, F.; Wieghardt, K., Octahedral non-heme oxo and non-oxo Fe(IV) complexes: an experimental/theoretical comparison. *J. Am. Chem. Soc.* **2006**, *128*, 13515-13528; (d) Chanda, A.; Popescu, D.-L.; Tiago de Oliveira, F.; Bominaar, E. L.; Ryabov, A. D.; Muenck, E.; Collins, T. J., High-valent iron complexes with tetraamido macrocyclic ligands: Structures, Moessbauer spectroscopy, and DFT calculations. *J. Inorg. Biochem.* **2006**, *100*, 606-619; (e) Scepianiak, J. J.; Vogel, C. S.; Khusniyarov, M. M.; Heinemann, F. W.; Meyer, K.; Smith, J. M., Synthesis, Structure, and Reactivity of an Iron(V) Nitride. *Science* **2011**, *331*, 1049-1052.

85. Banerjee, S.; Ghosh, A.; Wu, B.; Lassahn, P.-G.; Janiak, C., Polymethylene spacer regulated structural divergence in cadmium complexes: Unusual trigonal prismatic and severely distorted octahedral coordination. *Polyhedron* **2005**, *24*, 593-599.

86. (a) Aviv-Harel, I.; Gross, Z., Coordination chemistry of corroles with focus on main group elements. *Coord. Chem. Rev.* **2011**, *255*, 717-736; (b) Dagorne,

S.; Normand, M.; Kirillov, E.; Carpentier, J.-F., Gallium and indium complexes for ring-opening polymerization of cyclic ethers, esters and carbonates. *Coord. Chem. Rev.* **2013**, 257, 1869-1886; (c) Chatterjee, C.; Chisholm, M. H., Ring-Opening Polymerization Reactions of Propylene Oxide Ring-Opening Polymerization Reactions of Propylene Oxide Catalyzed by Porphyrin Metal (3+) Complexes of Aluminum, Chromium and Cobalt. *Chem. Rec.* **2013**, 13, 549-560; (d) Decortes, A.; Castilla, A. M.; Kleij, A. W., Salen-Complex-Mediated Formation of Cyclic Carbonates by Cycloaddition of CO₂ to Epoxides. *Angew. Chem., Int. Ed.* **2010**, 49, 9822-9837; (e) Cokoja, M.; Bruckmeier, C.; Rieger, B.; Herrmann, W. A.; Kuehn, F. E., Transformation of Carbon Dioxide with Homogeneous Transition-Metal Catalysts: A Molecular Solution to a Global Challenge? *Angew. Chem., Int. Ed.* **2011**, 50, 8510-8537.

87. Duxbury, J. P.; Cawley, A.; Thornton-Pett, M.; Wantz, L.; Warne, J. N. D.; Greatrex, R.; Brown, D.; Kee, T. P., Chiral aluminum complexes as phospho-transfer catalysts. *Tetrahedron Lett.* **1999**, 40, 4403-4406.

88. Aluthge, D. C.; Patrick, B. O.; Mehrkhodavandi, P., A highly active and site selective indium catalyst for lactide polymerization. *Chem. Commun.* **2013**, 49, 4295-4297.

89. Shetti, V. S.; Pareek, Y.; Ravikanth, M., Sn(IV) porphyrin scaffold for multiporphyrin arrays. *Coord. Chem. Rev.* **2012**, 256, 2816-2842.

90. Jing, H.; Edulji, S. K.; Gibbs, J. M.; Stern, C. L.; Zhou, H.; Nguyen, S. T., (Salen)Tin Complexes: Syntheses, Characterization, Crystal Structures, and

Catalytic Activity in the Formation of Propylene Carbonate from CO₂ and Propylene Oxide. *Inorg. Chem.* **2004**, *43*, 4315-4327.

91. Darensbourg, D. J.; Ganguly, P.; Billodeaux, D., Ring-opening polymerization of trimethylene carbonate using aluminum(III) and tin(IV) salen chloride catalysts. *Macromolecules* **2005**, *38*, 5406-5410.

92. (a) Braunschweig, H.; Dewhurst, R. D.; Hammond, K.; Mies, J.; Radacki, K.; Vargas, A., Ambient-Temperature Isolation of a Compound with a BoroN-Boron Triple Bond. *Science* **2012**, *336*, 1420-1422; (b) Wang, Y.; Quillian, B.; Wei, P.; Wannere, C. S.; Xie, Y.; King, R. B.; Schaefer, H. F., III; Schleyer, P. v. R.; Robinson, G. H., A Stable, Neutral Diborene Containing a B:B Double Bond. *J. Am. Chem. Soc.* **2007**, *129*, 12412-12413.

93. Wang, Y.; Xie, Y.; Wei, P.; King, R. B.; Schaefer, H. F., III; Schleyer, P. v. R.; Robinson, G. H., A Stable Silicon(0) Compound with a Si:Si Double Bond. *Science* **2008**, *321*, 1069-1071.

94. Wang, Y.; Xie, Y.; Wei, P.; King, R. B.; Schaefer, H. F., III; Schleyer, P. v. R.; Robinson, G. H., Carbene-Stabilized Diphosphorus. *J. Am. Chem. Soc.* **2008**, *130*, 14970-14971.

95. (a) Nakai, H.; Tang, Y.; Gantzel, P.; Meyer, K., A new entry to *N*-heterocyclic carbene chemistry: synthesis and characterization of a triscarbene complex of thallium(I). *Chem. Commun.* **2003**, 24-25; (b) Dutton, J. L.; Tuononen, H. M.; Ragogna, P. J., Tellurium(II)-Centered Dications from the Pseudohalide "Te(OTf)₂". *Angew. Chem., Int. Ed.* **2009**, *48*, 4409-4413; (c)

Rupar, P. A.; Staroverov, V. N.; Ragogna, P. J.; Baines, K. M., A Germanium(II)-Centered Dication. *J. Am. Chem. Soc.* **2007**, 129 (49), 15138-15139; (d) Filippou, A. C.; Lebedev, Y. N.; Chernov, O.; Strassmann, M.; Schnakenburg, G., Silicon(II) Coordination Chemistry: *N*-Heterocyclic Carbene Complexes of Si²⁺ and Si¹⁺. *Angew. Chem., Int. Ed.* **2013**, 52, 6974-6978.

96. (a) Nieto, I.; Bontchev, R. P.; Smith, J. M., Synthesis of a bulky bis(carbene)borate ligand - contrasting structures of homoleptic nickel(II) bis(pyrazolyl)borate and bis(carbene)borate complexes. *Eur. J. Inorg. Chem.* **2008**, 2476-2480; (b) Nieto, I.; Cervantes-Lee, F.; Smith, J. M., A new synthetic route to bulky "second generation" tris(imidazol-2-ylidene)borate ligands: synthesis of a four coordinate iron(II) complex. *Chem. Commun.* **2005**, 3811-3813.

97. Bass, H. M.; Cramer, S. A.; McCullough, A. S.; Bernstein, K. J.; Murdock, C. R.; Jenkins, D. M., Employing Dianionic Macrocyclic Tetracarbenes To Synthesize Neutral Divalent Metal Complexes. *Organometallics* **2013**, 32, 2160-2167.

98. (a) Bass, H. M.; Cramer, S. A.; Price, J. L.; Jenkins, D. M., 18-Atom-Ringed Macrocyclic Tetra-imidazoliums for Preparation of Monomeric Tetracarbene Complexes. *Organometallics* **2010**, 29, 3235-3238; (b) Cramer, S. A.; Jenkins, D. M., Synthesis of Aziridines from Alkenes and Aryl Azides with a Reusable Macrocyclic Tetracarbene Iron Catalyst. *J. Am. Chem. Soc.* **2011**, 133, 19342-19345; (c) Lu, Z.; Cramer, S. A.; Jenkins, D. M., Exploiting a dimeric silver

transmetallating reagent to synthesize macrocyclic tetracarbene complexes.

Chem. Sci. **2012**, 3, 3081-3087.

99. (a) Black, S. J.; Hibbs, D. E.; Hursthouse, M. B.; Jones, C.; Abdul, M. K. M.; Smithies, N. A., Synthesis and characterization of stable carbene-indium(III) halide complexes. *J. Chem. Soc., Dalton Trans.* **1997**, 4313-4320; (b) Francis, M. D.; Hibbs, D. E.; Hursthouse, M. B.; Jones, C.; Smithies, N. A., Carbene complexes of Group 13 trihydrides: synthesis and characterization of $[MH_3\{CN(Pr^i)C_2Me_2N(Pr^i)\}]$, M = Al, Ga or In. *J. Chem. Soc., Dalton Trans.* **1998**, 3249-3254.

100. Goehner, M.; Herrmann, F.; Kuhn, N.; Stroebele, M., $(Carb)_2SnF_4$ (Carb = 2,3-Dihydro-1,3-diisopropyl-4,5-dimethylimidazol-2-ylidene) - a Carbene Complex of Tetravalent Tin. *Z. Anorg. Allg. Chem.* **2012**, 638, 2196-2199.

101. Still, B. M.; Kumar, P. G. A.; Aldrich-Wright, J. R.; Price, W. S., ^{195}Pt NMR - theory and application. *Chem. Soc. Rev.* **2007**, 36, 665-686.

102. (a) Cornman, C. R.; Geiser-Bush, K. M.; Rowley, S. P.; Boyle, P. D., Structural and Electron Paramagnetic Resonance Studies of the Square Pyramidal to Trigonal Bipyramidal Distortion of Vanadyl Complexes Containing Sterically Crowded Schiff Base Ligands. *Inorg. Chem.* **1997**, 36, 6401-6408; (b) Addison, A. W.; Rao, T. N.; Reedijk, J.; Van, R. J.; Verschoor, G. C., Synthesis, structure, and spectroscopic properties of copper(II) compounds containing nitrogen-sulfur donor ligands: the crystal and molecular structure of aqua[1,7-

bis(*N*-methylbenzimidazol-2'-yl)-2,6-dithiaheptane]copper(II) perchlorate. *J. Chem. Soc., Dalton Trans.* **1984**, 1349-56.

103. Baker, R. J.; Cole, M. L.; Jones, C.; Mahon, M. F., Bidentate *N*-heterocyclic carbene complexes of Group 13 trihydrides and trihalides. *J. Chem. Soc., Dalton Trans.* **2002**, 1992-1996.

104. Carmalt, C. J., Main Group Carbenes. In *Encyclopedia of Inorganic and Bioinorganic Chemistry*, John Wiley & Sons, Ltd: 2011.

VITA

Steven Alan Cramer was born November 29, 1984 in Austell, Georgia. He spent his youth living in Powder Springs, Georgia with his parents. After graduating from McEachern High School in 2003, Alan enrolled at Kennesaw State University in Kennesaw Georgia. Initially he was preparing to attend pharmacy school when a period of soul searching led him to follow his passion for experimental science and change his major to chemistry. In December of 2008, Alan graduated with his B.S. in Chemistry from Kennesaw State University while also keeping his HOPE scholarship for the entire duration of his collegiate education.

In the time leading up to graduation Alan began applying to graduate schools in chemistry. Shortly after graduation he was accepted into the University of Tennessee's chemistry graduate program for the Fall of 2009. Upon visitation he knew that Knoxville was the place he wanted to continue his education and he promptly accepted the offer. During graduate school he has contributed to several peer-reviewed publications, won multiple departmental achievement awards, and gave four presentations at ACS national meetings.